

# **Assessment of the effect of selected African plants on an *in vitro* model of Parkinson's disease**

by

**Keagile H. Lepule**

A dissertation submitted in fulfilment for the degree

**Magister Scientiae**

in

**Pharmacology**

in the

**Faculty of Health Sciences**

at the

**University of Pretoria**

**Supervisor: Prof V Steenkamp**

**Co-supervisors: Mrs M Nell and Dr W Cordier**

2017

# Declaration

**University of Pretoria**  
**Faculty of Health Sciences**  
**Department of Pharmacology**

**Student name:** Keagile Hilda Lepule

**Student number:** 29243239

**Subject of the work:** Assessment of the effect of selected African plants on an *in vitro* model of Parkinson's disease

## Declaration

1. I understand what plagiarism is and am aware of the University's policy in this regard.
2. I declare that this dissertation is my own original work. Where other people's work has been used (either from a printed source, Internet or any other source), this has been properly acknowledged and referenced in accordance with departmental requirements.
3. I have not used work previously produced by another student or any other person to hand in as my own.
4. I have not allowed, and will not allow, anyone to copy my work with the intention of passing it off as his or her own work.

**Signature:**

# Dedication

*To my mom, Thandi Victoria Lepule, for the encouragements and support that you granted me throughout my life and mostly for teaching me to walk by FAITH.*

# Acknowledgements

*'The Lord is my shepherd; I have everything I need...'*

*Psalm 23*

I would like to give my sincere gratitude to following people and organisations:

To my supervisor, Prof V Steenkamp, thank you for the continuous support, advice and for believing in me throughout my study. I hope we will continue with this mentorship.

To my co-supervisor, Dr W Cordier, thank you for the guidance, training, patience and assistance in this project.

To my co-supervisor, Mrs. M Nell thank you for the unremitting constant support and for sacrificing multiple weekends to assist me in the lab. Your efforts are highly appreciated.

To my colleagues at Tshwane University Technology, thank you for your constant motivation and support.

To my mentor and academic mom, Prof GE Enslin, thank you for the encouragement and counsel you give.

To my mom, sister and brother, thank you for your unconditional love, support, care and including me in your prayers. There really is no bond stronger than family.

To my friends, Lois, Kim, Chanelle, Hafiza, Akanyang and Tracey, thank you for encouraging me to take well deserved breaks in between experiments and for understanding my late arrival for our hangout sessions because I had to pop-in and check the cells.

To the National Research Fund, thank you for the continued financial support.

*'God's delay is not his denial'*

# Abstract

Parkinson's disease (PD) is an incurable, progressive disease characterised by loss of dopaminergic neurons in the substantia nigra of the brain. The main cause of dopaminergic neuron loss is attributed to oxidative stress and mitochondrial dysfunction. Although treatments are available, focus is placed on symptomatic relief, and thus over time disease progression still occurs. Herbal remedies offer a wide range of chemical entities that may prove beneficial in treating neurodegeneration. The aim of this study was to evaluate the neuroprotective effects of selected African medicinal plants using 6-hydroxydopamine (6-OHDA)-induced cytotoxicity in the SH-SY5Y human neuroblastoma cell line as model of PD.

Eight plants, used ethnomedicinally for the treatment of neurological disorders, were extracted using methanol and acetone ultrasonic maceration. Neurotoxicity was induced by exposing cells to 33.3  $\mu$ M 6-OHDA for 2 h, followed by 24 h incubation with the crude extracts. Neuroprotection was initially assessed using the sulforhodamine B staining assay. Plants that displayed neuroprotective activity (*Acokanthera oppositifolia*, *Boophane disticha* and *Xysmalobium undulatum*) were further assessed (0.5-15  $\mu$ g/mL) using mechanistic assays. Reduced glutathione (GSH) content, mitochondrial membrane potential, reactive oxygen species (ROS) levels, intracellular calcium ( $\text{Ca}^{2+}$ ) flux and adenosine triphosphate (ATP) levels were assessed using the monochlorobamine adduct formation, JC-1 ratiometric, dihydrodichlorofluorescein cleavage assays, Fura-2 AM and a bioluminescence assay kit, respectively. Cell morphology was visualized using phase contrast and polarisation-optical transmitted light differential interference contrast (PlasDIC) microscopy.

6-Hydroxydopamine reduced cell density by 91% and increasing ROS (3-fold) and GSH (2-fold) levels. Mitochondrial depolarisation (2-fold) was evident, most likely due to blockage of mitochondrial complex I with subsequent ROS leakage. Reduced glutathione levels increased adaptively possibly in response to the ensuing oxidation. Crude extracts attenuated cytotoxicity by reducing ROS, sustaining ATP production and maintaining threshold intracellular  $\text{Ca}^{2+}$  effects. This was confirmed by microscopic analyses. A trend for greater protection at lower concentrations was observed. Results suggest that intermediate-polarity extracts of *A. oppositifolia*, *B. disticha* and *X. undulatum* may assist with reducing the detrimental effects associated with PD. In conclusion, extracts of *A. oppositifolia*, *B. disticha* and *X. undulatum* offer *in vitro* neuroprotective effects.

# Table of Contents

Declaration.....	i
Dedication .....	ii
Acknowledgements.....	iii
Abstract .....	iv
List of Figures .....	viii
List of Tables .....	xi
List of Abbreviations .....	xii
Glossary.....	xviii
Chapter 1: Introduction .....	1
1.1. Parkinson’s disease .....	1
1.2. Classification of Parkinson’s disease.....	3
1.2.1. Familial Parkinson’s disease.....	3
1.2.1.1. $\alpha$ -Synuclein.....	3
1.2.1.2. Leucine-rich repeat kinase 2 .....	4
1.2.1.3. Parkin .....	4
1.2.1.4. Phosphatase and tensin homolog induced kinase-1 .....	4
1.2.1.5. DJ-1.....	4
1.2.2. Sporadic Parkinson’s disease .....	4
1.3. Neurochemical factors involved in Parkinson’s disease.....	4
1.3.1. Mitochondrial dysfunction .....	4
1.3.2. Oxidative stress.....	7
1.3.3. Aging .....	10
1.3.4. Cell death .....	10
1.3.4.1. Apoptosis .....	10
1.3.4.2. Necrosis .....	12
1.3.4.3. Autophagy.....	12
1.3.4.4. Caspase-independent cell death (CICD) .....	13

1.4.	Experimental models of Parkinson’s disease.....	13
1.4.1.	6-Hydroxydopamine .....	14
1.4.2.	1-Methyl-4-phenylpyridinium (MPP <sup>+</sup> ) .....	14
1.4.3	Human neuroblastoma cells .....	16
1.5.	Treatment of Parkinson’s disease.....	17
1.5.1.	Conventional treatment .....	17
1.5.2.	Herbal remedies.....	19
1.5.2.1.	<i>Acokantera oppositifolia (Lam.) Codd</i> .....	20
1.5.2.2.	<i>Boophane disticha(L.f.) Herb</i> .....	20
1.5.2.3.	<i>Hypericum perfoatum (L.)</i> .....	20
1.5.2.4.	<i>Leonotis leonurus (L.) R.Br</i> .....	21
1.5.2.5.	<i>Siphonochillus aethipicus (schweinf.) B.L. Brutt</i> .....	21
1.5.2.6.	<i>Terminalia sericea Burch. ex DC</i> .....	21
1.5.2.7.	<i>Xysmalobium undulatum (L.) Aiton.F.</i> .....	21
1.5.2.8.	<i>Ziziphus mucronata Willd</i> .....	21
1.5.3.	The blood brain barrier and medicinal plants .....	22
1.6.	Aim.....	23
1.7.	Objectives of the study.....	23
1.8.	Project overview .....	24
Chapter 2: Materials and methods .....		25
2.1.	Plant material.....	25
2.2.	Preparation of the plant extracts.....	25
2.3.	Phytochemical screening .....	26
2.4.	Cell culture and maintenance .....	26
2.5.	Effect of neurotoxins and crude extracts on cell density .....	27
2.6.	Preliminary screening of neuroprotective effects of crude extracts in the Parkinson’s disease model .....	28
2.7.	Determination of intracellular reactive oxygen species concentrations.....	28

2.8.	Quantification of intracellular glutathione content .....	29
2.9.	Mitochondrial membrane potential .....	29
2.10.	Quantification of intracellular calcium flux .....	30
2.11.	Quantification of intracellular ATP levels .....	31
2.12.	Cellular morphology .....	31
2.13.	Data analysis and statistics .....	32
Chapter 3: Results and Discussion .....		33
3.1.	Phytochemical screening of crude extracts .....	33
3.2.	Cytotoxicity of crude extracts .....	36
3.3.	The effect of neurotoxins on cell density .....	39
3.4.	The effect of crude extracts on 6-OHDA-induced cytotoxicity .....	41
3.5.	The effect of crude extracts on 6-OHDA-induced mitochondrial depolarisation.....	46
3.6.	The effect of crude extracts on 6-OHDA-induced oxidative stress.....	49
3.7.	The effect of crude extracts on 6-OHDA-induced alterations to reduced glutathione .....	52
3.8.	The effect of crude extracts on 6-OHDA-induced decreased intracellular adenosine tri- phosphate .....	55
3.9.	The effect of crude extracts on 6-OHDA-induced decreased intracellular calcium flux .....	58
3.10.	The effect of plant extracts and 6-OHDA on cellular morphology .....	61
Chapter 4: Conclusion .....		65
4.1.	Concluding remarks .....	65
4.2.	Recommendations and limitations .....	66
References .....		67
Appendix I: Ethical approval .....		77
Appendix II: Reagent preparation.....		78

# List of Figures

**Figure 1:** The nigrostriatal dopaminergic pathway in a (A) healthy patient and (B) PD patient. Immunohistochemical image (C) of Lewy bodies observed post-mortem. Lewy bodies have been shown to stain positive for  $\alpha$ -synuclein and ubiquitin aggregates. Reproduced with permission: Elsevier.<sup>16</sup> ..... 3

**Figure 2:** The mitochondrial electron transport chain. Adenosine tri-phosphate is produced and reactive oxygen species are generated in the process. s. Reproduced with permission: Elsevier.<sup>27</sup> ..... 6

**Figure 3:** Functions of reduced glutathione in a brain. Reduced glutathione blocks oxidation of macromolecules (protein, lipids, DNA) and oxidative stress induced mitochondrial dysfunction. Reproduced with permission: Elsevier.<sup>16</sup> ..... 9

**Figure 4:** The extrinsic and intrinsic apoptotic pathway. Reproduced with permission: Cold Spring Harbor Laboratory press.<sup>40</sup> ..... 11

**Figure 5:** Structural similarity of 6-hydroxydopamine and dopamine..... 14

**Figure 6:** Structural similarity of 1-methyl-4-phenylpyridinium and dopamine..... 15

**Figure 7:** There are four well-established PD models, namely the 6-OHDA, MPP+, paraquat and rotenone models. Reproduced with permission.<sup>28</sup> ..... 16

**Figure 8:** Plants selected for the present study. (A) *Acokanthera oppositifolia*, (B) *Boophane disticha*, (C) *Hypericum perforatum*, (D) *Leonotis leonurus*, (E) *Siphonochilus aethiopicus*, (F) *Terminalia sericea*, (G) *Xyralobium undulatum* and (H) *Ziziphus mucronata*. Reproduced with permission: Briza Publications.<sup>60</sup> ..... 22

**Figure 9:** Project overview is the summation of the methodology used to achieve set objectives..... 24

**Figure 10:** The effect of (●) acetone and (●) methanol extracts on SH-SY5Y cell density. (A) *A. oppositifolia*, (B) *B. disticha*, (C) *H. perforatum*, (D) *L. leonurus*, (E) *S. aethiopicus*, (F) *T. sericea*, (G) *X. undulatum* and (H) *Z. mucronata*. The black dashed line represents a 50% reduction in cell density. .... 37

**Figure 11:** The effect of controls used during cytotoxicity assessment on the SH-SY5Y cell line. Significant difference to the 6-OHDA treatment relative to the NC<sub>a</sub>,\*\*\*  $p < 0.001$ ..... 40

**Figure 12:** The effect of (A) 6-OHDA and (B) MPP<sup>+</sup> on the SH-SY5Y cell line after (●) 24 h and (●) 48 h exposure. .... 41

**Figure 13:** The neuroprotective effect of the crude (A) acetone and (B) methanol extracts against 6-OHDA-induced neurotoxicity in the SH-SY5Y cell line after 24 h exposure. The black dashed line represents the cytotoxicity induced by 6-OHDA.. ..... 43

**Figure 14:** The neuroprotective effect of crude (A) acetone and (B) methanol extracts against 6-OHDA-induced neurotoxicity in the SH-SY5Y cell line after 48 h exposure. .... 44

**Figure 15:** The neuroprotective effect of crude (A) acetone and (B) methanol extracts against 6-OHDA-induced neurotoxicity in the SH-SY5Y cell line after 72 h exposure. .... 45

**Figure 16:** Effect of controls used during mitochondrial membrane potential assessment on the SH-SY5Y cell line. Significant difference to the 6-OHDA treatment relative to the NC<sub>a</sub>, \*\*\* p < 0.001. .... 47

**Figure 17:** Effect of crude (A) acetone and (B) methanol extracts against 6-OHDA-induced mitochondrial membrane depolarisation in the SH-SY5Y cell line after 24 h incubation. .... 48

**Figure 18:** Effect of controls used during reactive oxygen species assessment on the SH-SY5Y cell line. Significant difference to the 6-OHDA treatment relative to the NC<sub>a</sub>, \* p < 0.05 and \*\* p < 0.01. .... 50

**Figure 19:** The effect of crude (A) acetone and (B) methanol extracts against 6-OHDA-induced ROS in the SH-SY5Y cell line after 24 h incubation. Significant difference to the 6-OHDA treatment relative to the NC<sub>a</sub>, \* p < 0.05, \*\* p < 0.01 and \*\*\* p < 0.001. .... 51

**Figure 20:** Effect of controls used during intracellular glutathione assessment on the SH-SY5Y cell line. Significant difference to the 6-OHDA treatment relative to the NC<sub>a</sub>, \*\* p < 0.01. .... 53

**Figure 21:** Effect of crude (A) acetone and (B) methanol extracts against 6-OHDA-induced increase in intracellular glutathione levels in the SH-SY5Y cell line after 24 h incubation. Significant difference to the 6-OHDA treatment relative to the NC<sub>a</sub>. .... 54

**Figure 22:** Effect of controls used during intracellular ATP assessment on the SH-SY5Y cell line. Significant difference to the 6-OHDA treatment relative to the NC<sub>a</sub>, \*\* p < 0.01. .... 56

**Figure 23:** Effect of crude (A) acetone and (B) methanol extracts on ATP levels after pre-treatment with 6-OHDA on SH-SY5Y cell line after 24 h incubation. .... 57

**Figure 24:** Effect of controls on intracellular calcium levels on the SH-SY5Y cell line. Significant difference to the 6-OHDA treatment relative to the NC<sub>a</sub>, \* p < 0.05. .... 59

**Figure 25:** Effect of crude (A) acetone and (B) methanol extracts on intracellular calcium levels after pre-treatment with 6-OHDA in the SH-SY5Y cell line after 24 h incubation. Significant difference to the 6-OHDA treatment relative to the NC<sub>a</sub>, \* p < 0.05 and \*\*\* p < 0.001. .... 60

**Figure 26:** The effect of controls and 6-OHDA on cellular morphology of the SH-SY5Y cell line using phase contrast microscopy and polarisation-optical transmitted light differential interference contrast (PlasDIC) microscopy. A magnification of 5x and 40x was used for phase contrast and PlasDIC, respectively. Arrows indicate apoptotic bodies. .... 62

**Figure 27:** Effect of acetone and methanol extracts (0.5 and 5  $\mu\text{g}/\text{mL}$ ) on cellular morphology in SH-SY5Y cell line pre-treated with 6-OHDA and incubated for 24h. A magnification of 5x and 40x was used for phase contrast and PlasDIC microscopy, respectively. Arrows indicate apoptotic bodies.. ..... 64

# List of Tables

<b>Table 1:</b> Conventional treatment of PD.....	18
<b>Table 2:</b> Plants selected for study against neurotoxin-induced Parkinson’s disease. ....	25
<b>Table 3:</b> Mobile phases and detection reagent used to visualise phytochemical classes.....	26
<b>Table 4:</b> Extraction yields and presence of major phytochemical classes in the crude extracts of the selected medicinal plants. ....	35
<b>Table 5:</b> The cytotoxicity of the acetone and methanol extracts in the SH-SY5Y cell line expressed as the IC <sub>50</sub> .....	36

# List of Abbreviations

## Symbols and numerical indicators

°C	Degrees Celsius
%	Percentage
µg	Micrograms
6-OHDA	6-Hydroxydopamine

## A

AAPH	2,2'-Azobis (2-methylpropionamide) dihydrochloride
ABTS	2,2'-Azino-bis(3-ethylbenzothiazoline-6-sulphonic acid
ADP	Adenosine di-phosphate
AGT 5	Autophagy related protein
AIF	Apoptosis inducing factor
ANOVA	Analysis of variance
ANT	Adenine nucleotide translocator
Apaf-1	Apoptotic protease- activating factor-1
ATCC	American Tissue Culture Collection
ATP	Adenosine tri-phosphate
AUC	Area under the curve

## B

BAGS	Bcl-2 associated anthogene
Bad	Bcl-2 antagonist of cell death
Bax	Bcl-2 associated X protein
BBB	Blood brain barrier
Bcl-2	B-cell lymphoma protein 2
Bcl-10	B-cell lymphoma protein 10
Bcl-w	Bcl-2 like 2 protein
Bcl-X	Bcl-2 like 1 protein

Bcl-XL	Bcl-2 related protein, long isoform
BID	BH <sub>3</sub> only pro-apoptotic protein
Bik	Bcl-2 interacting killer

## C

CAT	Catalase
CICD	Caspase-independent cell death
CO <sub>2</sub>	Carbon dioxide
COMT	Catechol-O-methyl transferase

## D

DAQ	Dopamine quinone
DAT	Dopamine transporter
DMSO	Dimethyl sulfoxide
DNA	Deoxyribonucleic acid
DMEM	Dulbecco's Modified Eagle's Medium
DOPAC	3,4-Dihydroxyphenylacetic acid
DPPH	2,2-Diphenyl-1-picrylhydrazyl

## E

EGTA	Ethylene glycol-bis(2-aminoethylether)-N,N,N',N'-tetraacetic acid
ETC	Electron transport chain

## F

FAD	Flavin adenine dinucleotide
FADD	Fas-associated death domain
FADH	Flavin adenine dinucleotide hydroquinone
FADH <sub>2</sub>	Flavin adenine dinucleotide semiquinone
FasR	Fas receptor
FCS	Foetal calf serum
Fe <sup>2+</sup>	Ferrous ion

Fe <sup>3+</sup>	Ferric ion
FITC	Fluorescein isothiocyanate
FR	Fluorescence ratio
FURA-2	2-[6-[Bis[2-[(acetyloxy)methoxy]-2-oxoethyl]amino]-5-[2-[2-[bis[2-[(acetyloxy)methoxy]-2-oxoethyl]amino]-5-methylphenoxy]ethoxy]-2-benzofuranyl]-5-oxazolecarboxylic acid
FURA-2 AM	FURA-2-acetoxymethyl ester
<b>G</b>	
g	Grams
<i>g</i>	Relative centrifugal force
GCS	Glutamylcysteine
GPx	Glutathione peroxidase
GSH	Glutathione
GSSG	Glutathione disulphide
<b>H</b>	
h	Hour
H <sup>+</sup>	Hydrogen ion
H <sub>2</sub> DCF-DA	Dihydrodichlorofluorescein diacetate
HBSS	Hanks Balanced Salt Solution
H <sub>2</sub> O	Water
H <sub>2</sub> O <sub>2</sub>	Hydrogen peroxide
<b>I</b>	
IC <sub>50</sub>	Half maximal inhibitory concentration
<b>J</b>	
JC-1	5,5',6,6'-Tetrachloro-1,1,3,3'- tetraethylbenzimidazolylcarbocyanine iodide

## K

kDa                      Kilodaltons

## L

L                              Liter

L-dopa                      L-3,4-Dihydrophenylalanine

LDH                        Lactic acid dehydrogenase

LRRK-2                    Leucine-rich repeat kinase

## M

MAO                        Monoamine oxidase

MCB                        Monochlorobimane

mg                         Milligram

mL                         Milliliter

MLKL                      Mixed-lineage kinase domain like protein

mM                        Millimolar

MMP                        Mitochondrial membrane potential

MnSOD                    Manganese superoxide

MPP<sup>+</sup>                      1-Methyl-4-phenylpyridinium

MPPP                      1-Methyl-4-propion-oxypiperidine

MPT                        Mitochondrial permeability transition

MPTP                      1-Methyl-4-phenyl-1,2,3,6-tetrahydropyridine

## N

nM                         Nanomolar

NAD<sup>+</sup>                      Nicotinamide adenine dinucleotide

NADH                      Reduced nicotinamide adenine dinucleotide

NCX                        Sodium-calcium exchanger

NICE                        National Institute for Health and Clinical Excellence

NO<sup>•</sup>                        Nitric oxide radical

## O

O <sub>2</sub>	Oxygen
O <sub>2</sub> <sup>•-</sup>	Superoxide radical
OH <sup>•</sup>	Hydroxyl radical
ONOO <sup>-</sup>	Peroxynitrite

## P

PARP	Poly-ADP-ribose polymerase
PBS	Phosphate-buffered saline
Pink-1	Phosphatase and tensin homolog induced kinase-1
PlasDIC	Polarisation-optical transmitted light differential interference contrast

## R

RIPK	Serine/threonine protein kinase
RNS	Reactive nitrogen species
ROS	Reactive oxygen species

## S

SANBI	South African National Biodiversity Institute
SEM	Standard error of the mean
SOD	Superoxide dismutase
SRB	Sulforhodamine B

## T

tBID	Truncated BH3 only pro-apoptotic protein
TCA	Trichloroacetic acid
TPx	Thioredoxin reductase
TLC	Thin layer chromatography
TNF-α	Tumour necrosis factor-α
TNF-αR	Tumour necrosis factor-α receptor

**U**

U Units

UV Ultraviolet

**V**

VDAC Voltage-dependant anion channels

VMAT-2 Vesicle monoamine transporter 2

# Glossary

<b>Aerobic respiration:</b>	An oxygen requiring process for the production of energy in form adenosine tri-phosphate.
<b>Bradykinesia:</b>	Slowness of movement.
<b>Eukaryotes:</b>	Organisms with complex cellular structure, with the genetic material inside the nucleus.
<b>Deamination:</b>	A chemical reaction, where an amine group is removed from an amino acid.
<b>DNA methylation:</b>	The addition of methyl-groups to the nucleotides on the DNA molecule.
<b>DNase:</b>	An enzyme that fragment s DNA, by means of hydrolysis
<b>Endonuclease:</b>	An enzyme that fragments DNA by cleaving phosphodiester bonds.
<b>Endopeptidase:</b>	An enzyme that cleaves inner peptide bonds.
<b>Familial Parkinson's disease:</b>	Parkinson's disease as a result of genetic mutations carried from generation to generation.
<b>Fas ligand:</b>	A signalling molecule that triggers cell death upon binding to the death receptor.
<b>Fas recetor:</b>	A death receptor belonging to the family of the tumour necrosis factor- $\alpha$ .

<b>Glycoslation:</b>	An enzyme requiring reaction by adding sugar molecule to macromolecule such as a protein.
<b>Idiopathic Parkinson's disease:</b>	See Sporadic Parkinson's disease.
<b>Mendelian rules of inheritances:</b>	A set of rules which explains how genes are carried from parents to offspring
<b>Metallothioein:</b>	Low molecular weight protein containing thiol groups that can neutralise free radical.
<b>Morbidity:</b>	A diseases state.
<b>Nitrosylation:</b>	Chemical incorporation of nitric oxide to other molecules.
<b>Peroxinitrite:</b>	An unstable form of nitrate.
<b>Redox chaperone:</b>	A protein involved in the neutralisation of free radicals
<b>Senescence:</b>	A stage where cells cease to divide
<b>Sporadic Parkinson's disease:</b>	Parkinson's disease that results from definitive cause.
<b>Tumour necrosis factor-<math>\alpha</math>:</b>	A cell signalling molecule protein involved in inflammation and cell death

# Chapter 1: Introduction

Neurodegenerative diseases result in the functional loss of neurons and associated brain cells. The ultimate effect is irreversible brain damage with morbidity and mortality.<sup>1-3</sup> The incidence of neurodegenerative disease is thought to escalate parallel to the increase in the age of the population (65 years and older) due to cessation of cell proliferation and increased cell death.<sup>4</sup> Examples of neurodegenerative diseases include Parkinson's disease (PD), Alzheimer's disease, Huntington's disorder and Amyotrophic lateral sclerosis; all which increase morbidity and mortality.<sup>2,3</sup> Apart from increasing age, neurodegenerative diseases share some similarities, however the associated brain cells vary from disease to disease. Therefore depending on the aetiology and pathogenesis each disease will present with its own panel of symptoms.<sup>3</sup> The aetiologies of neurodegenerative disease are not fully understood, however, mitochondrial dysfunction, oxidative stress, and genetic mutations have been implicated in the pathology.<sup>3</sup> Neurodegenerative diseases remain incurable; as current treatment only relieves symptoms which with time becomes inadequate.<sup>3,5</sup>

## 1.1. Parkinson's disease

Parkinson's disease is the second most common neurodegenerative disease, affecting 1% of the population over the age of 60, with a lifetime risk of developing PD estimated at 1.5%.<sup>6,7</sup> The incidence of the disease increases steeply with age, and has a prevalence of 17.4 and 93 in 100 000 people between the age of 50-59 years and 70-79 years, respectively.<sup>8</sup> Aging plays a critical role in the progression of disease, and thus the increasing life expectancy observed in Western countries<sup>7</sup> has been suggested to increase the occurrence of the disease to one in every 800 people over the age of 65 years.<sup>8</sup>

Parkinson's disease is characterised by the loss of dopaminergic neurons in the substantia nigra pars compacta of the brain.<sup>9</sup> The primary function of dopaminergic neurons is to synthesise and release dopamine.<sup>6,9,10</sup> The loss of dopaminergic neurons results in dopamine deficiency or hypodopaminergic activity (Figure 1A-B).<sup>6,9,10</sup> Dopamine is synthesised from the amino acid L-tyrosine,<sup>11,12</sup> which undergoes hydroxylation by tyrosine hydroxylase to produce L-3,4-dihydroxyphenylalanine (L-dopa).<sup>13</sup> L-Dopa undergoes further decarboxylation by L-amino acid decarboxylase to form dopamine,<sup>13</sup> which is involved in the control of voluntary movements, moods, gastric function, memory and neuroendocrine

regulation.<sup>13,14</sup> Parkinson's disease patients present with severe motor complications, such as progressive rigidity, bradykinesia, postural instability and tremors.<sup>5,7,9</sup> Non-motor complications include autonomic disturbances (gastrointestinal, cardiac and respiratory) and neuropsychiatric dysfunction (depression, dementia, impulse control disorders and psychosis).<sup>5,15</sup> The combination of these motor and non-motor complications result in poor quality of life for PD patients.<sup>15</sup> Symptoms typically present at an 80% drop in dopamine levels and 60-70% loss of dopaminergic neurons.<sup>16,17</sup> Current treatment only offers symptomatic relief as the progressive loss of dopaminergic neurons remains irreversible.<sup>5,8,15</sup>

Parkinson's disease has long been associated with declined dopamine activity, however, recent evidence indicates concurrent disruption of other neurotransmitters such as acetylcholine, glutamate and serotonin.<sup>18,19</sup> For example loss of dopaminergic neurons is followed by excessive release of acetylcholine that is contributing to the functional motor deficits associated with PD.<sup>18</sup> Furthermore, low levels of serotonin have been detected in PD patients as compared to same age control groups. This has led to conclusions that reduced serotonin levels may contribute to PD-related depression.<sup>18,19</sup> Similar studies shown glutamate-mediated excitotoxicity subsequent to loss of dopaminergic neurons.

The pathological hallmarks of familial and sporadic PD are Lewy bodies, oxidative stress and neuro-inflammation.<sup>15,17,20</sup> Lewy bodies are pathological protein-containing inclusions inside neurons.<sup>20,21</sup> They have a diameter of 15  $\mu\text{m}$  and dense hyaline cores surrounded by a halo-like structure (Figure 1C).<sup>16,20</sup> The protein aggregates in Lewy bodies contain  $\alpha$ -synuclein, parkin, ubiquitin and neurofilaments.<sup>20</sup> The above mentioned neuroproteins are normally highly soluble but have the ability to form insoluble aggregates in PD patients.<sup>6,22</sup> Insoluble aggregates are formed by increased oxidative stress, misfolded proteins and posttranslational mutations such as glycosylation or nitrosylation.<sup>6,22</sup> Unaffected cells use the proteolytic process, ubiquitination, to clear damaged proteins; this system, is impaired in PD resulting in the accumulation of aggregates.<sup>6,20,22</sup>

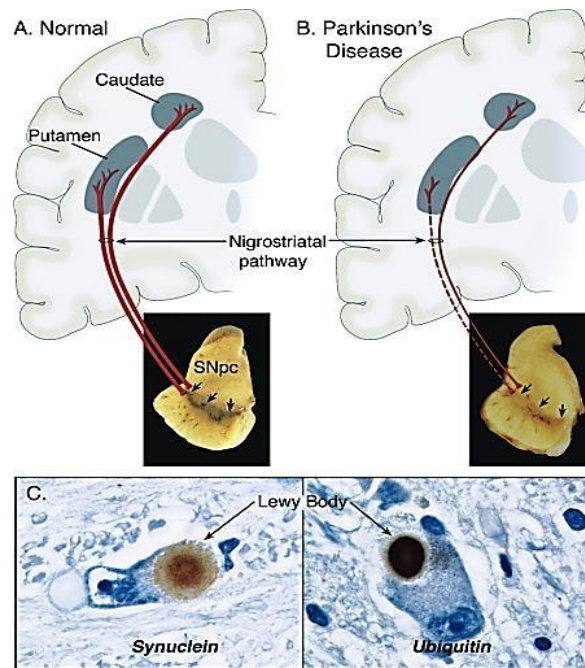


Figure 1: The nigrostriatal dopaminergic pathway in a (A) healthy patient and (B) PD patient. Immunohistochemical image (C) of Lewy bodies observed post-mortem. Lewy bodies have been shown to stain positive for  $\alpha$ -synuclein and ubiquitin aggregates. Reproduced with permission: Elsevier.<sup>16</sup>

## 1.2. Classification of Parkinson's disease

### 1.2.1. Familial Parkinson's disease

Familial PD accounts for 10-15% of PD cases and has been associated with early onset PD.<sup>6,23</sup> Five genes have been linked to an increased susceptibility to the familial form of PD.<sup>6</sup> These include  $\alpha$ -synuclein, leucine-rich repeat kinase 2 (LRRK-2), parkin, phosphatase and tensin homolog-induced kinase-1 (Pink-1) and DJ-1 genes.<sup>6,9</sup> Mutations of these genes are carried over from generation to generation following Mendelian rules of inheritance.<sup>9</sup> Advances in genetic research have found that mitochondrial genetic defects result in PD, highlighting the role of mitochondrial dysfunction in pathogenesis of this disease.<sup>3</sup>

#### 1.2.1.1. $\alpha$ -Synuclein

The  $\alpha$ -synuclein gene encodes  $\alpha$ -synuclein, a small protein found in the adult brain.<sup>24,25</sup> Normal functions of  $\alpha$ -synuclein include the regulation of vesicle dynamics at the presynaptic membrane, neuronal plasticity and learning.<sup>24,25</sup>  $\alpha$ -Synuclein aggregates have been found in Lewy bodies.<sup>6,16</sup>

#### **1.2.1.2. Leucine-rich repeat kinase 2**

The LRRK-2 gene encodes for a protein called dardarin.<sup>6,24</sup> At least one mutation in the gene is associated with the pathogenesis of PD.<sup>6,24</sup> The functions of dardarin are not well understood, however, LRRK-2 mRNA has been detected in dopamine-rich areas of the brain such as the nigrostriatal and mesolimbic dopaminergic pathway.<sup>24</sup>

#### **1.2.1.3. Parkin**

The parkin gene encodes the protein parkin.<sup>8,16,24</sup> The N-terminal of parkin has E3 ubiquitin ligase which is responsible for degrading misfolded or damaged proteins.<sup>7,16,26</sup> Failure to recognise these substrates results in accumulation of misfolded proteins and aggregates,<sup>26</sup> which is exacerbated by oxidative stress.<sup>16,24</sup> Gene mutations of parkin are responsible for at least 50% of the juvenile onset of PD,<sup>6,16</sup> and 77% of sporadic cases of PD with the onset age of 20 years.<sup>8,24</sup>

#### **1.2.1.4. Phosphatase and tensin homolog induced kinase-1**

Phosphatase and tensin homolog-induced kinase-1 (Pink-1) mutations are the second most common cause of familial PD after parkin.<sup>6</sup> Pink-1 protein is found in the mitochondrial membrane.<sup>6</sup> Pink-1 has poor solubility in the human brain, which increases its tendency to form aggregates, usually present in Lewy bodies and neurites.<sup>24</sup>

#### **1.2.1.5. DJ-1**

The DJ-1 protein is localised inside the mitochondria.<sup>24</sup> The DJ-1 protein functions as a redox chaperon that binds to free radicals when cells are under oxidative stress.<sup>6,24</sup> Extensive oxidation has been found to result in protein aggregation.<sup>6,24</sup>

### **1.2.2. Sporadic Parkinson's disease**

The majority of PD cases are idiopathic.<sup>6,20</sup> Aging still plays a major role in the development of the disease.<sup>3</sup> Factors such as mitochondrial dysfunction, neuroinflammation and oxidative stress have been implicated in the development and progression of sporadic PD.<sup>6,16</sup>

## **1.3. Neurochemical factors involved in Parkinson's disease**

### **1.3.1. Mitochondrial dysfunction**

Mitochondrial dysfunction has been implicated in many neurodegenerative diseases, including PD.<sup>3,7,11,27</sup> Mitochondria are cytoplasmic organelles that regulate intracellular calcium ( $\text{Ca}^{2+}$ ) levels, produce energy

in the form of adenosine tri-phosphate (ATP),<sup>11</sup> release pro-apoptotic mediators and maintain redox homeostasis.<sup>3,27</sup> Structurally, the mitochondrion has an outer membrane which is porous and permeant to small molecules.<sup>3,27</sup> The inner membrane provides a barrier to ionic flow and houses the electron transport chain (ETC).<sup>3,27</sup> The inner membrane is filled with the mitochondrial matrix which contains enzymes and substrates required for the tricarboxylic acid cycle and  $\beta$ -oxidation.<sup>3,28</sup> Mitochondrial functioning is controlled by both nuclear and mitochondrial DNA.<sup>27</sup> Mitochondrial DNA encodes ETC proteins, while all other proteins are encoded by nuclear DNA.<sup>3,11,27</sup>

Mitochondria produce ATP, an intracellular energy molecule, through the ETC (Figure 2).<sup>3,11</sup> The by-products of the Krebs' cycle, reduced nicotinamide adenine dinucleotide (NADH) and reduced flavin adenine dinucleotide (FADH<sub>2</sub>) donate electrons to the ETC to produce a mitochondrial membrane potential (MMP) (Figure 2).<sup>23</sup> The MMP drives the phosphorylation of ADP through the action of ATP synthase.<sup>3,23,27</sup> During electron transport, mitochondrial complex I and complex III leak electrons to oxygen (O<sub>2</sub>), producing superoxide radicals (O<sub>2</sub><sup>•</sup>).<sup>3,11,27</sup> The O<sub>2</sub><sup>•</sup> is highly reactive and generates hydroxyl ions (OH<sup>-</sup>) and hydrogen peroxide (H<sub>2</sub>O<sub>2</sub>) through enzymatic conversion by manganese superoxide dismutase (MnSOD).<sup>3,11,27</sup> Additionally, O<sub>2</sub><sup>•</sup> is produced through the tricarboxylic acid cycle.<sup>3</sup>

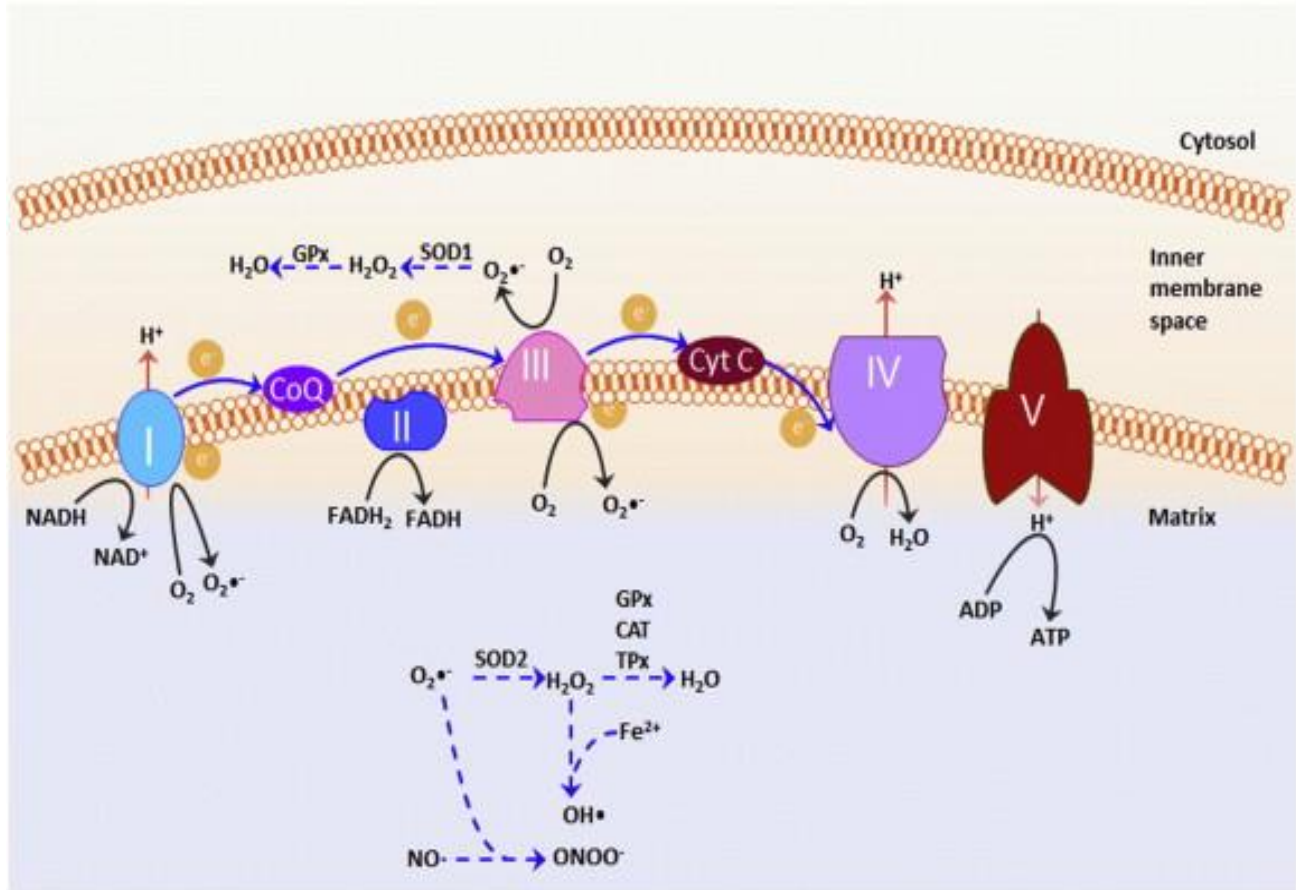


Figure 2: The mitochondrial electron transport chain. Adenosine tri-phosphate is produced and reactive oxygen species are generated in the process. Reproduced with permission: Elsevier.<sup>29</sup> ADP - adenosine di-phosphate, ATP - adenosine tri-phosphate, I/ II/ III/ IV/ V - mitochondrial complexes, CAT - catalase, e<sup>-</sup> - electrons, FADH<sup>-</sup> - Flavin adenine dinucleotide semiquinone, FADH<sub>2</sub> - Flavin adenine dinucleotide hydroquinone, Fe<sup>2+</sup> - Ferrous ion, GPx - glutathione peroxidase, H<sub>2</sub>O<sub>2</sub> - hydrogen peroxide, H<sup>+</sup> - hydrogen ion, H<sub>2</sub>O - water, NADPH - reduced NAD<sup>+</sup>, NAD<sup>+</sup> - Nicotinamide adenine dinucleotide, NO<sup>-</sup> - nitric oxide radical, O<sub>2</sub><sup>•-</sup> - superoxide, O<sub>2</sub> - oxygen, OH<sup>•</sup>/ OH<sup>-</sup> - hydroxyl ion, ONOO<sup>-</sup> - peroxynitrite, TPx - thioredoxin reductase, ROS - reactive oxygen species, SOD1/ SOD - superoxide dismutase, SOD2/MnSOD- manganese superoxide dismutase.

It has been observed that mitochondrial complex I (NADH dehydrogenase) is blocked in the brains of PD patients.<sup>6</sup> Mitochondrial complex I inhibitors, such as 6-hydroxydopamine (6-OHDA), 1-1-methyl-4-phenylpyridinium (MPP<sup>+</sup>) and rotenone, have been shown to induce PD like effects both *in vitro* and *in vivo*.<sup>30</sup> The inhibition of mitochondrial complex I hinders ETC functionality, which impairs ATP synthesis and subsequently increases free radicals production.<sup>20,22</sup> In humans, accidental administration and drug abuse of mitochondrial complex I inhibitors has been linked to early-onset PD.<sup>16,23</sup>

Free radicals are capable of impairing the Krebs' cycle, especially enzymes such as  $\alpha$ -ketoglutarate dehydrogenase, succinate dehydrogenase and isocitrate dehydrogenase. Processes such as these further reduce ATP output.<sup>23</sup> Furthermore, free radicals are transported to the cytosol through voltage-dependant anion channels (VDAC),<sup>3</sup> where they interact with mitochondrial DNA and proteins.<sup>27</sup> Mitochondrial DNA is susceptible to oxidation by free radicals because of its close association with sites of oxidation.<sup>3</sup> Oxidation reduces ATP and impairs ATP-dependent cytoprotective pathways, thus triggering cell death.<sup>23</sup>

Mitochondrial dysfunction impairs not only ATP biosynthesis but also allows for the dysregulation of intracellular  $\text{Ca}^{2+}$ .<sup>23</sup> In eukaryotes, intracellular  $\text{Ca}^{2+}$  levels are carefully controlled by interactions with pumps, channels and exchangers because of their low cell membrane permeability.<sup>31</sup> Calcium levels may be increased by two mechanisms. Firstly, by entry from the extracellular space through transporters, channels and pumps.<sup>31</sup> Alternatively, it may be released from intracellular  $\text{Ca}^{2+}$  stores, such as the endoplasmic reticulum and Golgi-apparatus.<sup>31</sup> Once in the cell,  $\text{Ca}^{2+}$  moves along the concentration gradient into the inner mitochondrial membrane. Together with hydrogen ions ( $\text{H}^+$ ),  $\text{Ca}^{2+}$  generates the MMP.<sup>31</sup>

In neurons,  $\text{Ca}^{2+}$  assists with cell signalling, such as the induction of apoptosis and neurotransmission.<sup>28</sup> Calcium homeostasis is an energy-dependent process using approximately 80% of the ATP produced.<sup>28</sup> To compensate for this the cell will stimulate the mitochondria to take up cytosolic  $\text{Ca}^{2+}$ , in turn activating ATP synthase,  $\alpha$ -ketoglutarate dehydrogenase and other enzymes involved in cellular ATP production.<sup>28, 32</sup> Calcium overload observed in PD, which is due to impaired ATP production, may trigger  $\text{Ca}^{2+}$ -induced opening of the mitochondrial permeability transition (MPT) pore and trigger cell death.<sup>11,33</sup>

### 1.3.2. Oxidative stress

Oxidative stress refers to a cellular state where free radical generation exceeds the removal thereof, thus an imbalance in redox homeostasis occurs.<sup>11,34</sup> Reactive oxygen species (ROS) and reactive nitrogen species (RNS) are collectively known as free radicals. These are molecules which possess an unpaired electron(s) in their orbital.<sup>11</sup> Normally, free radicals function as signalling molecules during neurotransmission and in the immune system, however, when in excess they may result in significant alterations to biological pathways.<sup>23</sup>

Post-mortem analysis of PD patient brains indicate increased levels of free radicals and iron, as well as low levels of reduced glutathione (GSH).<sup>6</sup> Metabolically-active organelles, such as the mitochondria, are

the primary source of free radicals.<sup>11</sup> Mitochondria undergo aerobic respiration, an oxygen-dependent process which produces ATP.<sup>11,23</sup> During aerobic respiration, oxygen is reduced to water and H<sub>2</sub>O<sub>2</sub>, however, premature leakage of electrons from the ETC may produce O<sub>2</sub><sup>•-</sup> and OH<sup>-</sup>.<sup>11,23</sup>

Inflammation also results in ROS as a defensive mechanism to combat pathogens.<sup>23</sup> Nitric oxide, a radical containing one unpaired electron, is normally produced as result of nitric oxide synthase activity.<sup>11</sup> Nitric oxide is a vasodilator and immunoregulator, however, excessive production of nitric oxide may generate more free radicals.<sup>11,23</sup> For example, nitric oxide reacts with O<sub>2</sub><sup>•-</sup> to form peroxynitrite (ONOO<sup>-</sup>), which may further be converted to nitrogen dioxide and OH<sup>-</sup> radicals.<sup>11,23</sup> Subsequently, these free radicals will attack DNA to alter expression profiles.<sup>3,6</sup> Modification of polyunsaturated fatty acids produce peroxy radicals, thus altering the structure of membranes, leading to impaired membrane permeability.<sup>11</sup>

Redox homeostasis is maintained by the activity of endogenous and exogenous antioxidants,<sup>11</sup> which are substances capable of removing and detoxifying free radicals.<sup>34</sup> Endogenous antioxidant enzymes include superoxide dismutase (SOD) (neutralises O<sub>2</sub><sup>•-</sup> to H<sub>2</sub>O<sub>2</sub>) and catalase (CAT) (H<sub>2</sub>O<sub>2</sub> converted to water and oxygen).<sup>23</sup>

The brain is susceptible to oxidative damage due to high rates of oxygen metabolism, high levels of polyunsaturated fatty acids and iron (ferritin) content, and lower antioxidant concentrations (that further decreases with age).<sup>10, 19, 24</sup> It has been demonstrated that the substantia nigra has the lowest GSH content, which is problematic due to high levels of dopamine metabolism taking place in this region, with subsequent ROS production.<sup>10,12</sup>

Reduced glutathione is the universal antioxidant found in mammalian cells which is oxidised by free radicals to oxidised glutathione disulphide (GSSG).<sup>12,34,35</sup> Reduced glutathione not only neutralises free radicals, but is also responsible for reducing thiol-groups on proteins, acting as a co-factor for isomerization reactions, transport and storage of the amino acid cysteine, as well as detoxification of xenobiotics during phase II metabolism (Figure 3).<sup>35</sup>

*De novo* synthesis of GSH is an energy-dependent reaction between glutamate and cysteine.<sup>12,35</sup>  $\gamma$ -Glutamylcysteine synthase (GCS) catalyses the reaction between glutamate and cysteine to form  $\gamma$ -glutamylcysteine.<sup>12</sup> The amino acid glycine is enzymatically bound to  $\gamma$ -glutamylcysteine to form GSH by GSH synthase.<sup>12,35</sup> Reduced glutathione may also be recycled through reduction of GSSG by GSH reductase.<sup>12,34-36</sup>

The severity of PD has been linked to GSH depletion,<sup>34</sup> indicating that GSH may be critical in the initial steps prior to mitochondrial dysfunction.<sup>35</sup> Oxidative stress becomes more problematic in individuals with impaired antioxidant capacity, such as the elderly population.<sup>3,6</sup>

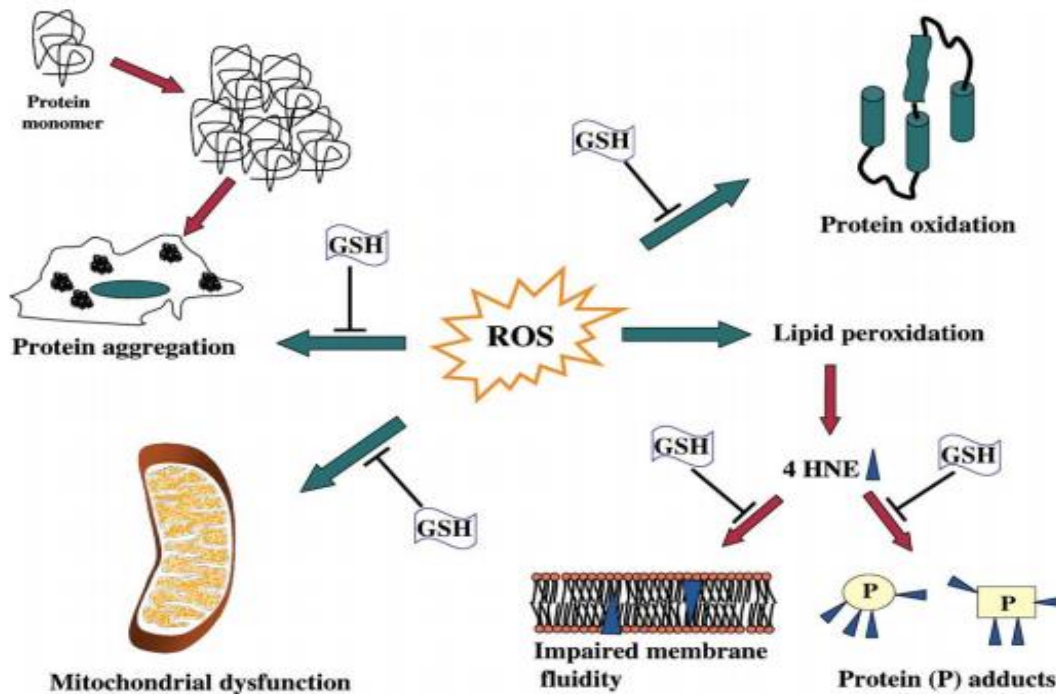


Figure 3: Functions of reduced glutathione in a brain. Reduced glutathione blocks oxidation of macromolecules (protein, lipids, DNA) and oxidative stress induced mitochondrial dysfunction. Reproduced with permission: Elsevier.<sup>12</sup> 4-HNE - 4-hydroxynonenal, GSH - reduced glutathione, ROS - reactive oxygen species.

Dopamine and the precursor molecule, L-dopa, auto-oxidise to produce neuromelanin and dopamine quinone (DAQ).<sup>11,13,14</sup> Neuromelanin is a black-brown molecule found in dopaminergic and noradrenergic neurons, and is generally neuroprotective.<sup>13,14</sup> It has a high affinity for ferric ion ( $Fe^{3+}$ ), though when bound to excess  $Fe^{3+}$  it becomes a pro-oxidant and reduces  $Fe^{3+}$  to ferrous ion ( $Fe^{2+}$ ).<sup>12</sup> Ferrous ion is released due to its low affinity for neuromelanin,<sup>12</sup> and promotes formation of neuromelanin by further generating more ROS.<sup>13,37</sup> Furthermore,  $Fe^{2+}$  alters mitochondrial  $Ca^{2+}$  homeostasis which in turn triggers apoptosis through the opening of the MPT pore.<sup>11,36,37</sup> Deamination of dopamine during catabolism by monoamine oxidase-B (MAO-B) forms 3,4-dihydroxyphenylacetic acid (DOPAC),  $O_2^{\bullet-}$ , and  $OH^{\bullet}$  radicals in the presence of iron, which further facilitates oxidation reactions.<sup>6,11,26</sup>

Nitric oxide may react with dopamine to form nitrisotoxic-conjugates.<sup>14</sup> Since a considerable amount of ROS is produced through dopamine metabolism and oxidation, it is therefore a likely explanation for the susceptibility of dopaminergic neurons to ROS-mediated toxicity seen in PD.<sup>13</sup>

### **1.3.3. Aging**

The post-reproductive phase, commonly known as ‘aging’, has been implicated in the development of many neurodegenerative diseases.<sup>3</sup> The basic definition of aging is a gradual growth process leading to maturation.<sup>3</sup> Biochemically, aging is defined as the accumulation of molecular, cellular and organ damage leading to loss of function, and increased risk of morbidity and mortality.<sup>3</sup> The biochemical pathways involved in the aging process include mitochondrial abnormalities, prolonged oxidative stress, shortening of telomeres, and DNA methylation.<sup>3</sup> Taking the latter into consideration, it has been hypothesized that oxidants produced by mitochondria cause damage to mitochondrial DNA and biomolecules resulting in gradual senescence.<sup>3</sup> Accumulation of mitochondrial mutations, increased production of ROS and RNS, reduction in mitochondrial respiration, low ATP production, and decreased antioxidant status has been found to occur in the brains of elderly people, making this population more susceptible to PD and other neurodegenerative diseases.<sup>3,4</sup>

### **1.3.4. Cell death**

In PD, perturbations in mitochondrial function and subsequent ROS generation results in cell death of dopaminergic neuron in the substantia nigra.<sup>6,9</sup> Cell death is a broad term that covers, among others, apoptosis, necrosis, necroptosis and autophagy.<sup>38</sup> The most well characterised mode of cell death is apoptosis.

#### **1.3.4.1. Apoptosis**

Apoptosis refers to a programmed cell death that is energy-dependent and required for normal development in mammals. However, it may be altered by diseases such as cancer and neurodegenerative diseases.<sup>38,39</sup> Apoptosis is highly controlled by Bcl-2 family of proteins; these proteins are divided into pro-apoptotic and anti-apoptotic proteins.<sup>39,40</sup> Pro-apoptotic Bcl-2 family proteins stimulate the induction of apoptosis; examples include Bcl-10, Bax, Bak, Bid, Bad, Bik and Blk.<sup>39,41</sup> Anti-apoptotic proteins of the Bcl-2 family of proteins include Bcl-2, Bcl-X, Bcl-XL, Bcl-w and bag.<sup>39,41</sup> Furthermore, apoptosis may follow an intrinsic or extrinsic pathway depending on the cell death signal’s origin, which may often occur in conjunction.<sup>39</sup>

The extrinsic pathway is initiated by activation of transmembrane receptor-mediated interactions, such as binding of tumour necrosis factor- $\alpha$  (TNF- $\alpha$ ) to the TNF- $\alpha$  receptor (TNF- $\alpha$ R), or binding of Fas ligand to the Fas receptor (FasR).<sup>39,42</sup> The death-receptor complex combines with adapter proteins which stimulates cleavage of pro-caspase-8 to caspase-8.<sup>39,42</sup> Caspases are a family of endopeptidases that hydrolyse peptide bonds.<sup>42</sup> Caspase-8 can directly cleave and activate executioner caspase-3, -6 and -7 which commits the cell to die (Figure 4).<sup>39,42</sup> Furthermore, caspase-8 indirectly activates the pro-apoptotic protein, Bid, which in turn stimulates release of mitochondrial cytochrome c.<sup>42 39</sup>

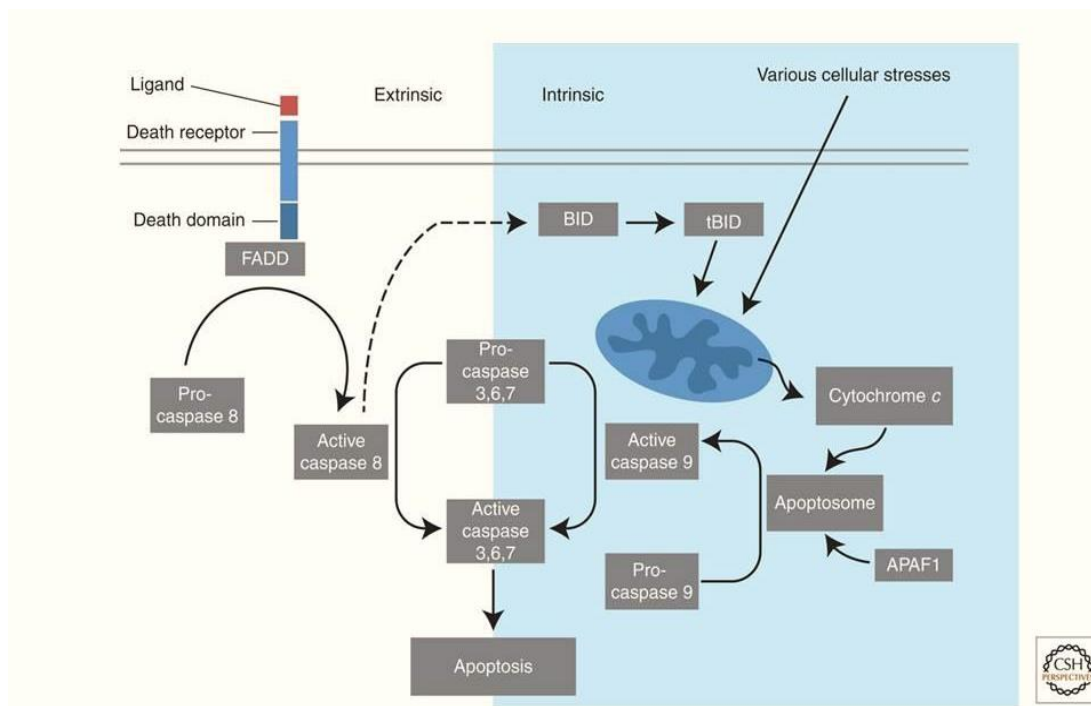


Figure 4: The extrinsic and intrinsic apoptotic pathway. Reproduced with permission: Cold Spring Harbor Laboratory press.<sup>40</sup> Apaf-1 - apoptotic protease- activating factor-1, BID - BH3 only pro-apoptotic protein, tBID - truncated form of Bid, FADD - Fas-associated death domain.

The intrinsic pathway doesn't require transmembrane receptor interactions. The stimuli often come from within the cell, such as increased ROS generation, reduced GSH and exposure to toxins (Figure 4).<sup>41</sup> These detriments impair inner mitochondrial membrane permeability, which results in a drop of MMP and subsequent opening of the MPT pore.<sup>39</sup> Once the MPT pore is open, cytochrome c leaks out and forms an apoptosome by combining with apoptotic protease activating factor (Apaf-1) and caspase-9,

which is an energy-dependent process.<sup>39</sup> The apoptosome recruits executioner caspases and additional apoptotic factors such as endonuclease G, caspase-activated DNase and apoptosis-inducing factor (AIF) to induce apoptosis (Figure 4).<sup>39</sup>

#### **1.3.4.2. Necrosis**

Necrosis is an uncontrolled energy-independent mode of cell death.<sup>39</sup> The two main stimuli for necrosis are i) disruption of intracellular ATP levels, and ii) direct alteration of the plasma membrane.<sup>39</sup> The latter cause osmotic imbalances, swelling and eventually cell rupture.<sup>39</sup> This effect releases cytoplasmic contents to the interstitial fluid, inducing local inflammation.<sup>39,43</sup> Hence, inflammation remains a marker for necrotic cell death rather than apoptosis.<sup>39</sup>

Recently, a more controlled form of necrosis that may occur has been described, as necroptosis.<sup>38,44</sup> Necroptosis shares morphological features with necrosis, however, some biochemical pathways may overlap with apoptosis.<sup>40,45</sup> For example, when apoptotic signalling is hindered, TNF- $\alpha$  and cytokines may trigger necroptosis.<sup>37,43</sup> In this way, activation of death receptors (TNF- $\alpha$ R and FasR) results in an interaction with serine/threonine protein kinase (RIPK)-1 and -3 to form a necrosome.<sup>38,46</sup> The necrosome is then translocated to the mitochondria where it induces cyclophilin D-dependent opening of the MPT-pore, inducing osmotic imbalances that impair ATP production.<sup>38,46</sup> Additionally, the necrosome activates mixed-lineage kinase domain-like (MLKL) protein, which causes disruptions of the plasma membrane and subsequent leakage of intracellular contents.<sup>38,46</sup> Local inflammation has been detected in the brains of PD patients at post-mortem,<sup>6,16</sup> suggesting that the mode of neuronal cell death may be necrosis or necroptosis.

#### **1.3.4.3. Autophagy**

Autophagic cell death is a lysosome-dependent process that degrades the cell and its contents.<sup>38,39</sup> Autophagy is induced by prolonged starvation, which causes the plasma membrane to engulf cellular contents to form a vesicle like autophagosome.<sup>38,39</sup> The autophagosome is able to fuse with a lysosome or vacuole which degrades cellular material.<sup>38</sup>

Cellular degradation is dependent on continuous protein synthesis and ATP supply.<sup>38</sup> The degraded material will then be recycled, this therefore brings about the controversy of whether autophagy is a mode of cell death or survival mechanism under stressful conditions.<sup>38</sup> Furthermore, autophagy is mediated by Beclin-1 and autophagy related protein (ATG 5), which are upregulated by inhibition of pro-apoptotic proteins Bax, Bak or caspase-8.<sup>38</sup>

#### **1.3.4.4. Caspase-independent cell death (CICD)**

The mitochondria is the main key player in caspase-independent cell death (CICD).<sup>38</sup> The MPT pore has been described as a 'megachannel', serving as a releaser apoptotic factors.<sup>33</sup> The pore is thought to consist of VDAC, adenine nucleotide translocase (ANT), cyclophilin D and the mitochondrial benzodiazepine receptor.<sup>33,47</sup> The mechanism of MPT pore opening is not completely understood, however, several models have been postulated.<sup>33</sup>

##### **1.3.4.4.1. The induced swelling model**

When the caspase pathway is blocked, AIF or  $Ca^{2+}$  overload<sup>40</sup> can directly open the MPT pore, resulting in osmotic imbalances, dissipation of the MMP and release of cytochrome c into the cytosol thus the intrinsic apoptotic pathway is initiated.<sup>33</sup>

##### **1.3.4.4.2. The non-swelling model**

The pro-apoptotic factors Bax and Bid can induce the release of cytochrome c by direct action on the mitochondria.<sup>33</sup> In this model there is dissipation of the MMP, but no swelling is observed.<sup>33</sup>

##### **1.3.4.4.3. The formation of conducting pore**

Pro-apoptotic proteins, such as Bax or Bid, can oligomerise with other Bax proteins or VDAC to create non-selective channels that allows for cytochrome c leakage out of the mitochondrion.<sup>33</sup>

##### **1.3.4.4.4. VDAC closure model**

During the VDAC closure model, the VDAC channel is closed, and is followed by hyperpolarisation of the mitochondrial membrane with subsequent disruption of ATP production and swelling of the mitochondria. Prolonged swelling causes rupture of the mitochondria and leakage of its contents into the cytoplasm.<sup>33</sup>

## **1.4. Experimental models of Parkinson's disease**

Several *in vitro* and *in vivo* models of PD exist that rely on exposure to toxins that simulate similar characteristics. There are four well-established PD models, namely the 6-OHDA, MPP<sup>+</sup>, paraquat and rotenone models.<sup>14,16</sup> 6-Hydroxydopamine and MPP<sup>+</sup> were selected based on literature as potential models for this *in vitro* study.

### 1.4.1. 6-Hydroxydopamine

6-Hydroxydopamine is a common neurotoxin used to study PD *in vitro* and *in vivo*.<sup>45,48,49</sup> 6-Hydroxydopamine may be naturally produced in the human body as a by-product of dopamine oxidation.<sup>4,45,48</sup> It shares structural similarities with dopamine and noradrenaline (Figure 5); hence it has high affinity to bind to the dopamine transporter (DAT).<sup>14,48</sup> 6-Hydroxydopamine-induced *in vitro* neurotoxicity is characterised by increased free radical production and mitochondrial dysfunction.<sup>48</sup> Once in the cytoplasm 6-OHDA accumulates and undergoes a non-catalysed auto-oxidation process to form  $O_2^{\bullet-}$ ,  $H_2O_2$  and quinones.<sup>14,16,48</sup>

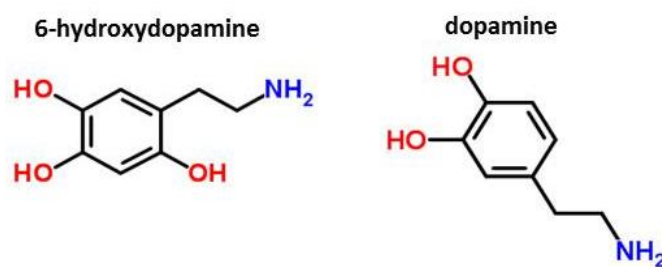


Figure 5: Structural similarity of 6-hydroxydopamine and dopamine.

6-Hydroxydopamine interferes with the ETC and redox capacity of the cell by blocking mitochondrial complex I.<sup>14,45,48</sup> This leads to reduced ATP production and increased ROS generation, ultimately producing mitochondrial dysfunction.<sup>14</sup> Additional ROS, in the form of  $H_2O_2$  may arise from deamination of 6-OHDA by MAO-B.<sup>14</sup> *In vivo*, 6-OHDA may be converted to neuromelanin which displaces  $Fe^{2+}$  from the ferritin- $Fe^{3+}$  complex.<sup>14,45</sup> Displaced  $Fe^{2+}$  together with  $H_2O_2$  oxidises dopamine to 6-OHDA and other radicals.<sup>14</sup> Intracellular ROS oxidise macromolecules and alters their function leading to cell death.<sup>3,45,48</sup> Mitochondrial defects induced by 6-OHDA stimulate the opening of the MPT pore to release pro-apoptotic factors to induce cell death.<sup>11,28,45</sup> The burden of oxidative stress reduces the cell's antioxidant capabilities and impairs redox regulation.<sup>14,45</sup>

### 1.4.2. 1-Methyl-4-phenylpyridinium (MPP<sup>+</sup>)

In 1982, a high frequency of young drug users presented with rapidly-developing parkinsonism.<sup>14,16</sup> Research into these cases was traced back to the recreational drug 1-methyl-4-propion-oxypiperidine (MPPP), a structural analogue of the narcotic meperidine.<sup>16</sup> The major contaminant in the production of MPPP is 1-methyl-4-phenyl-1,2,3,6-tetrahydropyridine (MPTP), which was mainly found to be

responsible for the early-onset parkinsonism that was seen.<sup>16</sup> Both *in vitro* and *in vivo* MPTP exposure simulates PD characteristics.<sup>9,14</sup>

Due to its lipophilicity, MPTP passively diffuses across the plasma membrane and blood-brain barrier within minutes after administration (Figure 6).<sup>14,16</sup> The pro-toxin is converted to 1-methyl-4-phenyl-2,3-dihydropyridinium (MPDP<sup>+</sup>) by MAO,<sup>16</sup> which undergoes spontaneous oxidation to MPP<sup>+</sup>.<sup>16</sup> 1-Methyl-4-phenylpyridinium is an ionic molecule that has affinity for DAT,<sup>6,9</sup> as well as other noradrenaline/serotonergic transporters that allows it to enter cells.<sup>14,16</sup> Intracellular MPP<sup>+</sup> may accumulate in the cell by three mechanisms: i) complexation with neuromelanin and other negatively charged enzymes, ii) sequestration in synaptosomal vesicle after incorporation by vesicle monoamine transporter-2 (VMAT-2)<sup>14,16</sup> and iii) energy-dependent transport into the mitochondria. These processes delay cytoplasmic MPP<sup>+</sup> release.<sup>9,14,16</sup>

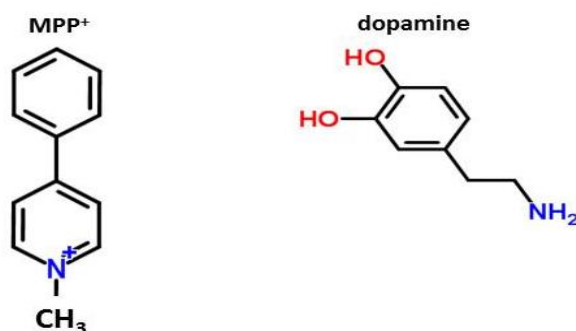


Figure 6: Structural similarity of 1-methyl-4-phenylpyridinium and dopamine.

1-Methyl-4-phenylpyridinium blocks mitochondrial complex I and  $\alpha$ -ketoglutarate dehydrogenase, which results in decreased ATP production (Figure 7).<sup>30</sup> Mitochondrial complex I blockage prevents reduction of nicotinamide adenine dinucleotide (NAD<sup>+</sup>), which maintains the redox state during ATP production.<sup>3,9</sup> This activates Ca<sup>2+</sup>-dependent nitric oxidase synthase that subsequently leads to the formation of peroxynitrite.<sup>14,16</sup> 1-Methyl-4-phenylpyridinium increases intracellular ROS by lowering GSH and metallothionein.<sup>14</sup> Ultimately, all these biochemical changes trigger both mitochondrial-dependent and independent cell death.<sup>14</sup>

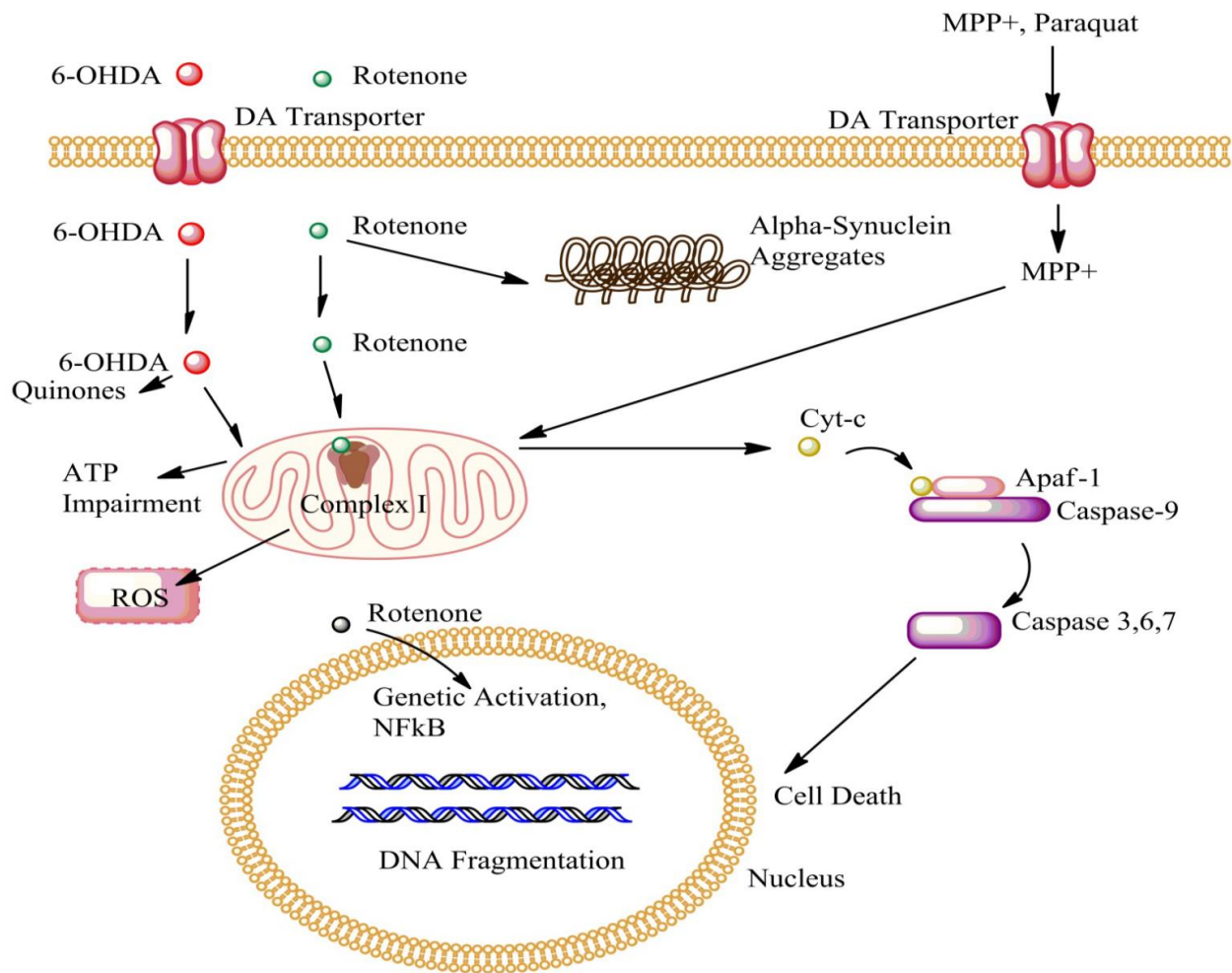


Figure 7: There are four well-established PD models, namely the 6-OHDA, MPP<sup>+</sup>, paraquat and rotenone models. Paraquat, 6-OHDA and MPP<sup>+</sup> are transported into the cell by the dopamine transporter, and once in the cytoplasm may induce oxidative stress and altered ATP synthesis, resulting in cell death. Rotenone is cell membrane-permeable, and also blocks mitochondrial complex I, forms  $\alpha$ -synuclein aggregates and it is also able to cross the nuclear membrane to influence gene transcription. Reproduced with permission.<sup>30</sup> ATP - adenosine tri-phosphate, Cyt-c – cytochrome c, DA - dopamine, DNA - deoxyribonucleic acid, ROS –reactive oxygen species.

### 1.4.3 Human neuroblastoma cells

The human neuroblastoma cells are an accepted *in vitro* model for studying Parkinson's disease using various neurotoxins.<sup>48</sup> These exponentially growing cells are catecholaminergic neuronal cells expressing, amongst others, dopamine receptors, dopamine transporters (DAT) and to some extent VMAT-2 which facilitates dopamine storage.<sup>48,50</sup> Furthermore, these cells express the DJ-1 protein,

associated with familial PD.<sup>48</sup> This indicates that there is some degree of homology between SH-SY5Y cells and dopaminergic neurons of the substantia nigra.<sup>48,50</sup> The latter makes them a candidate for PD modelling for primary drug screening assays. However, SH-SY5Y cells are cancer cells with proliferative potential, which is contradictory to dopaminergic neurons which are not mitogenic.

Apart from *in vitro* models, several *in vivo* models may be rodents (rats, mice) treated with neurotoxins (6-OHDA, MPP<sup>+</sup>) have long been used to study the complex pathogenesis of PD. However, the use of these animal models does not directly mimic what happens in the human body as the organisation of nervous system may differ.<sup>16</sup> For example, some motor deficits induced in rodents could not be paralleled to the motor effects present in PD patients.<sup>16</sup> Researchers agree that present PD models (*in vitro* and *in vivo*) only mimic a few aspects of the disease, hence it was suggested that non-humans primates could be the answer.<sup>16</sup> But the use of such animals is still hindered by expensive running costs and ethical considerations. With the above being said SH-SY5Y cells remain a cost-effective model for primary drug screening assay in PD.

## 1.5. Treatment of Parkinson's disease

### 1.5.1. Conventional treatment

Presently there is no cure for PD; however, symptomatic relief is available.<sup>5,8</sup> Symptomatic treatment focuses on increasing dopaminergic activity in the brain by increasing dopamine synthesis, inhibiting dopamine metabolism or stimulating dopamine receptors through mimetic activity.<sup>51</sup> Current treatment is focused on dopamine replacement strategies, which increases dopamine centrally.<sup>5,52</sup> Dopamine replacement therapy offers symptomatic relief with no effect on neuronal cell loss, therefore it does not offer sustained or curative benefits.<sup>5,18</sup> Furthermore, treatment is not beneficial to the non-motor effects mentioned earlier.<sup>5</sup> The dopamine replacement strategy is focused on restoring dopaminergic activity and balancing of dopaminergic and cholinergic inputs (Table 1).<sup>5,18,53</sup>

Table 1: Conventional treatment of PD

Class	Mechanism of action	Example	Side effects
Dopamine precursor	Precursor for dopamine synthesis <sup>5</sup>	L-dopa	Nausea, motor complications, confusion <sup>5,54,55</sup>
Decarboxylase inhibitors	Blocks peripheral metabolism of dopamine <sup>5,52</sup>	Carbidopa	Anorexia, visual and auditory hallucinations <sup>52</sup>
D <sub>2</sub> -receptor agonists	Mimics the action of dopamine at the D <sub>2</sub> -receptor <sup>5</sup>	Bromocriptine, Rotigotine, Apomorphine	Postural hypotension, impulse control disorders <sup>5,18,55</sup>
Selective MAO inhibitors	Blocks the metabolism of dopamine <sup>5</sup>	Selegine, Safinamide	Hypertension, insomnia <sup>52</sup>
Catechol-O-methyl transferase (COMT) inhibitors	Blocks peripheral degradation of L-dopa <sup>5</sup> Interferes with central dopamine metabolism <sup>18,54</sup>	Entacapone, Tolecapone	Nausea, dark coloured urine, dyskinesia <sup>18,54</sup>
Anticholinergics	Blocks excess acetylcholine associated with dyskinesia <sup>52</sup>	Benzotropine, Trihexyphenidyl	Blurred vision, cognitive impairment <sup>5,18,54</sup>
Adenosine A <sub>2A</sub> antagonist	Blockade of A <sub>2A</sub> -receptor enhances the activity of the D <sub>2</sub> -receptors <sup>5</sup>	Istadeffylline, Preladenant,	Undergoing clinical trials <sup>5,18</sup>
Other	Modulates the release of neurotransmitters <sup>5</sup>	Amantadine	Constipation, hallucination, confusions <sup>5,18,54</sup>

L-Dopa is considered the first-line treatment option for PD, however, as the disease progresses the efficacy is reduced.<sup>5,15,56</sup> L-Dopa is transported into the brain, where it is subsequently metabolised to dopamine.<sup>5,15,56</sup> It is used in combination with peripheral dopamine decarboxylase inhibitors (such as carbidopa), which prevent peripheral conversion of L-dopa to dopamine, thus increasing its bioavailability in the brain.<sup>5,52</sup> Dopamine decarboxylase inhibitors in combination with L-dopa not only bolster the increase in dopamine in the brain but also limit peripheral dopaminergic effects. Major side effects of prolonged L-dopa treatment include dyskinesia and 'wearing off' effects, which necessitates the introduction of other drug classes.<sup>18,52,56</sup> Studies report that more than 80% of patients who are on continuous L-dopa treatment develop dyskinesia within the first 10 years of treatment.<sup>15</sup> Furthermore, dyskinesia is also observed in nearly 100% of patients with early onset PD on L-dopa treatment,<sup>15</sup> indicative that younger populations are more susceptible to developing L-dopa-induced motor complications.<sup>55</sup> The National Institute for Health and Clinical Excellence (NICE) advises clinicians to use

a MAO inhibitor together with L-dopa as first line treatment in the mild form of the disease.<sup>55</sup> Furthermore, clinicians are advised to use a L-dopa, carbidopa, MAO inhibitor and/or COMT inhibitor in a single formulation (such as Stavelo consisting of L-dopa, carbidopa and safinamide) to avoid the number of tablets and help improve compliance.<sup>18,55</sup> Pharmacological intervention of PD remains complex and as the disease progresses the treatment becomes ineffective in controlling motor fluctuation and dyskinesia.<sup>5</sup>

Recently the Food and Drug Administration has approved deep brain stimulation as alternative non-pharmacological treatment for PD.<sup>15</sup> Deep brain stimulation sends electric signals to specific regions in the brain in order to modulate neural function.<sup>15</sup> So far deep brain stimulation has proven to be efficacious in relieving tremors, dystonia and obsessive compulsive disorder associated with PD.<sup>15</sup> However, the use of deep brain stimulation has variety of neuropsychological adverse effects which are limiting use.<sup>15</sup> Other non-pharmacological treatments include stem cell and gene therapy which are currently experimental.<sup>15,18</sup>

Researchers suggest that a combination of dopamine replacement therapy together with neuroprotection could slow the progression of the disease.<sup>18,57</sup> As PD remains an incurable disease, much research has been invested on producing more effective treatment strategies or discovery of efficacious chemical entities with less adverse effects. One such avenue of research involves that of herbal remedies.

### **1.5.2. Herbal remedies**

Medicinal plants have been used for millennia to treat various diseases.<sup>58</sup> It is estimated that approximately 27 million South Africans use herbal remedies for basic health care needs.<sup>59</sup> Various reasons exist why patients rely on herbal remedies, ranging from desperation to treat or cure chronic diseases, lack of available medical facilities, affordability to easy accessibility.<sup>59</sup>

Plants constitute a vast source of potential therapeutic drugs due to the presence of a diverse range of chemical entities that may possess bioactivity.<sup>58,60</sup> Cocaine, morphine, aspirin, digitoxin and quinines are medications which originated from plants and are in clinical use today.<sup>58,60</sup> Some herbals have displayed similar activity to that of conventional anti-Parkinson's disease drugs. Extracts from *Ruta graveolens* commonly known as herb-of-grace display MAO inhibitory effects, thus potentially inhibiting dopamine

metabolism and subsequently reducing oxidative stress.<sup>61</sup> Polyphenols from *Zingiber officinale*, commonly known as ginger, have been shown to possess acetylcholinesterase inhibitory activity.<sup>2</sup> This is relevant in PD because loss of dopaminergic activity increases the release of acetylcholine, leading to impaired mobility, a symptom of PD.<sup>52</sup> Furthermore, *Withania somnifera* commonly known as Indian ginseng, reverses oxidative stress in 6-OHDA- pre-treated rats indicative of an anti-Parkinson's disease effect.<sup>61</sup> For the purposes of this study, several plants commonly used for treatment of neurological disorders were selected for the assessment of neuroprotective activity.

#### **1.5.2.1. *Acokanthera oppositifolia* (Lam.) Codd.**

*Acokanthera oppositifolia* belongs to the family Apocynaceae. It is an evergreen tree that grows up to 3 metres tall, and has white flowers and plum-like fruits (Figure 8A).<sup>62</sup> *Acokanthera oppositifolia* is found in the northern parts of South Africa and its neighbouring countries Mozambique and Zimbabwe.<sup>62</sup> It is known by locals as the 'common poison bush' (English), 'gewone gifboom' (Afrikaans) and 'uhlunguyembe' (Zulu).<sup>62</sup> The plant is traditionally used for treatment of headaches, convulsions, gastrointestinal tract ailments and congestive heart failure.<sup>62-64</sup>

#### **1.5.2.2. *Boophone disticha* (L.f.) Herb.**

*Boophone disticha* is a member of the Amaryllidaceae family. It is bulbous plant with thin strap-like leaves.<sup>62</sup> The bulb is partially visible above ground and has pink flowers when it blooms (Figure 8B).<sup>62</sup> It grows in the southern parts of Africa, especially South Africa and Zimbabwe.<sup>62,65</sup> Common names include the 'bushman poison bulb' (English), 'gifbol' (Afrikaans) and 'incotha' (Zulu).<sup>62</sup> Traditionally, the bulb is used to treat paralysis, age-related dementia headaches and abdominal pain.<sup>62,66</sup> It is reported to induce hallucinations of a divine nature.<sup>62</sup> These psychoactive properties have resulted in the recreational abuse of *B. disticha* in parts of Zimbabwe.<sup>62,65</sup>

#### **1.5.2.3. *Hypericum perforatum* (L.)**

*Hypericum perforatum* belongs to the family Hypericaceae.<sup>62</sup> It is a perennial shrublet of about 1 metre high with protruding rhizomes, yellow flowers and shiny brown seeds (Figure 8C).<sup>62</sup> *Hypericum perforatum* is commonly known as St. John's wort, and is originally from Europe, Asia and North America.<sup>67</sup> It was introduced to South Africa where it has become known as a troublesome weed.<sup>62</sup> Preparations (aerial parts) are used as antidepressants, anxiolytics and diuretics.<sup>62,67,68</sup> In Germany a formulation of *H. perforatum* has been approved for use as a supportive treatment of excitotoxicity and sleep disturbances.<sup>62</sup>

**1.5.2.4. *Leonotis leonurus* (L.) R.Br.**

*Leonotis leonurus* is a shrub that grows up to 5 metres tall and contains woody branches and orange flowers (Figure 8D).<sup>62</sup> The shrub is widely distributed across southern Africa and remains a popular garden plant.<sup>62</sup> It belongs to the family Lamiaceae and is commonly known as ‘wild dagga’ (English), ‘wilde dagga’ (Afrikaans) and ‘umunyane’ (Zulu).<sup>62,69</sup> The leaves are smoked as a replacement for *Cannabis sativa* (marijuana) because of its mild narcotic effect, and is additionally used to relieve epilepsy and convulsions.<sup>62,69</sup>

**1.5.2.5. *Siphonochilus aethiopicus* (Schweinf.) B. L. Brutt**

*Siphonochilus aethiopicus* is a deciduous plant with pink/purple and white flowers. It belongs to the family Zingiberaceae (Figure 8E).<sup>62,70</sup> The leaves and rhizomes have a similar aroma to *Zingiber officinale* (ginger).<sup>62</sup> This plant is commonly known as the ‘African ginger’ (English) or ‘indungulo’ (Zulu) and mainly grows in the Mpumalanga and Limpopo provinces of South Africa.<sup>62,70</sup> Traditionally, rhizomes and roots are used to treat hysteria, epilepsy, headaches, and influenza.<sup>62,70</sup>

**1.5.2.6. *Terminalia sericea* Burch. ex DC.**

*Terminalia sericea* belongs to the family Combretaceae.<sup>62,71</sup> It grows up to 8 metres tall, and has a grey coloured bark and cream-coloured flowers when it blooming (Figure 8F).<sup>62</sup> It is mainly found in sandy savanna areas such as the Northern part of South Africa.<sup>62</sup> It is commonly referred to as the ‘silver cluster-leaf’ (English), ‘vaalboom’ (Afrikaans) and ‘amangwe’ (Zulu).<sup>62</sup> Traditional uses of *Terminalia* species ( roots and stems) include epilepsy and stomach complaints.<sup>62</sup>

**1.5.2.7. *Xysmalobium undulatum* (L.) Aiton.F.**

*Xysmalobium undulatum* is a perennial herb, belonging to the family Apocynaceae.<sup>62,72</sup> This herb has large leaves and yellow flowers with fluffy seeds encapsulated in hairy sacs (Figure 8G).<sup>62,72</sup> The leaves contain a milk-like exudate.<sup>62</sup> It has a wide distribution in South African grasslands and is found in KwaZulu-Natal, Limpopo and Mpumalanga provinces.<sup>62</sup> The roots are commonly used to treat hysteria, headaches and as a sedative.<sup>61,62</sup> It is marketed as Uzara, for a wide range of uses.<sup>62</sup>

**1.5.2.8. *Ziziphus mucronata* Willd.**

*Ziziphus mucronata* belongs to the family Rhamnaceae and is a tree that reaches a height of up to 10 metres. The bark is greyish-brown in colour; branches contain thorns, bright green leaves and small

yellowish flowers (Figure 8H).<sup>62</sup> It occurs in summer rainfall regions such as southern Africa, Ethiopia and Arabia.<sup>73</sup> Medicinally the roots or bark and leaves may be used as a sedative and to treat pain.<sup>62,73</sup>

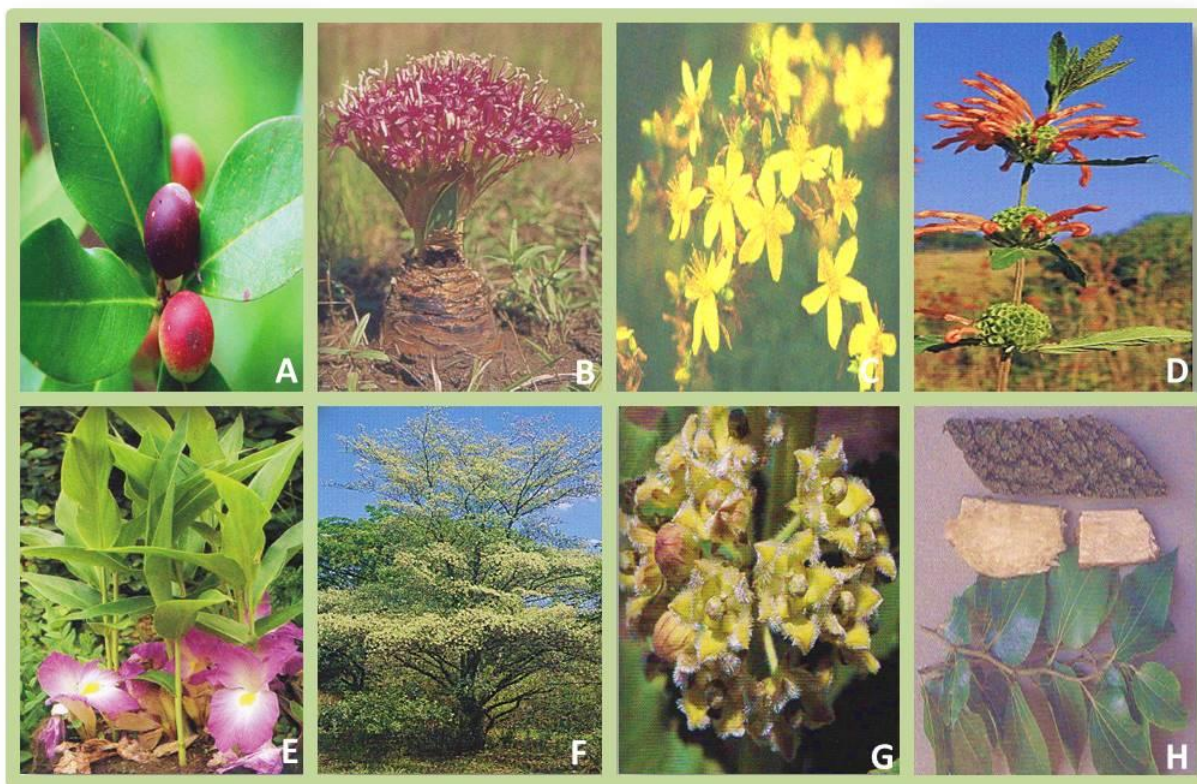


Figure 8: Plants selected for the present study. (A) *Acokanthera oppositifolia*, (B) *Boophane disticha*, (C) *Hypericum perforatum*, (D) *Leonotis leonurus*, (E) *Siphonochilus aethiopicus*, (F) *Terminalia sericea*, (G) *Xysmalobium undulatum* and (H) *Ziziphus mucronata*. Reproduced with permission: Briza Publications.<sup>62</sup>

### 1.5.3. The blood brain barrier and medicinal plants

By definition the blood brain barrier (BBB) is a physical barrier made of endothelial cells and capillaries that separates the brain from the blood, this is to control the brain's microenvironment.<sup>74</sup> This is essential for proper neural signalling. In drug discovery, this area is of concern because compounds need to access the brain. An intermediate polarity solvent, such as methanol or acetone, would yield compounds of a moderate lipophilicity, which should aid passive diffusion into the brain. However, the involvement of facilitated diffusion or active transport mechanisms cannot be excluded.

## 1.6. Aim

The aim of this study was to evaluate the neuroprotective effects of selected African medicinal plants traditionally used for neurodegenerative disorders in an *in vitro* SH-SY5Y neuroblastoma model of PD. *In vitro* neuroprotection is deemed as any attenuation of toxin-induced cytotoxicity in the neuroblastoma cell line.

## 1.7. Objectives of the study

The objectives of the study were to determine:

- The crude phytochemical classes present within acetone and methanol extracts of selected African herbal remedies.
- The effect of the neurotoxins (MPP<sup>+</sup> and 6-OHDA) on cell density using the sulforhodamine B (SRB) assay for selection of agent to use in a PD model.
- The effect of crude extracts on cell density using the SRB assay.
- The neuroprotective effects of crude extracts in the reversal of neurotoxicity in the PD model using the SRB assay for selection of ideal extract candidates.
- The neuroprotective mechanism of action of selected extracts in the PD model by assessing the following parameters:
  - Intracellular ROS generation using the dihydrodichlorofluorescein diacetate (H<sub>2</sub>-DCF-DA) cleavage assay.
  - Intracellular GSH concentrations using the monochlorobimane (MCB) adduct formation assay.
  - Mitochondrial membrane potential using the JC-1 ratiometric assay.
  - Intracellular Ca<sup>2+</sup> influx using the Fura-2 AM staining assay.
  - Intracellular ATP levels using bioluminescent assay kit.
  - Cellular morphology using phase contrast and PlasDIC microscopy.

## 1.8. Project overview

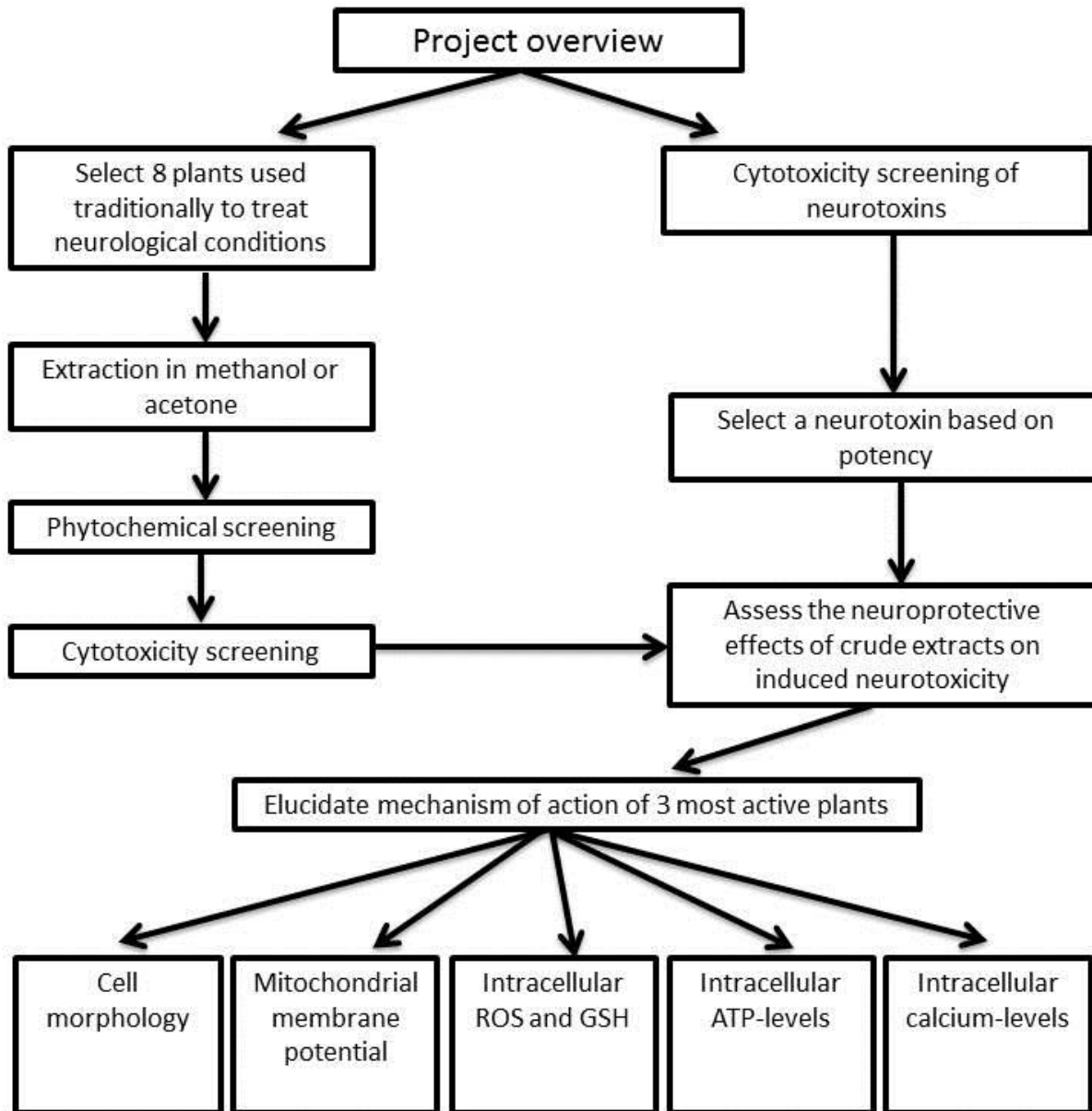


Figure 9: Project overview is the summation of the methodology used to achieve set objectives. GSH - reduced glutathione, ATP - adenosine tri-phosphate and ROS - reactive oxygen species.

## Chapter 2: Materials and methods

Approval to conduct this study was obtained from the Research Ethics Committee of the Faculty of Health Sciences, University of Pretoria (Appendix I). All reagents used, as well as the preparation thereof, are listed in Appendix II.

### 2.1. Plant material

Plant material (Table 2) was stored in closed, amber containers as a fine powder. Voucher specimens of *T. sericea* and *Z. mucronata* are deposited in the Soutpansbergensis herbarium (Makhado, Venda), whereas the voucher specimen of *A. oppositifolia* is deposited at the Department of Toxicology (Onderstepoort Veterinary Institute, Pretoria). All other plant material was received as gifts from the South African Natural Biodiversity Institute (SANBI, Pretoria) after confirmation by their in-house botanist, or purchased from a health shop.

Table 2: Plants selected for study against neurotoxin-induced Parkinson's disease.

Plant name and authority	Part used	Voucher number
<i>Acokanthera oppositifolia</i> (Lam.) Codd	Roots	LT0019
<i>Boophone disticha</i> (L.f.) Herb.	Bulb	SANBI
<i>Hypericum perforatum</i> (L.)	Leaves	Health Shop
<i>Leonotis leonurus</i> (L.) R.Br	Leaves	SANBI
<i>Siphonochilus aethiopicus</i> (Schweinf.) B. L.	Rhizomes	SANBI
<i>Terminalia sericea</i> Burch. ex DC.	Roots and leaves	NH1878
<i>Xysmalobium undulatum</i> (L.) Aiton.F.	Roots	SANBI
<i>Ziziphus mucronata</i> Willd.	Roots	NH1809

### 2.2. Preparation of the plant extracts

Although water extracts would have better simulated ethnomedicinal preparations, the purpose of this study was to opt for a broader drug discovery route, thus intermediate polarity solvents were used. Crude acetone and methanol extraction was done by sonicating 10 g ground plant material in 100 mL respective solvent for 30 min. The mixture was agitated for an additional 30 min and left overnight at 4°C. The supernatant was collected after centrifugation for 5 min at 1 000 g. The marc was re-extracted overnight in the respective solvent. Supernatants were combined and syringe-

filtered (0.22  $\mu\text{m}$ ). The filtrate was concentrated using a vacuum rotary evaporator (Büchi Rotovapor R-200, Büchi). Dried extracts were re-dissolved in dimethyl sulfoxide (DMSO) and stored at  $-80^{\circ}\text{C}$  to prevent phytochemical decomposition. Yields were determined gravimetrically.

## 2.3. Phytochemical screening

Thin-layer chromatography (TLC) was employed to identify major phytochemical classes (Table 3). Thin-layer chromatography was performed using guidelines outlined by Stahl<sup>75</sup> on pre-coated aluminium TLC plates (Merck, SIL G-25 ultraviolet light [UV] 254, 20 cm x 20 cm). Plates were spotted with 10  $\mu\text{g}$  crude extract and developed in different mobile phases. Visualisation was done using short-wave and long-wave UV light, as well as specific detection reagents (Table 3).

Table 3: Mobile phases and detection reagent used to visualise phytochemical classes.

Phytochemical class	Mobile phases	Detection reagent
Alkaloids	Chloroform:Acetone:Methanol (4:4:2)	Dragendorff's reagent
Flavonoids	Chloroform:Acetone:Methanol (4:4:2)	Aqueous 3% sodium nitrate and 1% aluminium chloride
Phenols	Methanol:Ammonium hydroxide (200:3)	Folin-Ciocalteu
Saponins	Chloroform:Methanol:Water (60:35:5)	1% Vanillin in 5% aqueous sulphuric acid
Terpenoids	Toluene:Ethyl acetate (93:7)	1% Vanillin in 5% aqueous sulphuric acid

## 2.4. Cell culture and maintenance

The SH-SY5Y neuroblastoma cell line (CRL-2266) was originally purchased from the American Tissue Culture Collection (ATCC) by the Department of Pharmacology, North-West University. Cells were received as a gift and were cultured in 75  $\text{cm}^2$  cell culture flasks. Cells were maintained in 1:1 Ham's F12 medium and Dulbecco's Modified Eagle's Medium (DMEM) supplemented with 1% non-essential amino acids, 1% L-glutamine, penicillin (100 U/mL), streptomycin (100 U/mL) and 10% heat-inactivated foetal calf serum (FCS) at  $37^{\circ}\text{C}$  in a humidified incubator with a 5%  $\text{CO}_2$  atmosphere. Cells were grown to 80% confluence, washed with sterilised phosphate-buffered saline (PBS) and chemically detached using Trypsin/Versene solution. Cells were centrifuged at 200  $g$  for 5 min and the pellet re-suspended in 1 mL medium. Cells were counted using the trypan blue exclusion assay (0.1% w/v) and re-suspended to  $1 \times 10^5$  cells/mL in 10% FCS-supplemented

medium, for experiments done in 96-well plates. Alternatively, cells were resuspended to  $2.5 \times 10^5$  cells/mL in 10% FCS-supplemented medium for experiments conducted in 24 well-plates.

## 2.5. Effect of neurotoxins and crude extracts on cell density

The SRB assay was performed following the guidelines of Vichai and Kirtikara<sup>76</sup> with minor modifications to volumes used. Cell suspensions (100  $\mu$ L) were added to 96-well plates and incubated for 24 h to allow for attachment. Attached cells were exposed to 100  $\mu$ L medium (negative control), acidified medium (pH  $\sim$ 5.8, acidified control), 0.5% DMSO (vehicle control), 1% saponin (positive control), MPP<sup>+</sup> (0.2 – 2 000  $\mu$ M) or 6-OHDA (0.2 - 200  $\mu$ M) prepared in FCS-free medium for 24 h and 48 h. Preliminary studies indicated that ascorbic acid did not influence any experimental workflow or outcomes at the concentration diluted to 0.00021% thus approximately 11.9 nM. The working solutions of 6-OHDA were prepared in medium supplemented with acetic acid to maintain a pH of 5.8 due to solubility issues. Blanks consisted of 5% FCS-supplemented medium alone to account for sterility and background noise. To assess the cytotoxicity of the crude extracts, cells were exposed to crude extracts (2 - 200  $\mu$ g/mL) for 48 h as described above.

After the incubation period, cells were fixed with 50  $\mu$ L trichloroacetic acid (TCA, 50%) and incubated overnight at 4°C. After fixation, plates were washed twice with tap water, dried and stained with 100  $\mu$ L SRB solution (0.057% w/v in 1% v/v acetic acid) for 30 min. Excess dye was removed by rinsing plates thrice with 1% acetic acid. Bound dye was extracted from fixed cells using 200  $\mu$ L Tris-base solution (10 mM, pH 10.5), followed by 30 min incubation on a shaker at room temperature. Plates were read spectrophotometrically using an EL-X 800 microplate reader (Biotek Inc, Winooski, USA) at 510 nm and a reference wavelength of 630 nm. Values were blank-excluded and cell density was determined by the following equation:

$$\text{Cell density (\% of negative control)} = \left( \frac{\text{absorbance of sample}}{\text{average absorbance of negative control}} \right) \times 100$$

## 2.6. Preliminary screening of neuroprotective effects of crude extracts in the Parkinson's disease model

Based on the neurotoxin cytotoxicity screening, 6-OHDA was selected to induce neurotoxicity in the SH-SY5Y cell line. To assess the neuroprotection offered by the crude extracts, cells were seeded as described in Section 2.5 and exposed to 6-OHDA (50  $\mu$ L, 33.3  $\mu$ M) for 2 h. Cells were treated with 50  $\mu$ L crude extracts at 20, 60 and 120  $\mu$ g/mL (5, 15 and 30  $\mu$ g/mL in-reaction), which further diluted the 6-OHDA to a final concentration of 25  $\mu$ M. Treated cells were incubated for 24 h, 48 h and 72 h, after which the SRB assay was done as described in Section 2.5. Crude extracts that reduced 6-OHDA-induced cytotoxicity were selected for mechanistic studies. All subsequent assays, apart from the  $\text{Ca}^{2+}$  flux assay were assessed after 24 h exposure.

## 2.7. Determination of intracellular reactive oxygen species concentrations

The intracellular ROS concentration was determined using the  $\text{H}_2$ -DCF-DA assay. The dye,  $\text{H}_2$ -DCF-DA, is a non-fluorescent molecule that passively enters the cell where it is cleaved by esterases and activated by ROS to release the fluorescent molecule, dichlorofluorescein (DCF).<sup>77</sup> 2,2'-Azobis (2-methylpropionamide) dihydrochloride (AAPH) (1 mM in-reaction) was used as positive control.

After 24 h exposure to the crude extracts, 20  $\mu$ L  $\text{H}_2$ -DCF-DA (220  $\mu$ M prepared in PBS) was added to all wells and incubated for 2 h at 37°C. Medium was aspirated and replaced with 100  $\mu$ L Hank's Balanced Salt Solution (HBSS). Fluorescence was measured using the H2 Synergy microplate reader (Analytical & Diagnostic Products (A.D.P.), SA) at an excitation wavelength of 485 nm and an emission wavelength of 535 nm. The SRB assay was used to normalise fluorescent data to cell density.

All values were blank-excluded and intracellular ROS concentrations determined using the following equations:

$$\text{Normalised fluorescence (NF)} = \frac{\text{fluorescence of well}}{\text{absorbance of well}}$$

$$\text{ROS concentration (\% of negative acidified control (NCa))} = \left( \frac{\text{NF of sample}}{\text{NF average of NCa}} \right) \times 100$$

## 2.8. Quantification of intracellular glutathione content

The intracellular GSH content was assessed by the MCB adduct formation assay.<sup>78</sup> The MCB dye passively enters the cell to bind exclusively to GSH to form a fluorescent GSH-MCB adduct.<sup>78</sup> Buthionine sulfoximine (1 mM in reaction) was used as positive control.

After 24 h exposure to the plant extracts, 20  $\mu$ L MCB (176  $\mu$ M prepared in PBS) was added and incubated for 2 h at 37°C. Medium was aspirated and replaced with 100  $\mu$ L HBSS. Fluorescence was measured at an excitation wavelength of 360 nm and an emission wavelength of 460 nm. The SRB assay used to normalise fluorescent data to cell density. All values were blank-excluded and intracellular GSH level was determined using the equation provided in Section 2.7.

## 2.9. Mitochondrial membrane potential

The MMP was monitored using the JC-1 dye. The JC-1 dye is a lipophilic cationic dye that enters the mitochondria and forms aggregates in 'healthy' cells to emit a red light.<sup>79</sup> In cells with mitochondrial dysfunction, the dye forms monomers and emits a green light.<sup>79</sup> The ratio of the red-to-green light can be measured and correlated with the loss of MMP.<sup>79</sup> Tamoxifen (10  $\mu$ M in reaction) was used as positive control.

After 24 h exposure to the plant extracts, 20  $\mu$ L JC-1 (150  $\mu$ M prepared in PBS) was added and incubated for 30 min at 37°C. Medium was aspirated and replaced with 100  $\mu$ L HBSS. Fluorescence was measured at an excitation wavelength of 485 nm and an emission wavelength of 525 nm for the monomeric form of JC-1 dye, and at an excitation wavelength of 545 nm and the emission wavelength of 595 nm for the aggregate form of the JC-1 dye. The MMP levels were determined using the following equations:

$$\text{Fluorescence ratio (FR)} = \frac{\text{fluorescence read at 485 nm}}{\text{fluorescence read at 545 nm}}$$

$$\text{MMP(\% of acidified negative control)} = \left( \frac{\text{FR of sample}}{\text{FR average of NCa}} \right) \times 100$$

## 2.10. Quantification of intracellular calcium flux

Intracellular  $\text{Ca}^{2+}$  was measured using the  $\text{Ca}^{2+}$  sensitive cationic dye, Fura-2 AM. Fura-2 is a ratiometric dye that provides more accurate calibration of values due to an increase in fluorescence emission upon  $\text{Ca}^{2+}$  binding, with a corresponding shift in excitation spectra.<sup>80</sup> The major drawback of using ratiometric probes is excitation in the UV wavelength ranges.<sup>80</sup> The UV excitation wavelengths are significantly absorbed by plastic microplates, which are normally used in cell culture, but this can be overcome by using optically clear bottom or opaque microplates. Intracellular  $\text{Ca}^{2+}$  flux assays using ratiometric dyes are more robust in that they are not as sensitive to cell density differences, concentration of the dye itself and other signal artefacts.<sup>80</sup> Ethylene glycol-bis(2-aminoethylether)-*N,N,N',N'*-tetraacetic acid (EGTA) (1 mM in-reaction) was used as positive control.

Cultured cells were washed twice with loading buffer (5.9 mM potassium chloride, 1.4 mM magnesium chloride, 10 mM 4-[2-hydroxyethyl]-1-piperazineethanesulfonic acid [HEPES], 1.2 mM monosodium phosphate, 5 mM sodium bicarbonate, 140 mM sodium chloride, 11.5 mM D-glucose and 1.8 mM calcium chloride). In a 1.5 mL tube, cells were loaded with 10  $\mu\text{L}$  of 1 mM Fura-2 AM and 5  $\mu\text{L}$  of 20% Pluronic F127 to a final concentration 10  $\mu\text{M}$  and 0.1%, respectively. Cells were incubated for 1 h at 37°C, and subsequently centrifuged at 200 *g* for 5 min. The supernatant was discarded and cells were re-suspended in 6 mL HBSS. The cell suspension (60  $\mu\text{L}$ ) was added to white 96-well plates, and incubated for an additional 10 min at 37°C. Subsequent to incubation, cells were read at the dual excitation wavelengths of 340 nm and 380 nm, and an emission wavelength of 508 nm every 1.53 min for 15 min to establish baseline readings. After an initial reading was obtained, 30  $\mu\text{L}$  of 100  $\mu\text{M}$  6-OHDA was manually added to respective wells and read for 30 min. Crude extracts (30  $\mu\text{L}$  of 2, 4, 20, 60  $\mu\text{g}/\text{mL}$  in HBSS) were manually added and the fluorescence measured for a further 3 h. The final concentration of 6-OHDA was 25  $\mu\text{M}$  and 0.5, 1, 5 and 15  $\mu\text{g}/\text{mL}$  for crude extracts.

Data was analysed using the equations below:

$$\text{Fluorescence ratio (FR)} = \frac{\text{fluorescence read at 380 nm}}{\text{fluorescence read at 340 nm}}$$

The FR was used to construct a fluorescence ratio vs time curve, which was then used to calculate the area under the curve (AUC).

$$\text{Intracellular calcium (\% of acidified negative control)} = \left( \frac{\text{AUC of sample}}{\text{average AUC of NCa}} \right) \times 100$$

## 2.11. Quantification of intracellular ATP levels

The monitoring of ATP may be used as an adjunct to assist with determination of cell death.<sup>43</sup> This uses the concept that ATP levels would be higher in proliferating cells than in apoptotic or necrotic cells.<sup>43</sup> Furthermore, fluctuations in intracellular ATP levels may be used as an indication of mitochondrial dysfunction.<sup>43</sup> The assay uses a bioluminescent enzyme luciferase to catalyse the formation of light ATP and luciferin. The amount of light can be correlated with the amount of ATP. Saponin (1% in reaction) was used as a necrotic control.

The ATP levels were determined using the ApoSENSOR ATP assay kit following the manufacturer's instructions. After 24 h exposure, culture medium was replaced with 90  $\mu$ L ATP buffer (containing the ATP-monitoring enzyme). Luminescence was measured after 1 min of incubation using the H2 Synergy microplate reader.

$$\text{ATP concentration (\% of acidified negative control)} = \left( \frac{\text{luminescence of sample}}{\text{average luminescence of NCa}} \right) \times 100$$

## 2.12. Cellular morphology

Cellular morphology was assessed using phase-contrast microscopy and polarisation-optical transmitted light differential interference contrast (PlasDIC) microscopy. PlasDIC microscopy uses enhanced linearity of polarised light emitted after the objective therefore generating quality images.<sup>81</sup> Staurosporine (20  $\mu$ M in reaction) was used as an apoptotic control.<sup>81</sup>

Cells were seeded into 24-well culture plates, and incubated for 24 h to allow attachment. Cells were exposed to 6-OHDA (60  $\mu$ L, 33.3  $\mu$ M) for 2 h. Cells were then treated with 60  $\mu$ L crude extracts at 2 and 20  $\mu$ g/mL (0.5 and 5  $\mu$ g/mL in-reaction), which further diluted the 6-OHDA to a final concentration of 25  $\mu$ M. Treated cells were incubated for 24 h, after which morphology was assessed. Microscopy images were taken using a Zeiss Axiovert-40 microscope (Göttingen, Germany) and Zeiss Axiovert MRm monochrome camera (Carl Zeiss MicroImaging GmbH, Göttingen, Germany). A magnification of 5x and 40x was used for phase contrast and PlasDIC microscopy, respectively. Two representative images per experiment were taken at the centre of each well.

## 2.13. Data analysis and statistics

All experiments were done with at least technical and biological triplicates ( $n \geq 9$ ). Data was compiled using Microsoft Excel, and analysed using GraphPad Prism 5.0. Numerical data was expressed as mean  $\pm$  standard error of the mean (SEM). Non-linear regression was used to determine the half maximal inhibitory concentration's ( $IC_{50}$ ) of samples. Statistical significance between controls and samples were assessed using the Kruskal Wallis test, using a post-hoc Dunn's test. The indicator of significance was  $p < 0.05$ . Microscopy images were taken on three separate occasions.

# Chapter 3: Results and Discussion

## 3.1. Phytochemical screening of crude extracts

Thin layer chromatography is a qualitative method that can be used for phytochemical screening. Phytochemicals are diverse chemicals with no nutritive value, but possess various preventative and curative properties.<sup>82</sup> The phytochemical classes assessed in the study have been described in literature to influence neurological activity.

Alkaloids are nitrogenous compounds containing carbon, hydrogen and oxygen.<sup>2</sup> The isoquinolone alkaloid morphine (from *Papaver somniferum*) is currently being used as an analgesic.<sup>2</sup> Galantamine, isolated from *Narcissus tazetta* and *Galanthus caucasicus* has been shown to improve cognition in Alzheimer's disease by inhibiting cholinesterase, an enzyme responsible for breaking down acetylcholine.<sup>2</sup>

Phenols and flavonoids are well-known antioxidants.<sup>2,73</sup> Phenolic compounds neutralise lipid reactive species and prevent decomposition of hydroxyperoxides into free radicals.<sup>73</sup> Furthermore, flavonoids act as ROS scavengers, and possess various benefits, such as anti-inflammatory, immunomodulatory and neuroprotective properties.<sup>73</sup> The citrus flavone, tangeretin, has been shown to protect nigro-striatal integrity after exposure to 6-OHDA.<sup>2</sup> Additionally, polyphenols from green tea have been shown to offer neuroprotection in rats after exposure to 6-OHDA.<sup>2</sup> Saponins from *Panax ginseng* stimulate muscarinic receptors and improve dopaminergic activity.<sup>2</sup>

In the study, both extracts of *A. oppositifolia* tested positive for alkaloids, flavonoids and phenolic compounds (Table 4). This is consistent with literature, where Sharma *et al.* reported the presence of phenols and flavonoids in the acetone and methanol extracts.<sup>63</sup> Contradictory to the present study, Sharma and colleagues did not detect alkaloids.<sup>63</sup>

*Boophane disticha* extracts were found to contain alkaloids, flavonoids and phenolic compounds (Table 4), which is consistent with literature apart from the absence of terpenoids in the present study.<sup>66</sup> Amaryllidaceae alkaloids that have been identified in *B. disticha* have been found to possess narcotic, hypotensive and analgesic properties.<sup>62</sup> Lycorine, an alkaloid isolated for *B. disticha*, displays anticholinergic activity *in vitro*.<sup>65</sup> 6-Hydroxycrinamine isolated from the methanolic extract of *B. disticha*

displays non-selective MAO inhibition.<sup>66</sup> Other phytochemicals that have been identified include the alkaloids crinine, buphanidrine, undulatin, buphansine and nerbodin.<sup>62</sup>

Both *H. perforatum* extracts possessed alkaloids, phenols and flavonoids; saponins were only present in the acetone extract, while terpenoids were only present in the methanol extract (Table 4). The presence of flavonoids, phenolic acids and terpenoids is supported by literature.<sup>83,84</sup> Active phytochemicals include hypericin, hyperforin, rutin and isoquercetin.<sup>62,67</sup> Hypericin and pseudohypericin inhibit MAO, and reduce synaptic reuptake of serotonin and dopamine.<sup>2</sup>

The acetone extract of *L. leonurus* tested positive for alkaloids, flavonoid, phenolics, terpenoids and saponins, whereas the methanol extract only possessed alkaloids, flavonoids and phenolics (Table 4). Aqueous extracts of *L. leonurus* are reported to contain alkaloids, flavonoids, phenolic acids, saponins and terpenoids.<sup>69</sup> *Leonotis Leonurus* contains marrubiin as the main diterpenoid,<sup>62</sup> which may be present only in acetone extracts.

*Siphonochilus aethiopicus* tested positive for alkaloids, phenols, saponins, flavonoids and terpenoids. Van Wyk *et al.* reported the presence of terpenoids with siphonochilone being the most active.<sup>62</sup>

*Xysmalobium undulatum* was found to possess alkaloids, flavonoids and phenols, however, this is contradictory to literature reports. Vermaak and colleagues reported the presence of saponins, but not alkaloids or tannins in *X. undulatum*.<sup>72</sup> Furthermore, Chatanga *et al.* did not detect alkaloids, flavonoids and diterpenes in their colorimetric assays of *X. undulatum* extracts.<sup>82</sup> Root extracts of *X. undulatum* contain cardenolide glycosides, which have digitalis-like effects on the heart and possess gastric inhibitory effects.<sup>62</sup> Isolated compounds include uzarin, xymalorin, uzarigenin and alloxymalorin.<sup>62,72</sup>

Alkaloids, flavonoids, phenolic acids and terpenoids were detected in the methanol extracts of *Z. mucronata* but lacked saponins. However, the latter was detected in the acetone extract. Olajuyigbe *et al.* reported the presence of phenols, flavonoids and proanthocyanidins in the ethanol, aqueous and acetone extracts of *Z. mucronata*.<sup>73</sup> An isolated compound includes mucronine D.<sup>62</sup>

The contradictions found when comparing the current findings to literature could be a factor of extraction and detection method, as well as the harvesting time of plants, geographic location and plant part used. The geographic location of cultivation, season of harvesting, the plant part used and extraction method would influence the phytochemistry which would in turn influence biological activity.<sup>85,86</sup>

Table 4: Extraction yields and presence of major phytochemical classes in the crude extracts of the selected medicinal plants.

Plant name	Extract	Extraction yield (%)	Alkaloids	Flavonoids	Phenolic acids	Saponins	Terpenoids
<i>A. oppositifolia</i>	Acetone	2.94	X	X	X		
	Methanol	8.30	X	X	X		
<i>B. disticha</i>	Acetone	1.20	X	X	X		
	Methanol	7.50	X	X	X		
<i>H. perforatum</i>	Acetone	4.40	X	X	X	X	
	Methanol	5.99	X	X	X		X
<i>L. leonurus</i>	Acetone	5.10	X	X	X	X	X
	Methanol	11.64	X	X	X		
<i>S. aethiopicus</i>	Acetone	7.28	X	X	X	X	X
	Methanol	8.13	X	X	X	X	X
<i>T. sericea</i>	Acetone	6.75	X	X	X		
	Methanol	14.10	X	X	X		
<i>X. undulatum</i>	Acetone	6.53	X	X	X		
	Methanol	9.45	X	X	X		
<i>Z. mucronata</i>	Acetone	1.31	X	X	X	X	X
	Methanol	6.83	X	X	X		X

In summary, plant extracts have been shown to possess variety of phytochemicals that may be beneficial in PD, for example 6-hydroxycrinamine and hypercin have been reported to inhibit dopamine metabolism by blocking MAO.<sup>2,66</sup> Furthermore, extracts of *H. perforatum*, *L. leonurus* and *S. aethiopicus* displayed a solvent dependent variability; this indicates that acetone and methanol may be extracting overlapping rather than similar phytochemicals. Solvent-dependent variability may be responsible for the intra-extract variability noted.

The acetone extract of *B. disticha* and *Z. mucronata* had lower percentage yields than their methanol counterparts. The methanol extracts of *T. sericea* and *L. leonurus* had higher percentage yields than the acetone counterparts. A similar trend was observed by Do *et al.*, whereby the acetone extracts had lower percentage yields than the methanol extracts.<sup>87</sup> However, *in vitro* activity cannot be attributed to

high percentage yields.<sup>87</sup> The authors further concluded that the extraction efficiency is affected by solvent polarity and phytochemical profile of the plant when pH, temperature and extraction time are kept constant.<sup>87</sup>

### 3.2. Cytotoxicity of crude extracts

Neuroblastoma cells were exposed to increasing concentrations of the crude acetone and methanol extracts for 48 h. The acetone extracts were more cytotoxic than their methanol counterparts (Figure 10 and Table 5), this further supports the statement that high percentage yield may not attribute to *in vitro* activity. The acetone and methanol extracts of *X. undulatum* were most cytotoxic, with IC<sub>50</sub>'s <10 µg/mL. Cytotoxicity of acetone extracts, in order of increasing potency, was *T. sericea* > *Z. mucronata* > *L. leonurus* > *A. oppositifolia* > *S. aethiopicus* > *H. perforatum* > *B. disticha* > *X. undulatum*. Methanol extracts displayed increasing cytotoxicity from *T. sericea* > *Z. mucronata* > *L. leonurus* > *H. perforatum* > *A. oppositifolia* > *S. aethiopicus* > *B. disticha* > *X. undulatum*.

Table 5: The cytotoxicity of the acetone and methanol extracts in the SH-SY5Y cell line expressed as the IC<sub>50</sub>.

Plant	Extract IC <sub>50</sub> ± SEM (µg/mL)	
	Methanol	Acetone
<i>A. oppositifolia</i>	41.4 ± 1.29	30.5 ± 1.09
<i>B. disticha</i>	22.4 ± 1.50	11.5 ± 1.62
<i>H. perforatum</i>	46.2 ± 1.10	16.1 ± 1.11
<i>L. leonurus</i>	>100	51.0 ± 1.07
<i>S. aethiopicus</i>	31.2 ± 1.19	25.3 ± 1.06
<i>T. sericea</i>	>100	86.8 ± 1.18
<i>X. undulatum</i>	7.3 ± 2.41	2.8 ± 3.29
<i>Z. mucronata</i>	>100	67.8 ± 1.13

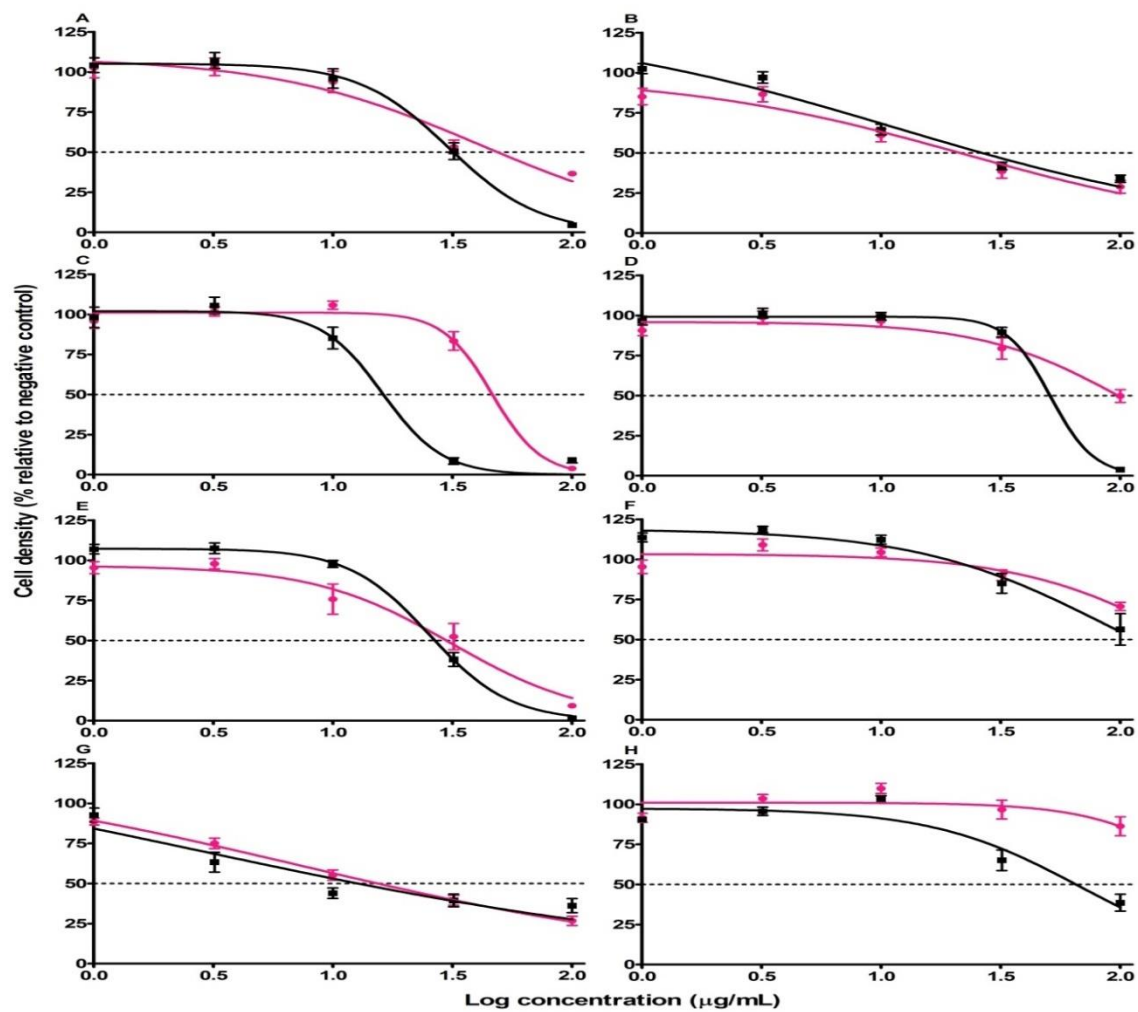


Figure 10: The effect of (●) acetone and (●) methanol extracts on SH-SY5Y cell density. (A) *A. oppositifolia*, (B) *B. disticha*, (C) *H. perforatum*, (D) *L. leonurus*, (E) *S. aethiopicus*, (F) *T. sericea*, (G) *X. undulatum* and (H) *Z. mucronata*. The black dashed line represents a 50% reduction in cell density.

The IC<sub>50</sub> value of *A. oppositifolia* was 30.5 and 41.4 µg/mL for the acetone and methanol extract respectively (Figure 10A and Table 5). Traditionally, *A. oppositifolia* has been used as an arrow poison,<sup>62</sup> which offers support to the cytotoxicity seen. The dichloromethane extract of *A. oppositifolia* induced total growth inhibition at 12.50 µg/mL and 6.25 µg/mL in the MCF-7 breast cancer cell line and UACC62 melanoma cell line, respectively.<sup>88</sup> Furthermore, Saeed *et al.* reported that the methanol crude extract of *A. oppositifolia* had an IC<sub>50</sub> of 2.5 µg/mL and 2.83 µg/mL in human drug-sensitive CCRF-CEM and multi-drug resistance CEM/ADR5000 leukaemia, respectively.<sup>89</sup> The authors further investigated the cytotoxicity of major phytochemicals (cardiac glycosides), acovenoside A and oubain, which were shown to incur cytotoxicity in various cell lines.<sup>89</sup> Cordier and Steenkamp reported that the methanol extract of *A. oppositifolia* had an IC<sub>50</sub> of 26.63 µg/mL in the HepG2 hepatocarcinoma cell line.<sup>90</sup> Variability between results and literature may be due to varying cytotoxicity assays and cell lines used.

In this study, the acetone extract of *B. disticha* had an IC<sub>50</sub> of 11.5 µg/mL, while presenting with an IC<sub>50</sub> of 22.4 µg/mL for the methanol extract after 48 h incubation. Adewusi and colleagues reported an IC<sub>50</sub> of 27.3 µg/mL in SH-SY5Y cells, for the methanol extract of *B. disticha* after 72 h of incubation.<sup>91</sup> It was suggested that cytotoxicity could be attributed to Amaryllidaceae alkaloids.<sup>91</sup> Furthermore, Lui and colleagues explored the cytotoxicity of isolated Amaryllidaceae alkaloids in eight different cell lines, and observed that lycorine-type alkaloids and aporphine-type alkaloids displayed potent cytotoxicity in all cell lines. Furthermore, lycorine-type alkaloids and aporphine-type alkaloids inhibited cyclooxygenase-2 by more than 90%,<sup>92</sup> which may be beneficial as neuroinflammation is a feature in PD. Lycorine- and crinine-type alkaloids isolated from *Zephyranthes carinata* inhibited acetylcholinesterase activity and displayed neuroprotective effects against glutamate-induced excitotoxicity.<sup>93</sup>

*L. leonurus* displayed an IC<sub>50</sub> of 51.0 µg/mL for the acetone extract, while little cytotoxicity was observed for the methanol extract. El-Anasari and colleagues reported no apparent cytotoxicity in various cell lines (MCF-7, Hela and HepG2) after exposure to a 70% methanol extract of *L. leonurus* (1 - 10 µg/mL).<sup>94</sup> Saeed *et al.* reported that methanol extracts of *L. leonurus* had an IC<sub>50</sub> of 2.57 µg/mL and 8.6 µg/mL in human drug-sensitive CCRF-CEM and multi-drug resistance CEM/ADR5000 leukaemia cells, respectively, however, marrubiin (diterpenoid lactone) was not responsible for this activity.<sup>89</sup>

The acetone extract of *S. aethiopicus* had an IC<sub>50</sub> of 25.3 µg/mL, while the methanol extract had an IC<sub>50</sub> of 31.2 µg/mL. An ethyl-acetate extract of *S. aethiopicus* displayed an IC<sub>50</sub> of 73.9 µg/mL in the Chinese hamster ovarian (CHO) cell line after 24 h incubation.<sup>95</sup>

The extracts with  $IC_{50}$ 's  $>100 \mu\text{g/mL}$  are indicative of low cytotoxicity, such as the methanol extracts of *L. leonurus*, *T. sericea* and *Z. mucronata*, making them ideal candidates for further assessment. The above trend was not evident with the acetone extracts, suggesting that the choice of extraction solvent would influence cytotoxicity based on the phytochemicals being extracted. As the solvent itself was evaporated to dryness, acetone did not contribute to any cytotoxicity. *Xysmalobium undulatum* displayed the most potent cytotoxicity. *Acokanthera oppositifolia*, also a member of the Apocynaceae family, induced less cytotoxicity, indicating intra-family differences that would alter bioactivity.<sup>85</sup> The level of cytotoxicity observed in both extracts of *X. undulatum* is concerning due to the wide use of the herbal remedy. Contradiction with literature may be due to different plant part used, incubation time, extraction solvent<sup>86</sup> and varying cell lines or the type of cytotoxicity assay used. Furthermore, there is limited availability of plant cytotoxicity profiles in literature with regards to the plants investigated in this study.

### 3.3. The effect of neurotoxins on cell density

The cytotoxicity of the two representative neurotoxins (6-OHDA and MPP<sup>+</sup>) was assessed after 24 h and 48 h to gain greater insight into the time-dependent reduction of cell density. According to Sigma Aldrich guidelines, 6-OHDA is prone to auto-oxidation, thus reconstitution needs to take place in an oxygen-free medium or be supplemented with an antioxidant. Lopes *et al.* suggested reconstitution in 0.1% ascorbic acid,<sup>48</sup> which was done for the present study. The in-well concentration of ascorbic acid could be considered negligible after dilution. As 6-OHDA precipitated in aqueous medium, it was reconstituted in acidified medium (pH 5.8). To account for the adjusted pH, an acidified negative control was included in all experiments. Results indicated that acidification of media did not alter the growth of the SH-SY5Y cell line significantly (Figure 11).

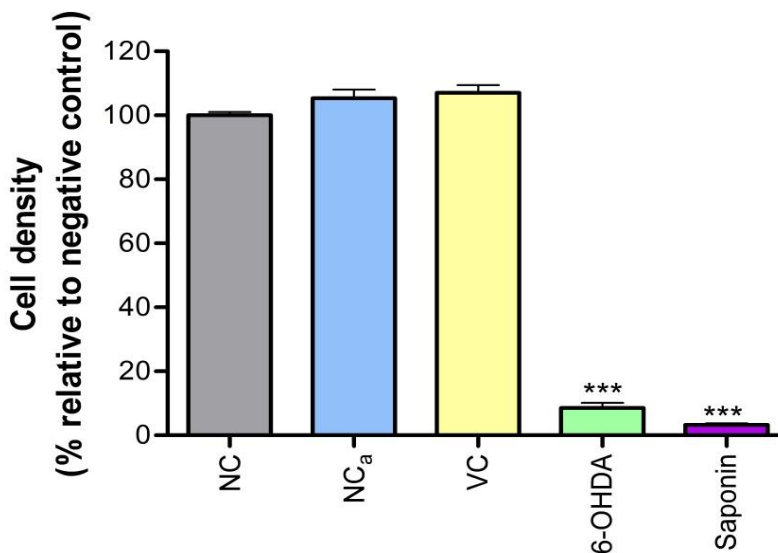


Figure 11: The effect of controls used during cytotoxicity assessment on the SH-SY5Y cell line. Significant difference to the 6-OHDA treatment relative to the NC<sub>a</sub>,\*\*\* p < 0.001. NC - negative control, NC<sub>a</sub> - acidified negative control, VC - vehicle control, 6-OHDA - 6-hydroxydopamine, saponin - positive control.

The IC<sub>50</sub> values of 6-OHDA in the present study were calculated to be  $23.4 \pm 1.32 \mu\text{M}$  and  $24.1 \pm 1.32 \mu\text{M}$  for 24 h and 48 h, respectively (Figure 12A). No further cytotoxicity was seen with longer exposure times (results not shown). This is in agreement with Kopalli and colleagues who obtained an IC<sub>50</sub> of 20  $\mu\text{M}$ .<sup>96</sup> Studies by Mahani *et al.*<sup>97</sup> and Ju *et al.*<sup>98</sup> only achieved cytotoxicity at concentrations exceeding 150  $\mu\text{M}$ , which could be explained by experimental conditions, such as the use of the 3-[4,5-dimethyl-2-thiazolyl]-2,5 diphenyl-tetrazolium bromide (MTT) assay and shorter incubation times.

Furthermore, no prominent cytotoxicity was observed for MPP<sup>+</sup> (Figure 12B). MPP<sup>+</sup> has been used as an *in vitro* model for PD in SH-SY5Y cells, however, in the present study the IC<sub>50</sub> exceeded the highest concentration tested (1 mM). Jantas and colleagues reported an IC<sub>50</sub> of 1 mM and 2 mM in undifferentiated and differentiated SH-SY5Y cells, respectively.<sup>99</sup> 6-Hydroxydopamine was thus selected as the neurotoxin for the *in vitro* PD model due to its potent cytotoxicity in relation to MPP<sup>+</sup>.

Even though both 6-OHDA and MPP<sup>+</sup> require DAT to enter the cell, 6-OHDA produced more cytotoxicity. 6-Hydroxydopamine, unlike MPP<sup>+</sup>, is able to undergo spontaneous auto-oxidation in an aqueous environment, such as in culture media, generating additional free radicals<sup>14</sup> which may exacerbate

cytotoxicity. Furthermore, 6-OHDA has a close structural resemblance with the endogenous ligand dopamine.

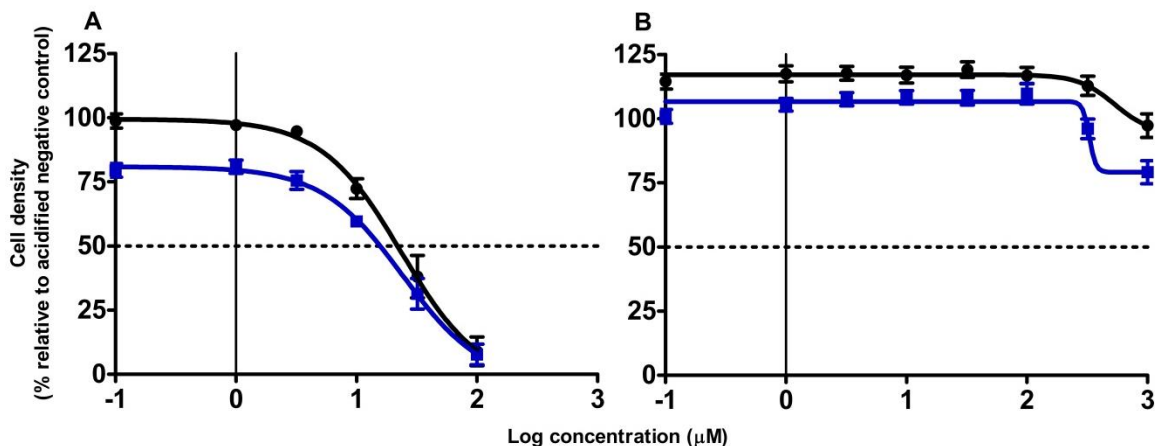


Figure 12: The effect of (A) 6-OHDA and (B) MPP<sup>+</sup> on the SH-SY5Y cell line after (●) 24 h and (●) 48 h exposure. 6-OHDA-hydroxydopamine, MPP<sup>+</sup> - 1-Methyl-4-phenylpyridinium.

Cellular differentiation status is also important as it results in up-regulation of transporters and enzymes, such as DAT and tyrosine hydroxylase.<sup>100</sup> Lopes and colleagues differentiated SH-SY5Y cells using retinoic acid and 1% FBS for 10 days; this treatment increased the cells' susceptibility to 6-OHDA-induced cytotoxicity.<sup>48</sup> This indicates that the differentiation and cytotoxicity assays amongst other effects may influence cytotoxicity.

### 3.4. The effect of crude extracts on 6-OHDA-induced cytotoxicity

In order to assess the neuroprotective effects of the crude extracts, SH-SY5Y cells were exposed to a cytotoxic concentration of 6-OHDA for 2 h, after which cells were treated with crude extracts for 24 h. At 24 h exposure, extracts of *A. oppositifolia*, *B. disticha*, *L. leonurus* and *X. undulatum* increased cell density by up to ~4-fold (Figure 13). Lower concentrations of *A. oppositifolia*, *B. disticha*, *H. perforatum*, *L. leonurus* and *T. sericea* had a greater neuroprotective effect than higher concentrations after pre-exposure to 6-OHDA. The acetone extracts of *Z. mucronata* displayed a trend of dose-dependent decrease in neuroprotection, however, this effect was not present in the methanol extract. The lower

neuroprotective activity of some of these extracts may be due to an additive cytotoxic effect between phytochemicals and 6-OHDA.

After 48 h both extracts of *B. disticha*, *L. leonurus*, *T. sericea* and *X. undulatum* displayed a trend dose-dependent decrease in neuroprotection (Figure 14). However, the lowest concentrations (5 and 15 µg/mL) of *A. oppositifolia* and *B. disticha* displayed a 4-fold increase in neuroprotection. The neuroprotective effect of the acetone extracts of *H. perforatum* observed at 24 h was completely diminished at 48 h, however, the methanol extract maintained the same trend of dose-dependent decrease in neuroprotection after both exposure periods (Figure 14). Both extracts of *L. leonurus* maintained the neuroprotective effects just below 40% (Figure 14). *Ziziphus mucronata* displayed the same trend as the 24 h exposure (Figure 14).

At 72 h, the crude extracts maintained the neuroprotective effects seen at previous exposure periods. Surprisingly, lower concentrations of *H. perforatum* and *S. aethiopicus* displayed improved neuroprotection than at 48 h, but similar to 24 h incubation. The neuroprotective effect of the acetone extract of *X. undulatum* decreased with longer incubation, however, this trend was not observed with the methanol extracts. In contrast, both extracts of *Z. mucronata* displayed an increase in neuroprotection with longer incubations. Extracts of *A. oppositifolia*, *B. disticha* and *X. undulatum*, displayed better neuroprotection than other extracts, specifically at lower concentrations.

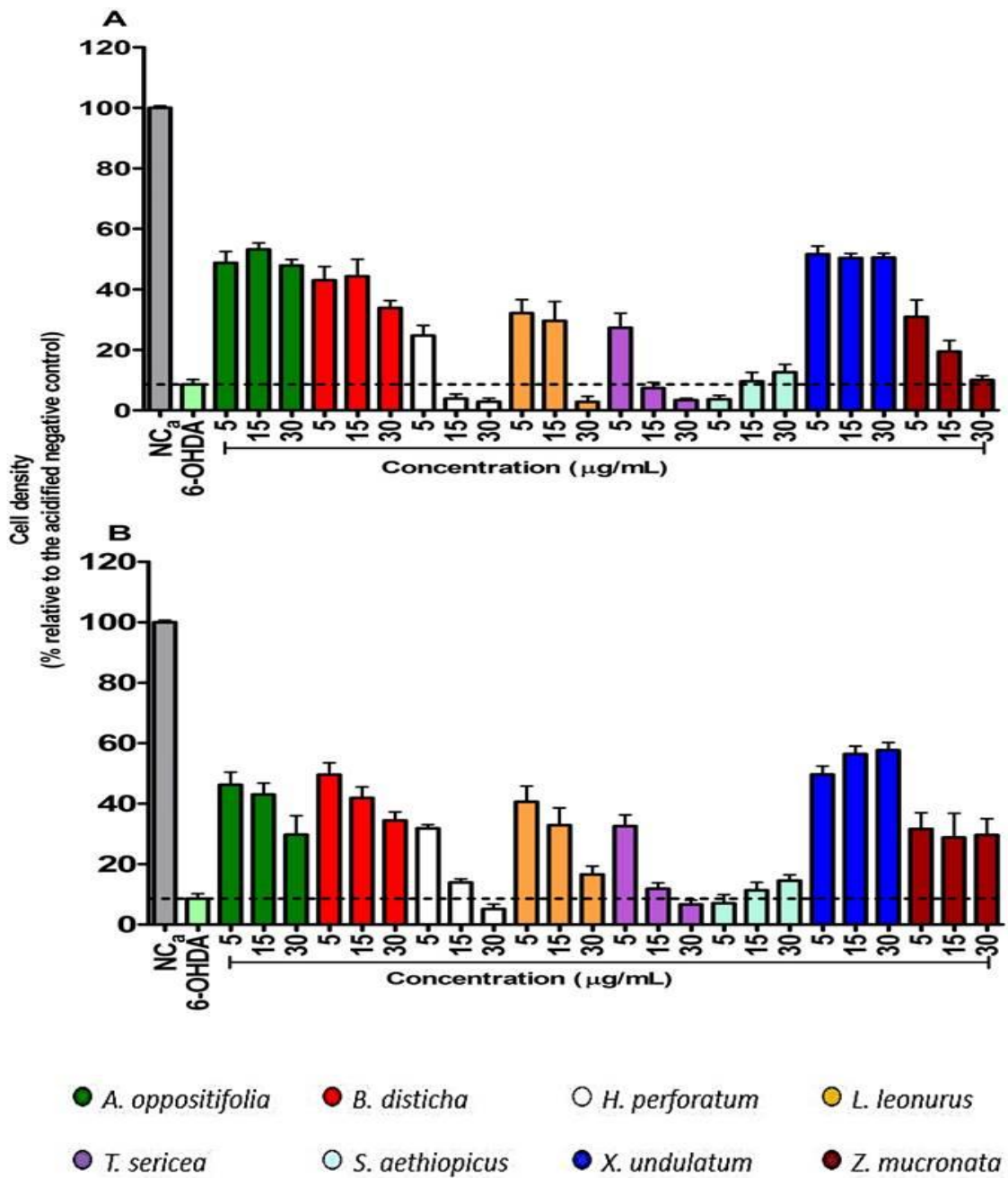


Figure 13: The neuroprotective effect of the crude (A) acetone and (B) methanol extracts against 6-OHDA-induced neurotoxicity in the SH-SY5Y cell line after 24 h exposure. The black dashed line represents the cytotoxicity induced by 6-OHDA. 6-OHDA- 6-hydroxydopamine, NC<sub>a</sub>- acidified negative control.

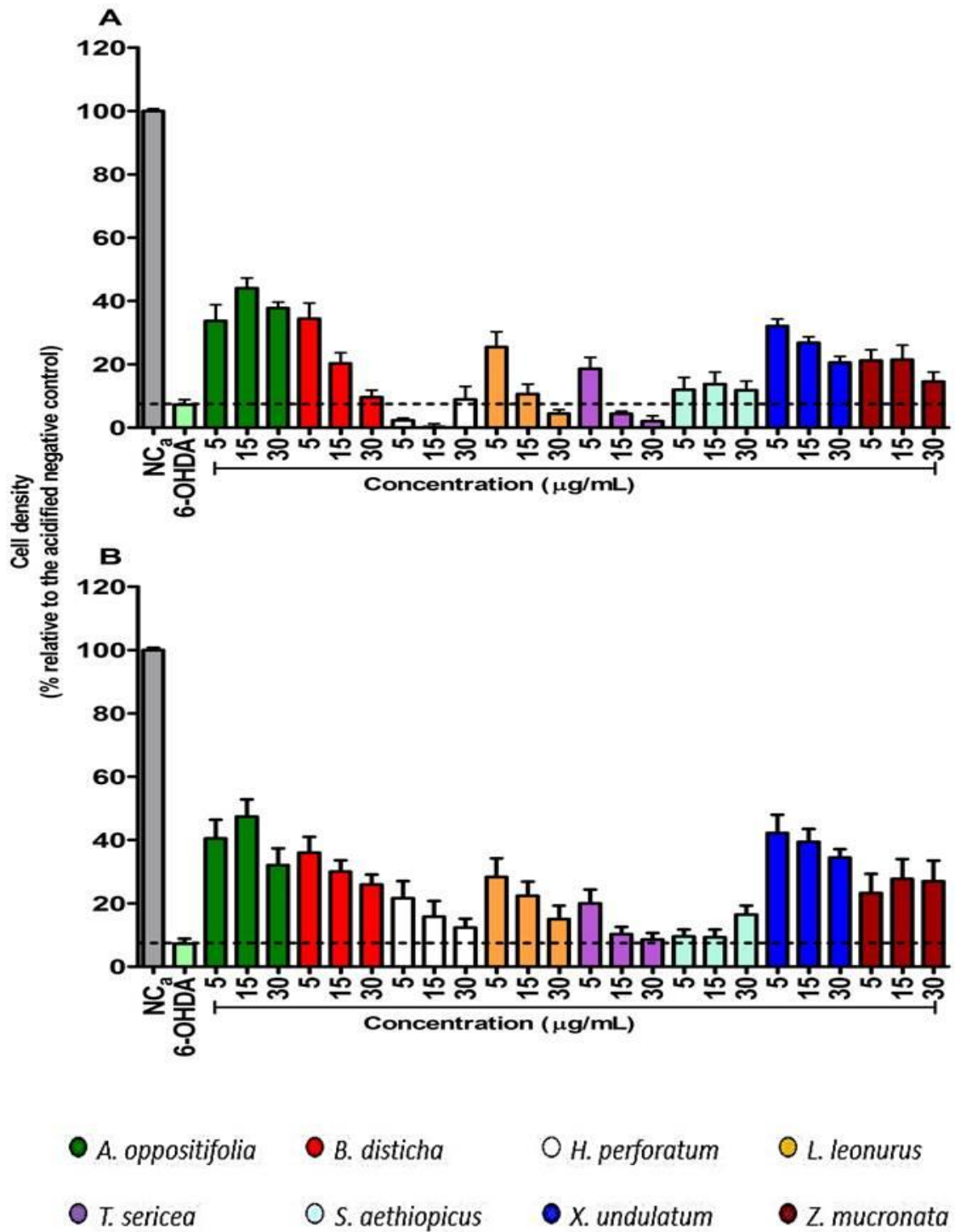


Figure 14: The neuroprotective effect of crude (A) acetone and (B) methanol extracts against 6-OHDA-induced neurotoxicity in the SH-SY5Y cell line after 48 h exposure. 6-OHDA- 6-hydroxydopamine, NC<sub>a</sub>- acidified negative control.

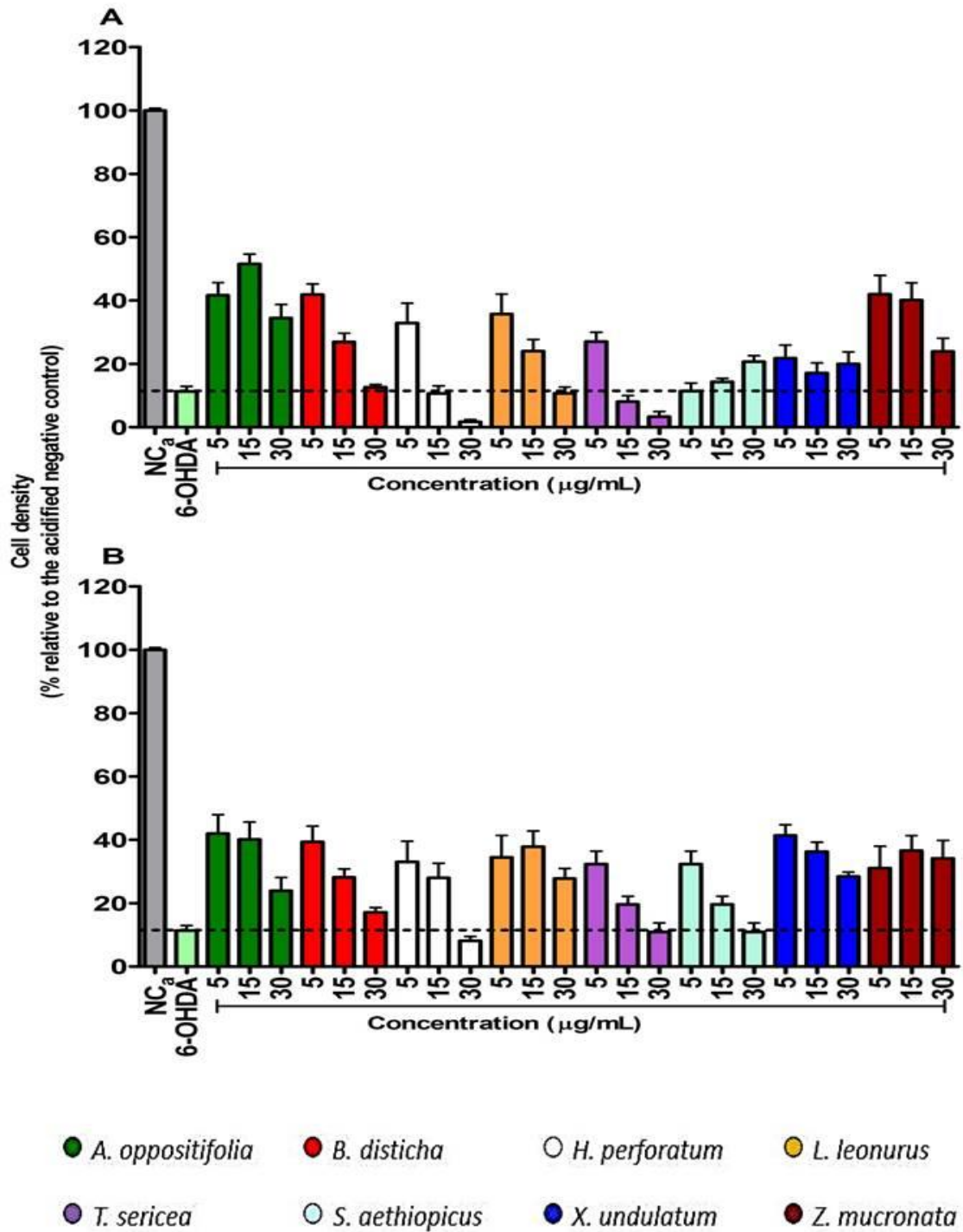


Figure 15: The neuroprotective effect of crude (A) acetone and (B) methanol extracts against 6-OHDA-induced neurotoxicity in the SH-SY5Y cell line after 72 h exposure. 6-OHDA- 6-hydroxydopamine, NC<sub>a</sub>- acidified negative control.

The variability between the acetone and methanol extracts of the same plant indicates that even though these solvents have the same polarity index, they are extracting different phytochemicals at varying quantities. Cytotoxicity studies are scarce on these plants, hence comparative literature is lacking. Furthermore, variability of literature that is available may also be due to different cell lines or incubation time and cytotoxicity assays used. Extracts of *S. aethiopicus* and *Z. mucronata* that initially showed poor neuroprotective effects (24 h exposure), had increased protection after 48 h, which may be due to the proliferative ability of the SH-SY5Y cell line or an artefact, rather than bioactivity. This may explain why previous studies<sup>97,98</sup> that used undifferentiated SH-SY5Y cells in the 6-OHDA PD model only looked at incubation times shorter than 24 h.

Although both extracts of *X. undulatum* displayed cytotoxicity, continuous neuroprotection was observed subsequent to 6-OHDA exposure at all incubation times. A different trend was observed with *T. sericea* which displayed low cytotoxicity but poor neuroprotection. This may therefore highlight that the presence of 6-OHDA may influence the pharmacodynamic profile due to interactions. On the other hand a paradoxical response was observed with *H. perforatum*, where neuroprotective effects were observed at 24 h and 72 h, but this was diminished at 48 h incubation.

The majority of the plant extracts induced greater neuroprotective activity at lower concentrations, suggesting that inherent cytotoxicity may be limiting their beneficial use at higher concentrations. Furthermore, the extracts of *A. oppositifolia*, *B. disticha* and *X. undulatum* showed consistent neuroprotection throughout the different exposure periods. Hence *A. oppositifolia*, *B. disticha* and *X. undulatum* were selected for further assessment. Subsequent experiments explored lower concentrations of *A. oppositifolia*, *B. disticha* and *X. undulatum* as lower concentration displayed better neuroprotection than higher concentration.

### **3.5. The effect of crude extracts on 6-OHDA-induced mitochondrial depolarisation**

Mitochondrial dysfunction has been implicated as an underlying cause of PD, and it is worth noting that the mitochondrion plays a key role in the coordination of mitochondrial-dependent apoptosis via the MPT pore.<sup>33</sup> Opening of the MPT pore is maintained by the MMP; depolarisation of the mitochondrial membrane will result in an opening of the MPT pore and ultimately cell death may occur.<sup>33</sup> Furthermore, the MMP needs to be maintained as it is essential for generation of ATP.<sup>33</sup>

Acidification of the medium, as well as exposure to DMSO (vehicle control), did not alter the MMP. The positive control tamoxifen (10  $\mu$ M), a non-steroidal anti-oestrogen drug, increased the MMP by approximately 0.5-fold. It has been reported that tamoxifen hyperpolarises the mitochondrial membrane by blocking the MPT pore.<sup>101,102</sup> Even though both studies were done in liver cells, it might still explain why the same trend was observed in the present study using the neuronal cell line (Figure 16).

The 6-OHDA-induced significant ( $p < 0.001$ ) 2-fold depolarisation of the mitochondrial membrane (Figure 16), as indicated by a reduced MMP, which is consistent with literature.<sup>48,98</sup> Lopes and colleagues monitored the effect of 6-OHDA on MMP every 3 h for 24 h, and found that after 12 h the MMP was similar for both proliferative and differentiated SH-SY5Y cells, and were both lower than the untreated control.<sup>48</sup>

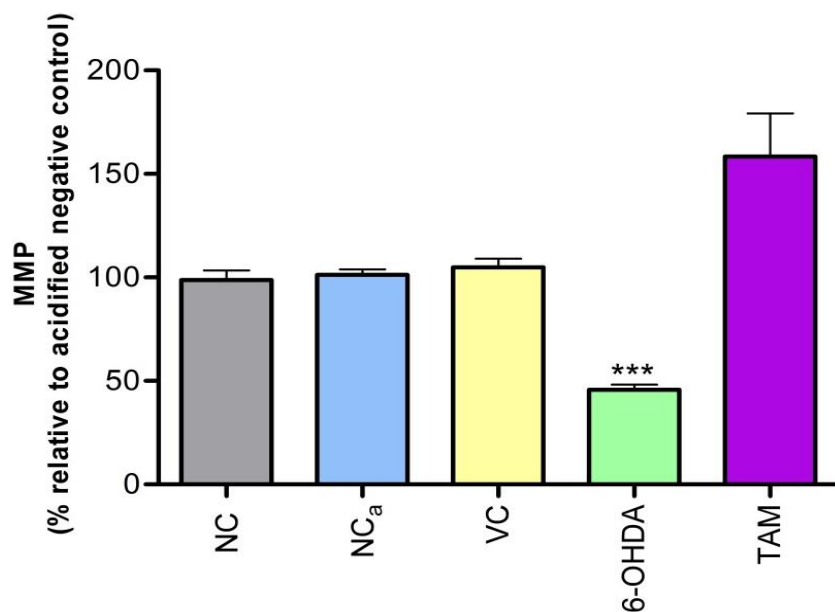


Figure 16: Effect of controls used during mitochondrial membrane potential assessment on the SH-SY5Y cell line. Significant difference to the 6-OHDA treatment relative to the NC<sub>a</sub>, \*\*\*  $p < 0.001$ . NC - negative control, NC<sub>a</sub> - acidified negative control, VC - vehicle control, 6-OHDA - 6-hydroxydopamine and TAM - tamoxifen (10  $\mu$ M) as positive control.

Plant extracts did not result in any marked improvement of MMP (Figure 17). The acetone extract of *A. oppositifolia* did not improve 6-OHDA-induced mitochondrial depolarisation, however, the methanol extract (1  $\mu$ g/mL) showed minimal attenuation thereof (Figure 17). Higher concentrations did not result in any improvement. Acetone extracts of *B. disticha* (5  $\mu$ g/mL) showed a non-significant increase in

MMP after treatment with 6-OHDA. Both extracts of *B. disticha* (15 µg/mL) potentiated 6-OHDA-induced MMP depolarisation. *Xysmalobium undulatum* increased MMP slightly; however, this was not statistically significant (Figure 17). Therefore the concentration range (0.5 - 15 µg/mL) of all extracts did not significantly improve 6-OHDA-induced depolarisation (Figure 17).

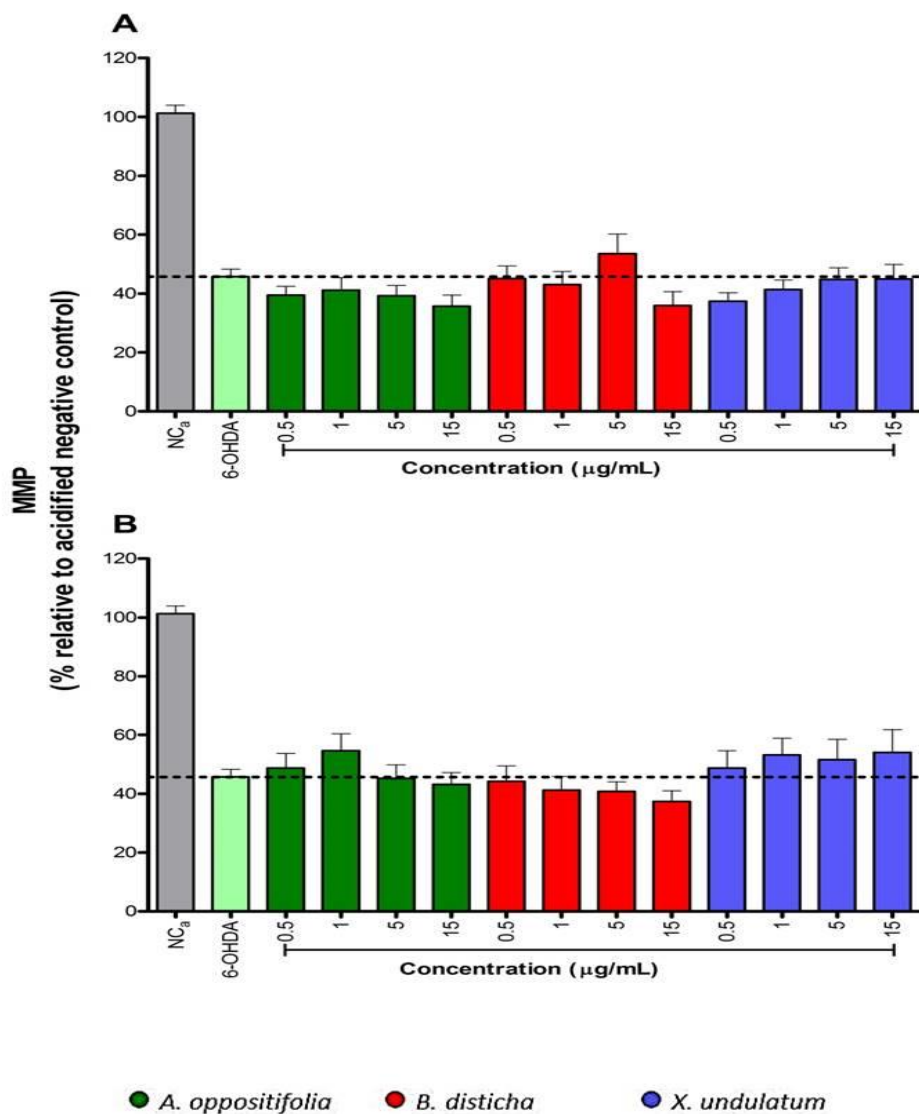


Figure 17: Effect of crude (A) acetone and (B) methanol extracts against 6-OHDA-induced mitochondrial membrane depolarisation in the SH-SY5Y cell line after 24 h incubation. 6-OHDA- 6-hydroxydopamine, NC<sub>a</sub>- acidified negative control.

Since mitochondria are the most metabolic active organelles, this makes it prone to injury or toxicity and crude extracts are rich in phytochemicals that may induce toxicity. Ly *et al.* found that cytochrome c

leaks out prior to mitochondrial membrane depolarisation.<sup>33</sup> Furthermore, loss of MMP is a common feature of apoptosis and necroptosis.<sup>38,39</sup> As cytotoxicity was attenuated, but mitochondrial depolarisation evident, it is possible that extracts may only be offering a protective effect downstream of mitochondrial toxicity. Furthermore, this brings to light the possibility that although a neuroprotective effect is offered with regards to cell density, mitochondrial damage may still be prevalent, which could result in further damage at a later stage.

### **3.6. The effect of crude extracts on 6-OHDA-induced oxidative stress**

Reactive oxygen species remain a major area of research and are implicated in many medical conditions such as cancer, inflammation and PD.<sup>3</sup> Reactive oxygen species which are produced as metabolic by-products, play a role in immune responses against pathogens and also function as signalling molecules.<sup>3</sup>

The vehicle control did not significantly increase ROS compared to the acidified negative control (Figure 18). AAPH significantly ( $p < 0.01$ ) increased ROS concentrations by 5-fold. The peroxy radical generator AAPH is known to be capable of oxidising proteins, lipids and DNA.<sup>103,104</sup>

6-Hydroxydopamine increased intracellular ROS generation 3-fold, which is consistent with previous studies.<sup>96,97,105</sup> Mahani *et al.* exposed SH-SY5Y cells to 150  $\mu\text{M}$  6-OHDA for 24 h, which induced a 40% increase in ROS.<sup>97</sup> Furthermore, Kopalli *et al.* observed more than 50% increase in ROS after exposure to 20  $\mu\text{M}$  6-OHDA for 2 h in SH-SY5Y cells.<sup>96</sup> Lee *et al.* observed a 2-fold increase of ROS in rat pheochromocytoma (PC12) cells after exposure to 50  $\mu\text{M}$  6-OHDA for 24 h.<sup>105</sup> In PC12 cells exposed to 75  $\mu\text{M}$  6-OHDA for 30 min, Fujita *et al.* observed a 4-fold increase in ROS measured using the hydroethidine assay.<sup>106</sup> The induction of ROS is dependent on the concentration of 6-OHDA, duration of incubation, type of cell line and ROS assay used. Furthermore, the fluorescence results in the present study were normalised to protein content (using the SRB assay) to account for varying cell density due to cell death, which was not done in the referenced literature.

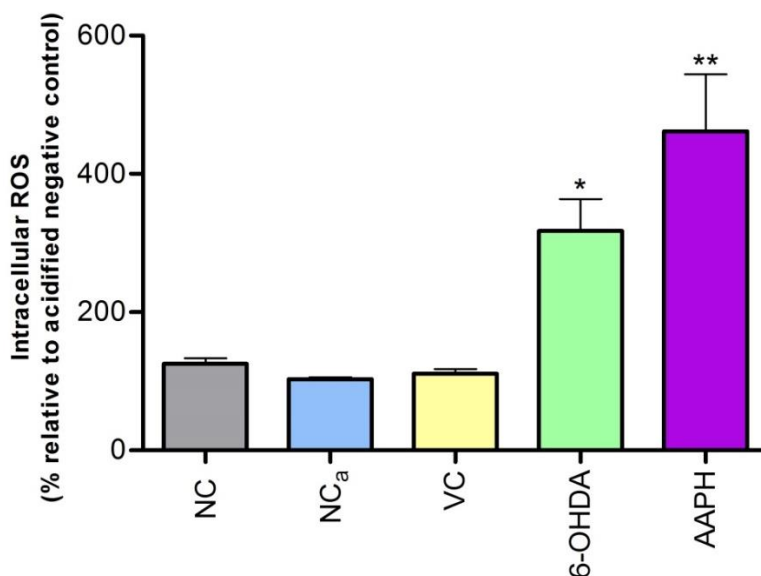


Figure 18: Effect of controls used during reactive oxygen species assessment on the SH-SY5Y cell line. Significant difference to the 6-OHDA treatment relative to the NC<sub>a</sub>, \*  $p < 0.05$  and \*\*  $p < 0.01$ . NC - negative control, NC<sub>a</sub> - acidified negative control, VC - vehicle control, 6-OHDA - 6-hydroxydopamine and AAPH - 2,2'-azobis (2-methylpropionamide) dihydrochloride as positive control.

Methanol and acetone extracts of *A. oppositifolia* prevented 6-OHDA-induced oxidative stress, most likely attenuated by flavonoid and phenolic content (Figure 19). Sharma and colleagues reported that methanol and acetone extracts *A. oppositifolia* have ROS scavenging ability.<sup>63</sup> Additionally, Sharma *et al.* reported that both acetone and methanol extracts displayed significant iron-chelating abilities,<sup>63</sup> which may be beneficial in PD as iron plays a significant role in the induction of oxidative stress.

Both extracts of *B. disticha* displayed a higher protective activity at lower concentrations (Figure 19). Higher concentrations of *B. disticha* may produce their own burden of free radicals, which reduces their ability to offer protection. This effect is consistent with the lower neuroprotection offered at higher concentrations in other assays. Adewusi *et al.* reported that the methanol extract of the *B. disticha* bulb did not have any ROS scavenging activity, however, the methanol extract of the roots did show sufficient antioxidant activity (86  $\mu\text{g}/\text{mL}$  and 130  $\mu\text{g}/\text{mL}$  using the ABTS and DPPH scavenging assays, respectively).<sup>91</sup>

Both extracts of *X. undulatum* decreased 6-OHDA-induced ROS (Figure 19). The ROS scavenging ability of *X. undulatum* was constant over all the concentrations assessed.

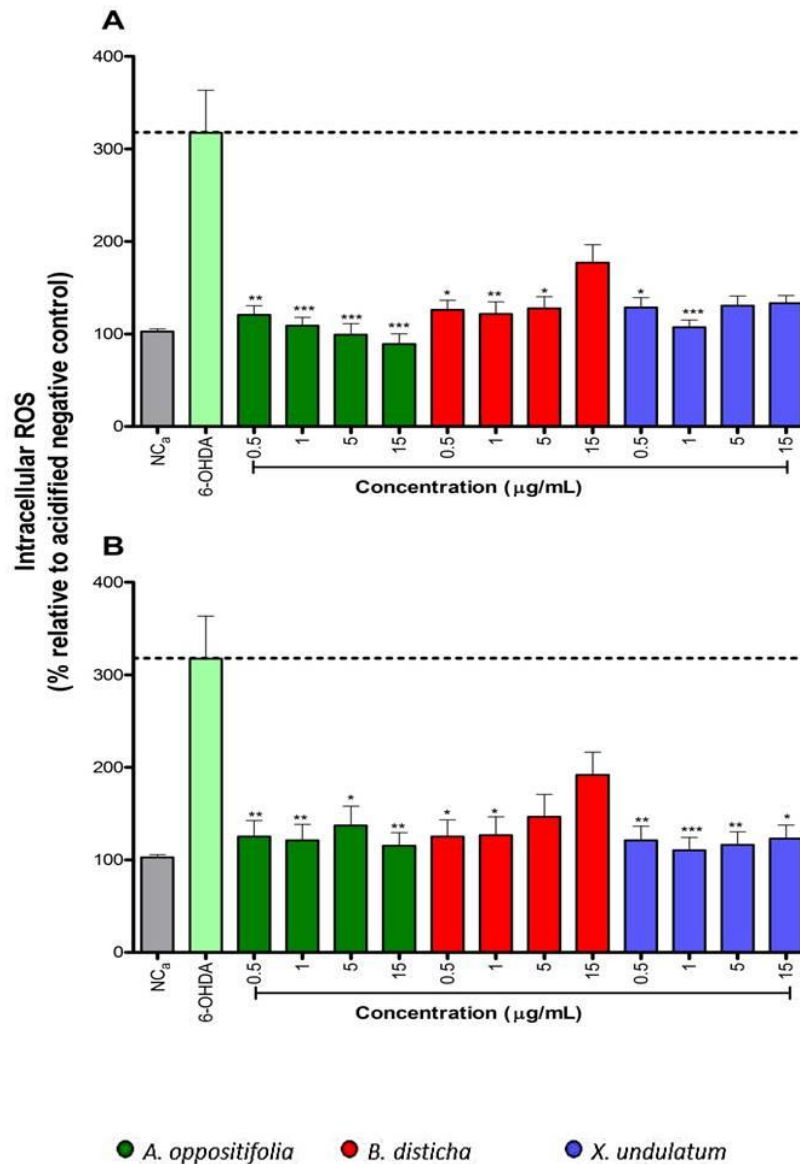


Figure 19: The effect of crude (A) acetone and (B) methanol extracts against 6-OHDA-induced ROS in the SH-SY5Y cell line after 24 h incubation. Significant difference to the 6-OHDA treatment relative to the NC<sub>a</sub>, \* p < 0.05, \*\* p < 0.01 and \*\*\* p < 0.001. 6-OHDA - 6-hydroxydopamine, NC<sub>a</sub> - acidified negative control.

Plant extracts decreased 6-OHDA-induced ROS generation, most likely due to flavonoid, diterpenoid and phenolic content.<sup>2,73</sup> 6-Hydroxydopamine induces ROS by auto-oxidation, deamination by MAO-B and by blocking mitochondrial complex 1.<sup>107</sup> Blum *et al.* reported the presence of H<sub>2</sub>O<sub>2</sub> in cell-free culture media subsequent to 6-OHDA exposure thus indicating that 6-OHDA is capable of inducing extracellular

ROS.<sup>107</sup> Taking the latter into account crude extracts may neutralize ROS through direct scavenging of extracellular ROS or by upregulating the expression of endogenous antioxidants, such as GSH to neutralise intracellular ROS, hence GSH levels were subsequently assessed.

Crude extracts attenuated 6-OHDA-induced ROS, but in previous experiments they did not have an effect on 6-OHDA-induced depolarisation of the mitochondrial membrane. This may indicate that the majority of the ROS generated may be extracellular rather than mitochondrial. Extracellular ROS induced by the auto-oxidation of 6-OHDA, may damage lipids in the plasma membrane. These results are consistent with the neuroprotection offered in the cytotoxicity assays, suggesting that a decrease in cytotoxicity may involve diminished ROS levels. Furthermore plant extracts may be beneficial in PD, as elevated ROS remains a common feature in PD.<sup>12</sup>

### **3.7. The effect of crude extracts on 6-OHDA-induced alterations to reduced glutathione**

The severity of PD has been linked to GSH depletion.<sup>34</sup> Buthionine sulfoximine, an inhibitor of GCS, induces PD-like characteristics both *in vitro* and *in vivo*, giving credence to the GSH-deficiency hypothesis.<sup>12</sup> Reduced glutathione depletion may cause oxidative stress<sup>11</sup> and ultimately induce ETC dysfunction.<sup>35</sup> Mitochondrial complex I is sensitive to ROS during GSH depletion because of oxidation-sensitive iron-sulphur centres within the enzyme and the high concentration of thiol groups that require GSH.<sup>35</sup>

Acidification or DMSO did not alter GSH levels (Figure 20). The positive control BSO, an irreversible inhibitor of  $\gamma$ -GCS, decreased intracellular GSH as compared to the negative control and the 6-OHDA-treated cells (Figure 20). The 6-OHDA induced a 2-fold increase in intracellular levels of GSH levels, which is contradictory to literature.<sup>108</sup> PC12 cells treated with 6-OHDA (150  $\mu$ M) for 48 h displayed a significant decrease in intracellular GSH levels however, this was observed without normalisation.<sup>108</sup> Furthermore, Lee *et al.* observed exposure to 50  $\mu$ M 6-OHDA depletes intracellular GSH after 24 h.<sup>105</sup> In contrast to the aforementioned studies, Tirmenstein and colleagues observed an increase in intracellular GSH levels after exposure to 6-OHDA (500  $\mu$ M) for 4 h.<sup>109</sup> This may therefore indicate that the duration of exposure and the concentration of 6-OHDA may affect intracellular GSH levels. Alternatively, the cells may increase the intracellular GSH levels as an adaptive response to increased ROS levels.<sup>109</sup> It is worth noting that studies that observed elevated intracellular GSH levels had normalised the fluorescence

readings to protein content, i.e. ratiometric monitoring, which is similar to what has been done in the present study. Ratiometric monitoring is more reliable as it accounts for signal artefacts such as varying cell density and dye concentration.<sup>80</sup>

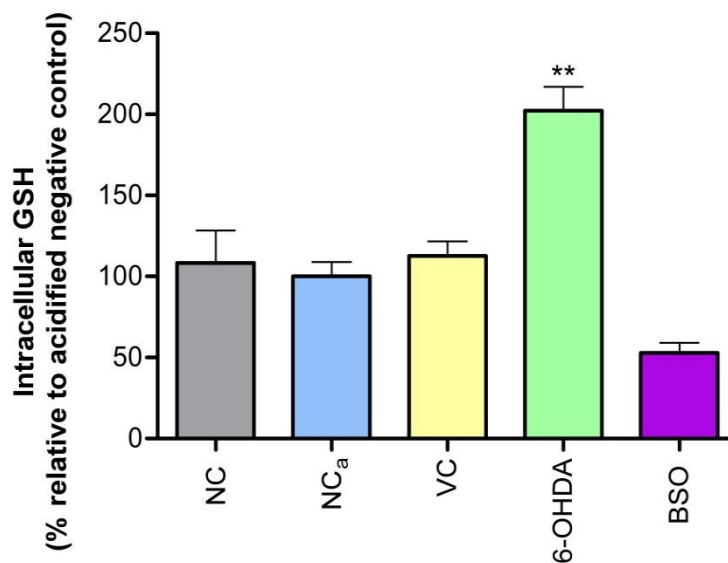


Figure 20: Effect of controls used during intracellular glutathione assessment on the SH-SY5Y cell line. Significant difference to the 6-OHDA treatment relative to the NC<sub>a</sub>,\*\*  $p < 0.01$ . NC - negative control, NC<sub>a</sub> - acidified negative control, VC - vehicle control, 6-OHDA - 6-hydroxydopamine and BSO - buthionine sulfoximine as a positive control (PC).

The methanol and acetone extract of *A. oppositifolia* reduced the 6-OHDA-induced GSH increase (Figure 21). Both extracts of *B. disticha* showed a trend of dose-dependent decrease of 6-OHDA-induced increase in GSH (Figure 21). The methanol extracts of *X. undulatum* significantly ( $p < 0.01$ ) reduced 6-OHDA-induced increase in GSH (Figure 21).

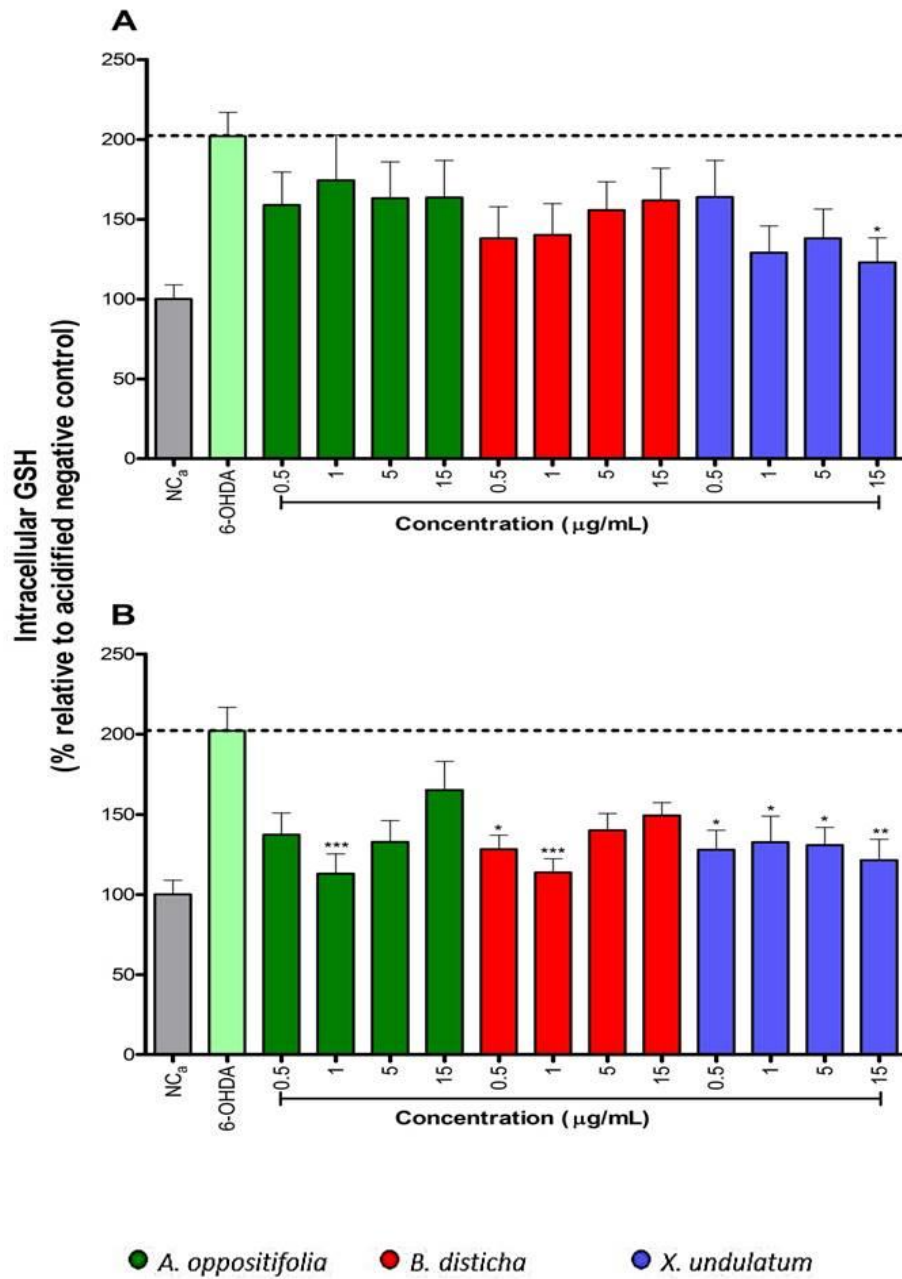


Figure 21: Effect of crude (A) acetone and (B) methanol extracts against 6-OHDA-induced increase in intracellular glutathione levels in the SH-SY5Y cell line after 24 h incubation. Significant difference to the 6-OHDA treatment relative to the NC<sub>a</sub>. 6-OHDA - 6-hydroxydopamine, NC<sub>a</sub> - acidified negative control.

In Section 3.6 the plant extracts were able to neutralise 6-OHDA-induced ROS, however, this could not be paralleled to intracellular GSH levels. This therefore may indicate that mechanism of ROS neutralisation used by crude extracts does not involve intracellular GSH.

Alternatively, during detoxification GSH is able to conjugate to xenobiotics (e.g. phytochemicals) to form phase II metabolites, a reaction catalysed by glutathione *S*-transferase.<sup>12,33</sup> Such a decrease in intracellular GSH would coincide with the reduced fluorescence observed during the MCB assay.

In PD patients, the GSH levels in the brain is critically low<sup>12</sup> and plant extracts that maintain intracellular GSH levels above threshold may be beneficial.

### **3.8. The effect of crude extracts on 6-OHDA-induced decreased intracellular adenosine tri-phosphate**

Adenosine tri-phosphate is an energy-rich molecule that is required for maintaining normal cellular processes. The production of ATP is dependent on glycolysis, the Krebs cycle and the ETC.<sup>110</sup> By definition, glycolysis is the metabolism of glucose and other sugars into pyruvate to produce ATP; this process is rapid and often preferred by cancer cells (such as the SH-SY5Y cell line).<sup>110</sup> Oxidative phosphorylation on the other hand is an oxygen-dependent pathway that couples oxidation of macromolecules to the ETC to generate ATP.<sup>110</sup> In PD models, the oxidative pathway is hindered by blocking mitochondrial complex I, thus impairing ATP production, inducing ROS generation, and subsequently inducing cell death.<sup>30</sup>

The vehicle control did not alter ATP levels (Figure 22). Saponin, abolished ATP levels, which is consistent with the cytotoxicity results, discussed earlier (Figure 11). Treatment with 6-OHDA induced more than 2-fold decrease in ATP levels (Figure 22). Tirmenstein *et al.* reported a decrease in intracellular ATP levels after exposure to 6-OHDA at varying concentrations and incubation times.<sup>109</sup> Mazzio *et al.* also reported a 6-OHDA-induced decrease in ATP levels in N-2A cells after treatment with 500  $\mu$ M 6-OHDA for 24 h.<sup>45</sup> These effects are most likely a product of mitochondrial toxicity due to interrupted ETC functions.

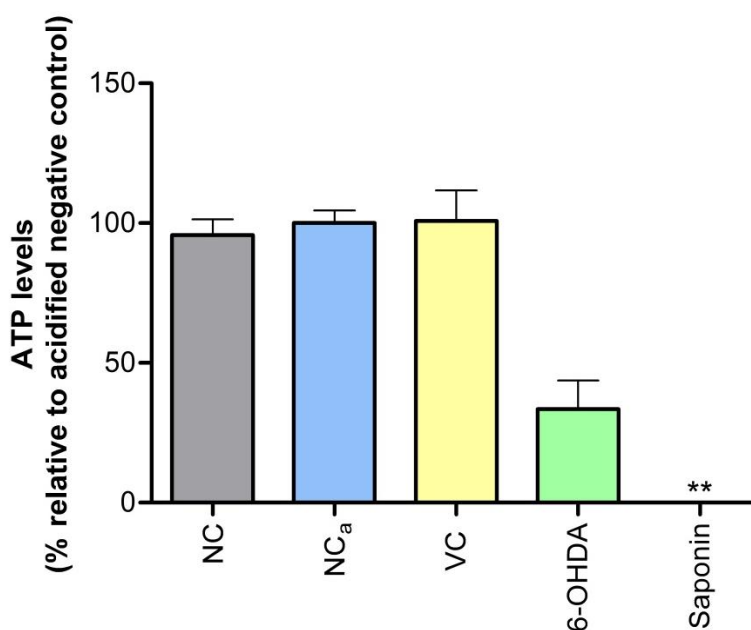


Figure 22: Effect of controls used during intracellular ATP assessment on the SH-SY5Y cell line. Significant difference to the 6-OHDA treatment relative to the NC<sub>a</sub>, \*\*  $p < 0.01$ . NC - negative control, NC<sub>a</sub> - acidified negative control, VC - vehicle control, 6-OHDA - 6-hydroxydopamine and 1% saponin as a positive control.

The acetone and methanol extracts of *A. oppositifolia* and *B. disticha*, respectively, a trend of increased ATP levels at  $<15 \mu\text{g/mL}$ . However, at  $15 \mu\text{g/mL}$ , ATP was decreased further (Figure 23). This effect supports the greater neuroprotection offered by lower concentrations, and the potential for additive cytotoxicity at higher concentrations. The methanol extracts of *A. oppositifolia* and *X. undulatum* displayed a plateaued effect, maintaining ATP levels 2-fold above the 6-OHDA-induced decrease (Figure 23). Overall, all extracts improved 6-OHDA-induced decrease in ATP levels, however, these effects were not statistically significant.

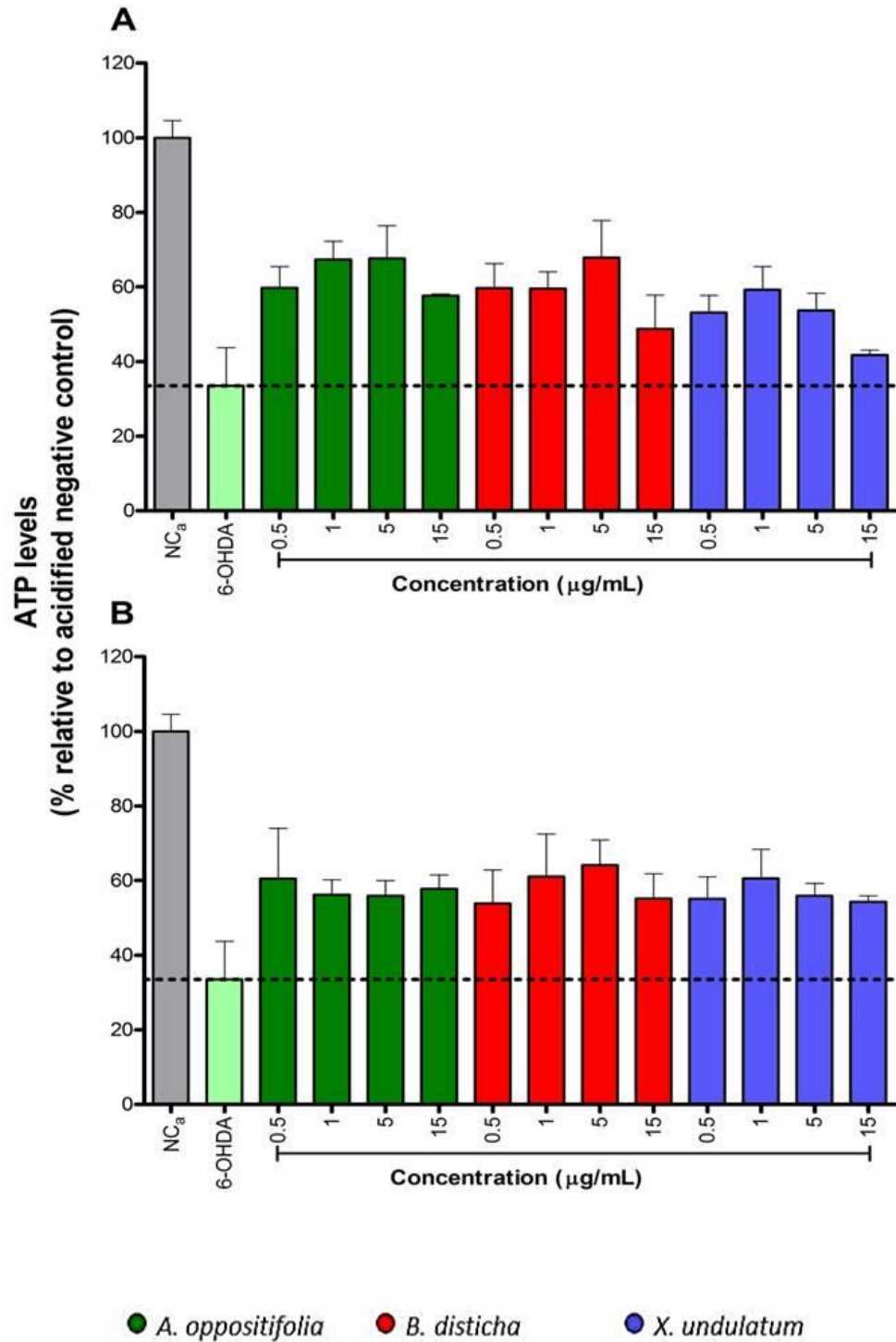


Figure 23: Effect of crude (A) acetone and (B) methanol extracts on ATP levels after pre-treatment with 6-OHDA on SH-SY5Y cell line after 24 h incubation. 6-OHDA - 6-hydroxydopamine, NC<sub>a</sub> - acidified negative control

Taking into account that the neuroblastoma cells are a cancerous cell line, these cells are capable of shifting their ATP-generation from oxidative phosphorylation to the less efficient, but rapid, glycolysis.<sup>110</sup> Furthermore, rapid glycolysis results in increased production of pyruvic acid which enters the Krebs cycle. In anaerobic conditions, pyruvic acid is converted to lactic acid by the enzyme lactic acid dehydrogenase (LDH). Tirmenstein *et al.* reported a significant increase in LDH in SH-SY5Y cells after exposure to 50  $\mu\text{M}$  6-OHDA for 24 h.<sup>109</sup> Zhu *et al.* observed the same trend in PC12 cells after exposure to 100  $\mu\text{M}$  6-OHDA for 24 h.<sup>111</sup> Both studies paralleled the 6-OHDA-induced increase in LDH to cytotoxicity.<sup>109,111</sup> Since crude extracts did not impact MMP, but improved ATP levels, it would suggest that the crude extract potentiated the glycolytic pathway rather than oxidative phosphorylation. However, the extracts could still be beneficial in PD, as one of the triggers for neuronal cell death is ATP depletion.<sup>11,33</sup>

### **3.9. The effect of crude extracts on 6-OHDA-induced decreased intracellular calcium flux**

Calcium is one of the most regulated ions in the cell. Homeostasis of intracellular  $\text{Ca}^{2+}$  requires high amounts of energy, as cells prefer to store  $\text{Ca}^{2+}$  in endoplasmic reticulum and mitochondria, which are released after appropriate stimulation.<sup>28,32</sup> Mitochondrial-stored  $\text{Ca}^{2+}$ , together with  $\text{H}^+$ , drives ATP production.<sup>28</sup> However, in PD the production of ATP is hindered, hence a subsequent intracellular  $\text{Ca}^{2+}$  overload is observed.<sup>28</sup> During  $\text{Ca}^{2+}$  overload,  $\text{Ca}^{2+}$  can directly interact with ANT on the MPT pore to stimulate its opening.<sup>28,33</sup> Once the MPT pore is opened it perturbs the ETC and intracellular osmolality, which results in the leakage of cytochrome c, and ultimately causes cell death if not remedied.<sup>11,33</sup>

Calcium levels were not altered by acidification of medium or the vehicle control (Figure 24). The positive control, EGTA, is a  $\text{Ca}^{2+}$  chelator, which depletes intracellular  $\text{Ca}^{2+}$  levels.<sup>112</sup> The exposure to 6-OHDA induced a decreasing trend in intracellular  $\text{Ca}^{2+}$  levels (Figure 24). Contradictory observations of 6-OHDA on intracellular  $\text{Ca}^{2+}$  levels have been reported. Lee and colleagues reported that treatment with 50  $\mu\text{M}$  6-OHDA for 24 h reduced intracellular  $\text{Ca}^{2+}$  levels.<sup>105</sup> Meng and colleagues found a 3-fold increase in intracellular  $\text{Ca}^{2+}$  in PC12 cells after treatment with 100  $\mu\text{M}$  6-OHDA for 24 h.<sup>113</sup> The study utilised a non-ratiometric dye, Fluo-3, which does not account for varying cell densities and other signal artefacts. Huang and colleagues observed an increase in intracellular  $\text{Ca}^{2+}$  in embryonic SNc of a transgenic mouse (SN4741 cells) after treatment with 6-OHDA (1  $\mu\text{M}$ ) for 20 min.<sup>114</sup> Subsequently the 6-OHDA-induced increase in intracellular  $\text{Ca}^{2+}$  was inhibited by addition of ryanodine, indicating that ryanodine- $\text{Ca}^{2+}$

channels may play a role in  $\text{Ca}^{2+}$  overload present in PD.<sup>114</sup> Another aspect that may explain contradictory reports is varying concentrations of 6-OHDA and the technique used to quantify intracellular  $\text{Ca}^{2+}$ .

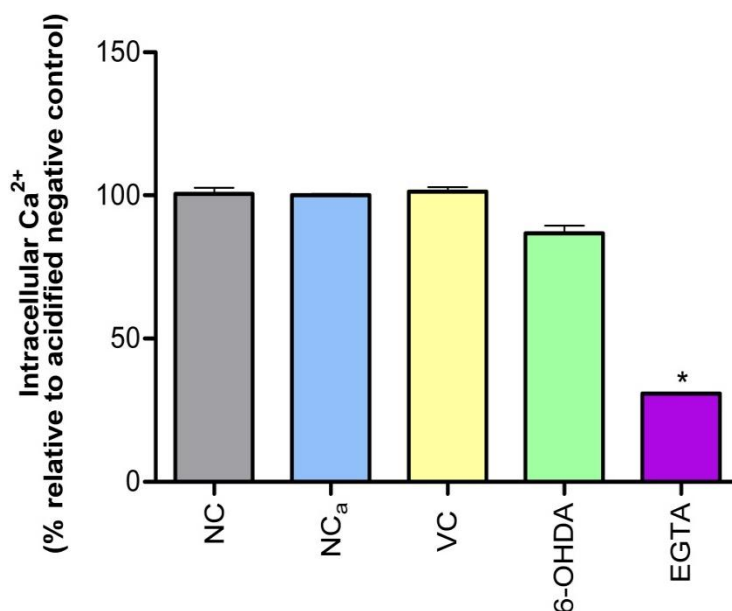


Figure 24: Effect of controls on intracellular calcium levels on the SH-SY5Y cell line. Significant difference to the 6-OHDA treatment relative to the  $\text{NC}_a$ , \*  $p < 0.05$ . NC - negative control,  $\text{NC}_a$  - acidified negative control, VC - vehicle control, 6-OHDA - 6-hydroxydopamine and EGTA - ethylene glycol-bis(2-aminoethylether)-N,N,N',N'-tetraacetic acid as positive control.

Extracts of *A. oppositifolia* decreased intracellular  $\text{Ca}^{2+}$  levels (Figure 25). The extracts of *B. disticha* maintained constant levels of intracellular  $\text{Ca}^{2+}$  across the concentrations tested (Figure 25). The acetone extract of *X. undulatum* displayed a trend of dose-dependent decrease in intracellular  $\text{Ca}^{2+}$  levels, whereas the treatment with the methanol extract decreased intracellular  $\text{Ca}^{2+}$  levels slightly (Figure 25). None of the crude extract increased intracellular  $\text{Ca}^{2+}$  levels to basal levels. Even more so, the extracts of *A. oppositifolia* potentiated 6-OHDA-induced decrease in intracellular  $\text{Ca}^{2+}$  levels.

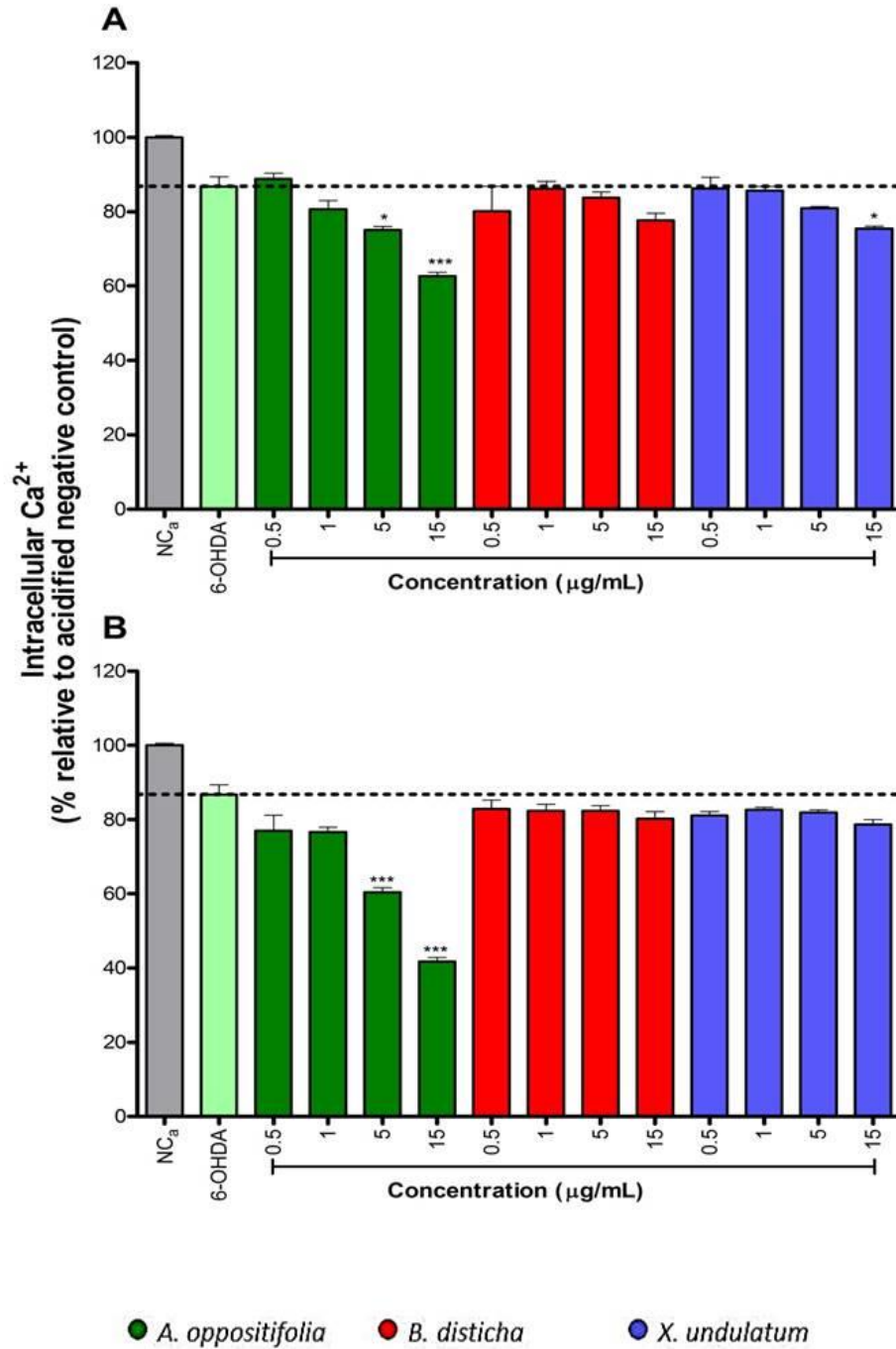


Figure 25: Effect of crude (A) acetone and (B) methanol extracts on intracellular calcium levels after pre-treatment with 6-OHDA in the SH-SY5Y cell line after 24 h incubation. Significant difference to the 6-OHDA treatment relative to the NC<sub>a</sub>, \* p < 0.05 and \*\*\* p < 0.001. 6-OHDA - 6-hydroxydopamine, NC<sub>a</sub> – acidified negative control

Plants such as *A. oppositifolia*, which are rich in cardiac glycosides,<sup>62</sup> were not expected to decrease intracellular  $\text{Ca}^{2+}$ . Cardiac glycosides are known to block the  $\text{Na}^+/\text{K}^+$  ATPase, thus increasing intracellular sodium levels which subsequently block the sodium-calcium exchanger (NCX).<sup>115</sup> The NCX is responsible for exchanging intracellular  $\text{Ca}^{2+}$  for two extracellular sodium ions, thus inhibiting the NCX will result in  $\text{Ca}^{2+}$  overload. Since none of the plants extracts induced intracellular  $\text{Ca}^{2+}$  overload it could mean that cardiac glycosides were not extracted or the pathway that mediates this effect may be blocked. Alternatively, the decrease in intracellular  $\text{Ca}^{2+}$  may be due to diterpenes, as Meng *et al.* reported that a diterpene from *G. biloba*, ginkgolide B, decreased intracellular  $\text{Ca}^{2+}$  subsequent to 6-OHDA-induced  $\text{Ca}^{2+}$  overload.<sup>113</sup> In summary, the plant extracts did not induce detrimental  $\text{Ca}^{2+}$  overload, suggesting they could be safe to use in PD. Furthermore, ionic fluxes are time dependent and manual addition of plants/6-OHDA could have influenced the results.

### **3.10. The effect of plant extracts and 6-OHDA on cellular morphology**

Polarisation-optical transmitted light differential interference contrast microscopy uses enhanced linearity of polarised light emitted after the objective therefore generating higher quality images.<sup>81</sup> Cell morphology studies are important to indicate cell death and other morphological factors that might affect cell viability.

The negative and the acidified negative control displayed healthy, dense cells, with minimal apoptotic features. Staurosporine induced significant cell death (Figure 26). Belmokhtar *et al.* reported that staurosporine is capable of inducing both caspase-dependent and caspase independent cell death in mouse leukaemia (L1210/0) cells and several other cell lines.<sup>116</sup> Treatment with 6-OHDA caused cells to become more round and lose density. These morphological changes are consistent with apoptosis.<sup>97</sup> Latchoumycandane *et al.* reported increased levels of cytoplasmic cytochrome c after rat mesencephalic dopaminergic neurons were exposed to 100  $\mu\text{M}$  6-OHDA for 3 h and 6 h.<sup>117</sup> Furthermore, Mahani *et al.* also reported increased levels of cytochrome c after exposure to 150  $\mu\text{M}$  of 6-OHDA for 24 h.<sup>97</sup> The cytochrome c released by mitochondria through the MPT pore is known to activate the caspase cascade. Caspase-3 is a major key player in oxidative stress-induced apoptosis, hence, elevated levels after exposure to 6-OHDA were reported.<sup>117</sup> Latchoumycandane *et al.* further reported a significant increase in both caspase-3 and -9 subsequent to exposure to 6-OHDA (100  $\mu\text{M}$ ) for 6 and 12 h.<sup>117</sup> Ju *et al.* further reported that treatment with 6-OHDA increased intracellular levels of caspase-3 and enhanced DNA

fragmentation and concluded that the mode of cell death for 6-OHDA could be apoptotic cell death or necroptosis.<sup>98</sup> Contradictory to these studies Li *et al* reported elevated levels of autophagy markers such lysosomal-associated membrane protein 1 and autophagy protein: light chain 3 after treatment with 6-OHDA (50  $\mu$ M) for 24 h in SH-SY5Y cells.<sup>118</sup> Furthermore, additional pre-treatment with 3-methyladine, autophagy repressor, increased caspase-3 indicating a switch from autophagy to apoptosis.<sup>118</sup>

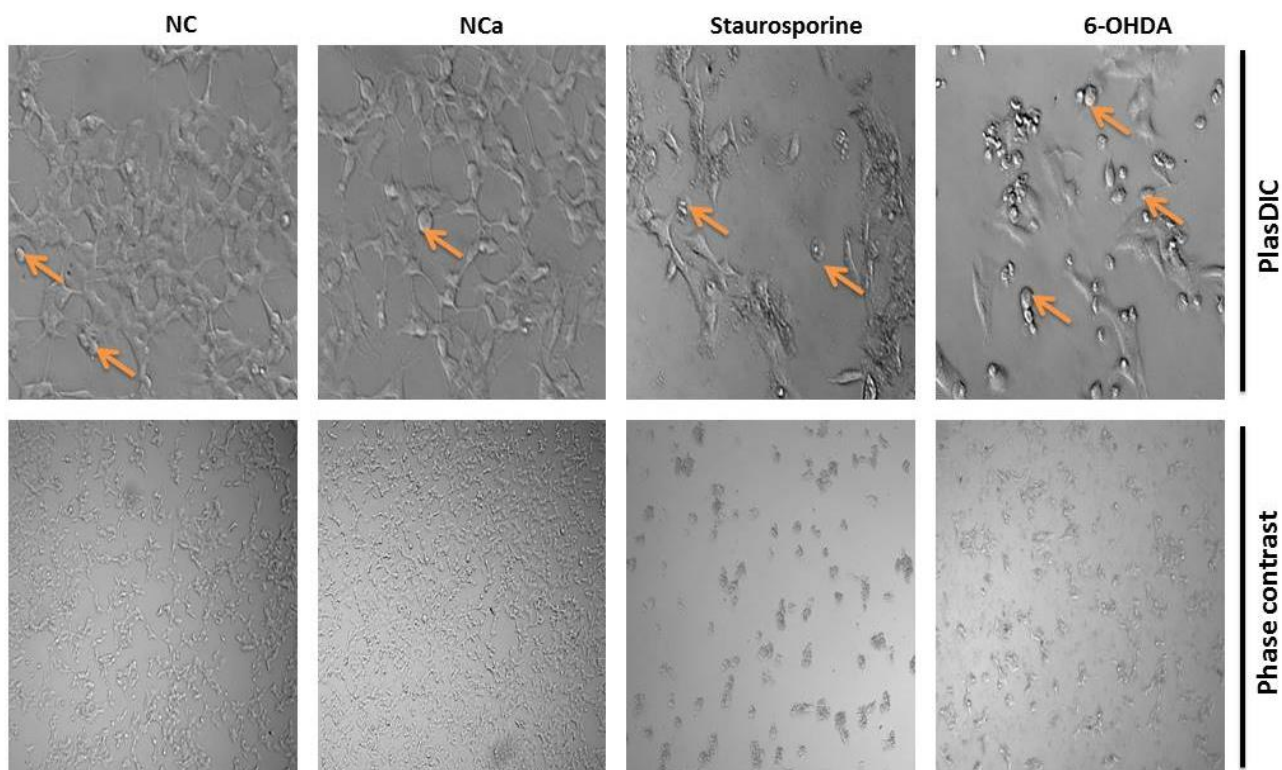


Figure 26: The effect of controls and 6-OHDA on cellular morphology of the SH-SY5Y cell line using phase contrast microscopy and polarisation-optical transmitted light differential interference contrast (PlasDIC) microscopy. A magnification of 5x and 40x was used for phase contrast and PlasDIC microscopy, respectively. Arrows indicate apoptotic bodies. NC - negative control, NC<sub>a</sub> - acidified negative control and staurosporine (20  $\mu$ M) as positive control.

Acetone extracts of *A. oppositifolia* (Figure 27) had less effect on cell morphology than methanol extracts (Figure 28), which is consistent with the neuroprotection results (Figure 14). Lower concentrations (0.5  $\mu$ g/mL) of both extracts of *B. disticha* displayed better neuroprotective effects than the 5  $\mu$ g/mL treated cells (Figure 27 and 28); the same trend was observed in the cytotoxicity assay

(Figure 14). Both extracts of *X. undulatum* indicated comparable neuroprotection, thus the neuroprotection was not dose-dependent (Figure 27 and 28).

Cell morphology results are consistent with cytotoxicity. However, morphology alone cannot be used to differentiate between necrosis and apoptosis. Even though the mode of cell death could not be deduced, crude extracts were still able to improve cell viability, thus creating a platform for further studies. Maintaining the viability of dopaminergic neurons in PD may greatly improve the efficacy of current PD treatment.

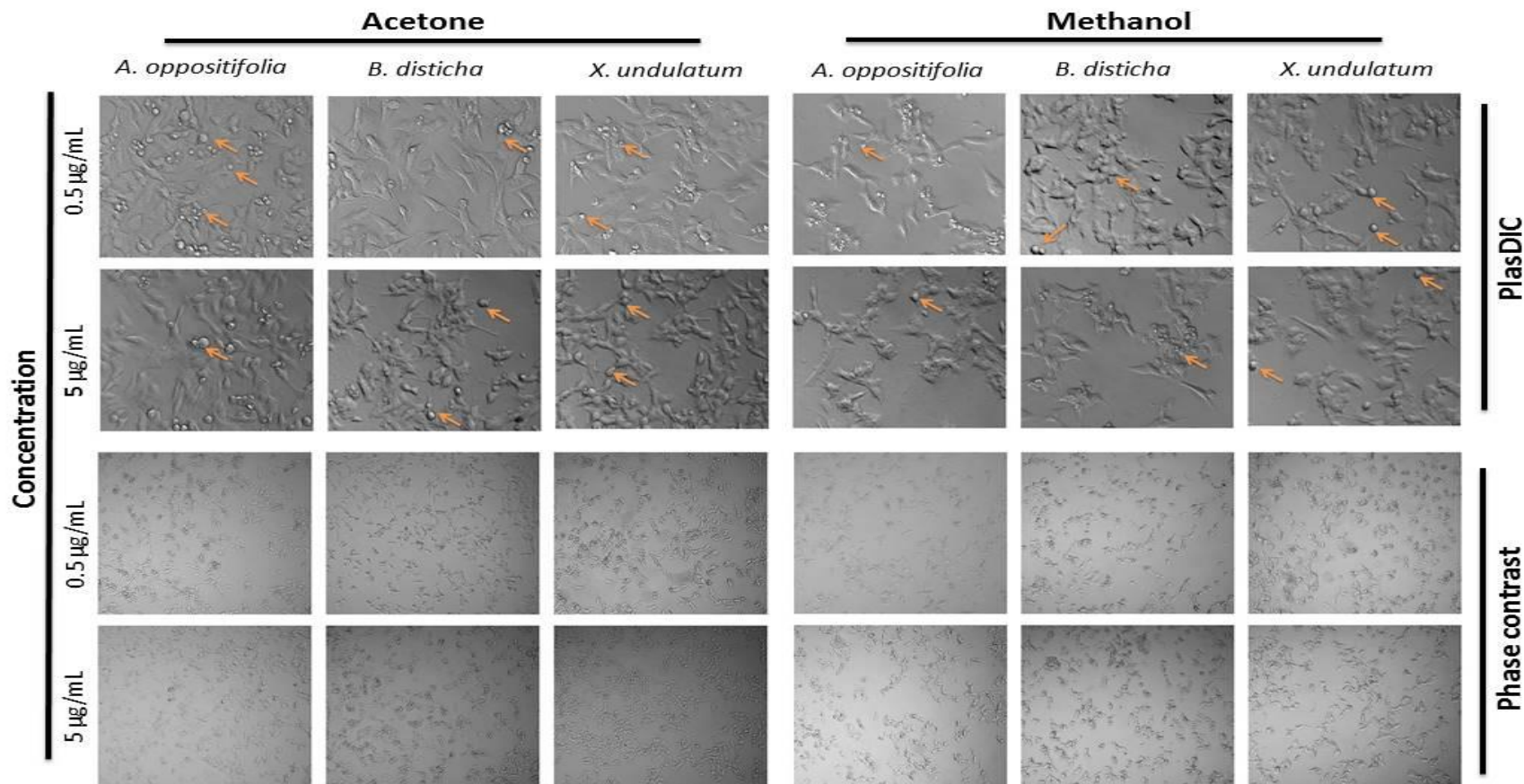


Figure 27: Effect of acetone and methanol extracts (0.5 and 5 µg/mL) on cellular morphology in SH-SY5Y cell line pre-treated with 6-OHDA and incubated for 24h. A magnification of 5x and 40x was used for phase contrast and PlasDIC microscopy, respectively. Arrows indicate apoptotic bodies. 6-OHDA- 6-hydroxydopamine, PlasDIC- polarisation-optical transmitted light differential interference contrast microscopy.

# Chapter 4: Conclusion

## 4.1. Concluding remarks

Parkinson's disease is the progressive loss of dopaminergic neurons in the brain, resulting in hypodopaminergic activity.<sup>6,9,10</sup> Hence, current treatment strategy aims to replace dopamine levels, which over time becomes ineffective and does not preserve existing neurons.<sup>5,8,15</sup> Researchers agree that dopamine replacement therapy together with neuroprotection may prove to be beneficial.<sup>57</sup> Several African medicinal plants have been used to treat various neurological conditions indicating that they may potentially be neuroprotective.

The neurotoxin, 6-OHDA, induced PD-like effects in the SH-SY5Y cell line, creating a model to study PD *in vitro*. Of the eight plant extracts screened only the crude extracts of *A. oppositifolia*, *B. disticha* and *X. undulatum* were selected for further assessment against 6-OHDA-induced cytotoxicity due to their neuroprotective effects. Neuroprotection appeared to be linked to reduced ROS generation, but not mitochondrial protection or Ca<sup>2+</sup> regulation. Adenosine tri-phosphate levels were maintained, suggesting unperturbed bioenergetics. Morphology studies were sufficient to support neuroprotective effects of the crude extracts; however, the mode of 6-OHDA-induced cell death remains controversial. Of note is that lower concentrations of the crude extracts (0.5 -5 µg/mL) offered greater neuroprotective activity, suggesting a potent effect that warrants further isolation studies. Although cell density and ATP levels were increased, it does appear that mitochondrial toxicity remains unaltered, suggesting that phytochemicals are not deterring mitochondrial-toxicity. This may result in delayed neurotoxic effects. Although the greatest level of neuroprotection was offered by *X. undulatum*, it is important to mention that the extracts themselves were highly cytotoxic, which may bolster further development. Isolation studies would be required to identify the phytochemicals producing the beneficial and cytotoxic effects, if not the same. Additionally, studies report that by the time PD symptoms are evident, more than 80% of the neurons have been lost and the remaining neurons will also die despite dopamine replacement therapy.<sup>16,17</sup> However, in this study crude extracts of *A. oppositifolia*, *B. disticha* and *X. undulatum* were able to maintain consistent cell viability providing neuroprotection. This indicates that the plants alone will not cure PD but they may potentially be used as adjuncts to current PD treatment to preserve existing dopaminergic neurons. Furthermore, the mechanism of neuroprotection may involve the ability to neutralise ROS, and sustain ATP production under pathological conditions. Future studies are

required to elucidate the mode of cell death used by 6-OHDA as well as the potential mitochondrial targets that sustains ATP production to stimulate survival.

## 4.2. Recommendations and limitations

The 6-OHDA and MPP<sup>+</sup> models are widely accepted as *in vitro* and *in vivo* models of PD; however, there were a few contradictions presented in literature about their pathological mechanisms. For example, several studies reported a decrease in intracellular GSH levels subsequent 6-OHDA exposure in different neuronal cell lines, whereas others gave a contradictory report. This therefore indicates that there is a need for an optimised *in vitro* model that can directly mimic the neurochemical pathogenesis of PD even *in vitro*. Furthermore, contradictory results with GSH and other assays was due to normalisation of fluorescence results with protein content; this practice should gradually be introduced in *in vitro* studies as it accounts for signal artefacts.

Additionally, no improvement in mitochondrial dysfunction was observed subsequent to treatment with neuroprotective plant extracts, this may be due to the array of plant constituent that may further strain the already injured mitochondria. This may require re-evaluation in future by testing the phytoconstituents individually rather than as crude extracts.

Neuronal cancer cell lines such as the SH-SY5Y cells are often a cell line of choice for primary screening assays, therefore it cannot be ignored that these cells have a proliferative nature and varying bioenergetics that may influence results.

Ionic flux studies are gaining popularity in neurochemistry, however, due to their rapid occurrence there is a need to develop a new high throughput automated ionic flux monitoring. This will reduce time delays caused by manual addition of reagents.

In future studies, it would be recommended to assess alterations to dopamine levels or dopaminergic activity, which could present with other mechanisms for disease improvement.

## References

1. Sertbaş M, Ülgen K, Çakır T. Systematic analysis of transcription-level effects of neurodegenerative diseases on human brain metabolism by a newly reconstructed brain-specific metabolic network. *FEBS Open Bio*. 2014;4:542-53.
2. Kumar GP, Khanum F. Neuroprotective potential of phytochemicals. *Pharmacogn Rev*. 2012;6:81-90.
3. Reddy PH, Reddy TP. Mitochondria as a therapeutic target for aging and neurodegenerative diseases. *Curr Alzheimer Res*. 2011;8:393-409.
4. Giordano S, Darley-Usmar V, Zhang J. Autophagy as an essential cellular antioxidant pathway in neurodegenerative disease. *Redox Biol*. 2014;2:82-90.
5. Kakkar AK, Dahiya N. Management of Parkinson's disease: Current and future pharmacotherapy. *Eur J Pharmacol*. 2015;750:74-81.
6. Kim SW, Ko HS, Dawson VL, Dawson TM. Recent advances in our understanding of Parkinson's disease. *Drug Discov Today Dis Mech*. 2006;2:427-33.
7. Kones R. Mitochondrial therapy for Parkinson's disease: neuroprotective pharmaconutrition may be disease-modifying. *Clin Pharmacol*. 2010;2:185-98
8. Lees AJ, Hardy J, Revesz T. Parkinson's disease. *Lancet*. 2009;373:2055-66.
9. Banerjee R, Starkov AA, Beal MF, Thomas B. Mitochondrial dysfunction in the limelight of Parkinson's disease pathogenesis. *Biochim Biophys Acta*. 2009;1792:651-63.
10. Ham A, Lee S-J, Shin J, Kim K-H, Mar W. Regulatory effects of costunolide on dopamine metabolism-associated genes inhibit dopamine-induced apoptosis in human dopaminergic SH-SY5Y cells. *Neurosci Lett*. 2012;507:101-5.
11. Bhat AH, Dar KB, Anees S, Zargar MA, Masood A, Sofi MA, Ganie SA. Oxidative stress, mitochondrial dysfunction and neurodegenerative diseases; a mechanistic insight. *Biomed Pharmacother*. 2015;74:101-10.
12. Bharath S, Hsu M, Kaur D, Rajagopalan S, Andersen JK. Glutathione, iron and Parkinson's disease. *Biochem Pharmacol*. 2002;64:1037-48.

13. Allen GF, Ullah Y, Hargreaves IP, Land JM, Heales SJ. Dopamine but not L-dopa stimulates neural glutathione metabolism. Potential implications for Parkinson's disease and other dopamine deficiency states. *Neurochem Int.* 2013;62:684-94.
14. Blum D, Torch S, Lambeng N, Nissou M-F, Benabid A-L, Sadoul R, Verna JM. Molecular pathways involved in the neurotoxicity of 6-OHDA, dopamine and MPTP: contribution to the apoptotic theory in Parkinson's disease. *Prog Neurobiol.* 2001;65:135-72.
15. Yadav HP, Li Y. The development of treatment for Parkinson's disease. *Adv Parkinson's Dis.* 2015;4:59-78.
16. Dauer W, Przedborski S. Parkinson's disease: Mechanisms and models. *Neuron.* 2003;39:889-909.
17. Ren R, Sun Y, Zhao X, Pu X. Recent advances in biomarkers for Parkinson's disease focusing on biochemicals, omics and neuroimaging. *Clin Chem Lab Med.* 2015;53:1495-506
18. Stayte S, Vissel B. Advances in non-dopaminergic treatments for Parkinson's disease. *Front Neurosci.* 2014;8:113-39.
19. Brichta L, Greengard P, Flajolet M. Advances in the pharmacological treatment of Parkinson's disease: targeting neurotransmitter systems. *Trends Neurosci.* 2013;36:543-54.
20. Dawson TM, Dawson VL. Molecular pathways of neurodegeneration in Parkinson's disease. *Science.* 2003;302:819-22.
21. Lee D-H, Kim C-S, Lee YJ. Astaxanthin protects against MPTP/MPP<sup>+</sup>-induced mitochondrial dysfunction and ROS production *in vivo* and *in vitro*. *Food Chem Toxicol.* 2011;49:271-80.
22. Gandhi S, Wood NW. Molecular pathogenesis of Parkinson's disease. *Hum Mol Genet.* 2005;14:2749-55.
23. Tsang AH, Chung KK. Oxidative and nitrosative stress in Parkinson's disease. *Biochim Biophys Acta.* 2009;1792:643-50.
24. Wood-Kaczmar A, Gandhi S, Wood N. Understanding the molecular causes of Parkinson's disease. *Trends Mol Med.* 2006;12:521-8.
25. Lee VM-Y, Trojanowski JQ. Mechanisms of Parkinson's disease linked to pathological  $\alpha$ -synuclein: new targets for drug discovery. *Neuron.* 2006;52:33-8.

26. Shen J, Cookson MR. Mitochondria and dopamine: new insights into recessive parkinsonism. *Neuron*. 2004;43:301-4.
27. Duchen MR. Mitochondria in health and disease: perspectives on a new mitochondrial biology. *Mol Aspects Med*. 2004;25:365-451.
28. Abeti R, Abramov AY. Mitochondrial Ca<sup>2+</sup> in neurodegenerative disorders. *Pharmacol Res*. 2015;99:377-81.
29. Jin H, Kanthasamy A, Ghosh A, Anantharam V, Kalyanaraman B, Kanthasamy AG. Mitochondria-targeted antioxidants for treatment of Parkinson's disease: Preclinical and clinical outcomes. *Biochim Biophys Acta*. 2014;1842:1282-94.
30. Cabezas R, Avila MF, Torrente D, El-Bachá RS, Morales L, Gonzalez J, Barreto GE. Astrocytes role in Parkinson: A double-edged sword. *Neurodegener Dis*. 2013;10:491-517.
31. Rizzuto R, Marchi S, Bonora M, Aguiari P, Bononi A, De Stefani D, Giorgi C, Leo S, Rimessi A, Siviero R, Zecchini E. Ca<sup>2+</sup> transfer from the ER to mitochondria: When, how and why. *Biochim Biophys Acta*. 2009;1787:1342-51.
32. Contreras L, Drago I, Zampese E, Pozzan T. Mitochondria: The calcium connection. *Biochim Biophys Acta*. 2010;1797:607-18.
33. Ly JD, Grubb D, Lawen A. The mitochondrial membrane potential ( $\Delta\psi_m$ ) in apoptosis; an update. *Apoptosis*. 2003;8:115-28.
34. Ruzskiewicz J, Albrecht J. Changes in the mitochondrial antioxidant systems in neurodegenerative diseases and acute brain disorders. *Neurochem Int*. 2015;88:66-72.
35. McBean GJ, Aslan M, Griffiths HR, Torrão RC. Thiol redox homeostasis in neurodegenerative disease. *Redox Biol*. 2015;5:186-94.
36. Roberts RA, Laskin DL, Smith CV, Robertson FM, Allen EM, Doorn JA, Slikker W. Nitrate and oxidative stress in toxicology and disease. *Toxicol Sci*. 2009;112:4-16.
37. Ward RJ, Dexter DT, Crichton RR. Neurodegenerative diseases and therapeutic strategies using iron chelators. *J Trace Elem Med Biol*. 2015;31:267-73.
38. Tait SW, Ichim G, Green DR. Die another way—non-apoptotic mechanisms of cell death. *J Cell Sci*. 2014;127:2135-44.

39. Gogvadze V, Orrenius S, Zhivotovsky B. Multiple pathways of cytochrome c release from mitochondria in apoptosis. *Biochim Biophys Acta*. 2006;1757:639-47.
40. Elmore S. Apoptosis: a review of programmed cell death. *Toxicol Pathol*. 2007;35:495-516.
41. Circu ML, Aw TY. Reactive oxygen species, cellular redox systems, and apoptosis. *Free Radic Biol Med*. 2010;48:749-62.
42. McIlwain DR, Berger T, Mak TW. Caspase functions in cell death and disease. *Cold Spring Harb Perspect Biol*. 2013;5: a008656.
43. Lemasters JJ, Nieminen A-L, Qian T, Trost LC, Elmore SP, Nishimura Y, Crowe RA, Cascio WE, Bradham CA, Brenner DA, Herman B. The mitochondrial permeability transition in cell death: a common mechanism in necrosis, apoptosis and autophagy. *Biochim Biophys Acta*. 1998;1366:177-96.
44. Berghe TV, Vanlangenakker N, Parthoens E, Deckers W, Devos M, Festjens N, Guerin CJ, Brunk UT, Declercq W, Vandenabeele P. Necroptosis, necrosis and secondary necrosis converge on similar cellular disintegration features. *Cell Death Differ*. 2010;17:922-30.
45. Mazzi EA, Reams RR, Soliman KF. The role of oxidative stress, impaired glycolysis and mitochondrial respiratory redox failure in the cytotoxic effects of 6-hydroxydopamine *in vitro*. *Brain Res*. 2004;1004:29-44.
46. Feoktistova M, Leverkus M. Programmed necrosis and necroptosis signalling. *FEBS J*. 2015;282:19-31.
47. Green DR, Reed JC. Mitochondria and apoptosis. *Science*. 1998;281:1309-12.
48. Lopes FM, Schröder R, da Frota Júnior MLC, Zanotto-Filho A, Müller CB, Pires AS, Meurer RT, Colpo GD, Gelain DP, Kapczinski F, Moreira JC. Comparison between proliferative and neuron-like SH-SY5Y cells as an *in vitro* model for Parkinson disease studies. *Brain Res*. 2010;1337:85-94.
49. Lastres-Becker I, Molina-Holgado F, Ramos JA, Mechoulam R, Fernández-Ruiz J. Cannabinoids provide neuroprotection against 6-hydroxydopamine toxicity *in vivo* and *in vitro*: Relevance to Parkinson's disease. *Neurobiol Dis* 2005;19:96-107.
50. Fasano M, Alberio T, Colapinto M, Mila S, Lopiano L. Proteomics as a tool to investigate cell models for dopamine toxicity. *Parkinsonism Relat. Disord*. 2008;14:135-8.
51. Martin W, Wieler M. Treatment of Parkinson's disease. *Can J Neurol Sci*. 2003;30:27-33.

52. Pazdernik T. Lippincott's Illustrated Reviews: Pharmacology. Med Sci Sports Exerc. 2009;41:1531.
53. Jones T, Murray R. Current research in and development of treatments for Parkinson's disease. Pharm J. 2011;287:293-300.
54. Connolly BS, Lang AE. Pharmacological treatment of Parkinson disease: A review. Jama. 2014;311:1670-83.
55. Worth PF. How to treat Parkinson's disease in 2013. Clin Med. 2013;13:93-6.
56. Katzenschlager R, Lees AJ. Treatment of Parkinson's disease: Levodopa as the first choice. J Neurol. 2002;249:19-24.
57. Hu S, Han R, Mak S, Han Y. Protection against 1-methyl-4-phenylpyridinium ion (MPP<sup>+</sup>)-induced apoptosis by water extract of ginseng (*Panax ginseng*) in SH-SY5Y cells. J Ethnopharmacol. 2011;135:34-42.
58. Balunas MJ, Kinghorn AD. Drug discovery from medicinal plants. Life Sci. 2005;78:431-41.
59. Street R, Stirk W, Van Staden J. South African traditional medicinal plant trade—challenges in regulating quality, safety and efficacy. J Ethnopharmacol. 2008;11:705-10.
60. Rishton GM. Natural products as a robust source of new drugs and drug leads: Past successes and present day issues. Am J Cardiol. 2008;101:43-9.
61. Stafford GI, Pedersen ME, van Staden J, Jäger AK. Review on plants with CNS-effects used in traditional South African medicine against mental diseases. J Ethnopharmacol. 2008;119:513-37.
62. van Wyk BE, VanOudtshoorn B, Gericke N. Medicinal Plants of South Africa: Briza; 2009.
63. Sharma P, Chaurasia S. Evaluation of total phenolic, flavonoid contents and antioxidant activity of *Acokanthera oppositifolia* and *Leucaena leucocephala*. Int J Pharmacogn Phytochem Res. 2014;7:175-180.
64. Adedapo AA, Jimoh FO, Afolayan AJ, Masika PJ. Antioxidant activities and phenolic contents of the methanol extracts of the stems of *Acokanthera oppositifolia* and *Adenia gummifera*. BMC Complement Altern Med 2008;8:54-61.

65. Gadaga LL, Tagwireyi D, Dzungare J, Nhachi CF. Acute oral toxicity and neurobehavioural toxicological effects of hydroethanolic extract of *Boophone disticha* in rats. *Hum Exp Toxicol.* 2011;30:972-80.
66. Nair JJ, Van Staden J. Traditional usage, phytochemistry and pharmacology of the South African medicinal plant *Boophone disticha* (L.f.) Herb. (Amaryllidaceae). *J Ethnopharmacol.* 2014;151:12-26.
67. Dhingra D, Sharma A. A review on antidepressant plants. *Nat Prod Radiance.* 2006;5:144-52.
68. Benedí J, Arroyo R, Romero C, Martín-Aragón S, Villar AM. Antioxidant properties and protective effects of a standardized extract of *Hypericum perforatum* on hydrogen peroxide-induced oxidative damage in PC12 cells. *Life Sci.* 2004;75:1263-76.
69. Bienvenu E, Amabeoku G, Eagles P, Scott G, Springfield E. Anticonvulsant activity of aqueous extract of *Leonotis leonurus*. *Phytomedicine.* 2002;9:217-23.
70. Holzapfel CW, Marais W, Wessels PL, Van Wyk B-E. Furanoterpenoids from *Siphonochilus aethiopicus*. *Phytochemistry.* 2002;59:405-7.
71. Eldeen IM, Elgorashi EE, Mulholland DA, van Staden J. Anolignan B: A bioactive compound from the roots of *Terminalia sericea*. *J Ethnopharmacol.* 2006;103:135-8.
72. Vermaak I, Enslin GM, Idowu TO, Viljoen AM. *Xysmalobium undulatum* (uzara)—review of an antidiarrhoeal traditional medicine. *J Ethnopharmacol.* 2014;156:135-46.
73. Olajuyigbe OO, Afolayan AJ. Phenolic content and antioxidant property of the bark extracts of *Ziziphus mucronata* Willd. subsp. *mucronata* Willd. *BMC Complement Altern Med.* 2011;11:130-8.
74. Gilgun-Sherki Y, Melamed E, Offen D. Oxidative stress induced-neurodegenerative diseases: The need for antioxidants that penetrate the blood brain barrier. *Neuropharmacol.* 2001;40:959-75.
75. Stahl E. Thin-layer chromatography. A laboratory handbook. 1967
76. Vichai V, Kirtikara K. Sulforhodamine B colorimetric assay for cytotoxicity screening. *Nat Protoc.* 2006;1:1112-6.
77. Kalyanaraman B, Darley-Usmar V, Davies KJ, Dennery PA, Forman HJ, Grisham MB, Mann GE, Moore K, Roberts LJ, Ischiropoulos H. Measuring reactive oxygen and nitrogen species with fluorescent probes: Challenges and limitations. *Free Radic Biol Med.* 2012;52:1-6.

78. Kamencic H, Lyon A, Paterson PG, Juurlink BH. Monochlorobimane fluorometric method to measure tissue glutathione. *Anal Biochem.* 2000;286:35-7.
79. Gravance CG, Garner DL, Baumber J, Ball BA. Assessment of equine sperm mitochondrial function using JC-1. *Theriogenology.* 2000;53:1691-703.
80. Robinson JA, Jenkins NS, Holman NA, Roberts-Thomson SJ, Monteith GR. Ratiometric and nonratiometric Ca<sup>2+</sup> indicators for the assessment of intracellular free Ca<sup>2+</sup> in a breast cancer cell line using a fluorescence microplate reader. *J Biochem Biophys Methods.* 2000;58:227-37.
81. Nkandeu DS, Mqoco TV, Visagie MH, Stander BA, Wolmarans E, Cronje MJ, Joubert AM. *In vitro* changes in mitochondrial potential, aggresome formation and caspase activity by a novel 17- $\beta$ -estradiol analogue in breast adenocarcinoma cells. *Cell Biochem Funct.* 2013;31:566-74.
82. Mugomeri E, Chatanga P, Hlapisi S, Rahlao L. Phytochemical characterization of selected herbal products in Lesotho. *Lesotho Med Assoc J.* 2014;12:38-47.
83. Wojdyło A, Oszmiański J, Czemerys R. Antioxidant activity and phenolic compounds in 32 selected herbs. *Food Chem.* 2007;105:940-9.
84. Radulović N, Đorđević A, Palić R, Zlatković B. Essential oil composition of *Hypericum annulatum* Moris (Hypericaceae) from Serbia. *J Essent Oil Res.* 2010;22:619-24.
85. Joshi K, Chavan P, Warude D, Patwardhan B. Molecular markers in herbal drug technology. *Curr Sci.* 2004;87:159-65.
86. Oleszek W, Stochmal A, Karolewski P, Simonet AM, Macias FA, Tava A. Flavonoids from *Pinus sylvestris* needles and their variation in trees of different origin grown for nearly a century at the same area. *Biochem Syst Ecol.* 2002;30:1011-22.
87. Do QD, Angkawijaya AE, Tran-Nguyen PL, Huynh LH, Soetaredjo FE, Ismadji S, Ju YH. Effect of extraction solvent on total phenol content, total flavonoid content, and antioxidant activity of *Limnophila aromatica*. *J Food Drug Anal.* 2014;22:296-302.
88. Fouche G, Cragg GM, Pillay P, Kolesnikova N, Maharaj VJ, Senabe J. *In vitro* anticancer screening of South African plants. *J Ethnopharmacol.* 2008;119:455-61.
89. Saeed ME, Meyer M, Hussein A, Efferth T. Cytotoxicity of South-African medicinal plants towards sensitive and multidrug-resistant cancer cells. *J Ethnopharmacol.* 2016;186:209-23.

90. Cordier W, Steenkamp V. Evaluation of four assays to determine cytotoxicity of selected crude medicinal plant extracts *in vitro*. Br J Pharm Res. 2015;7:16-21.
91. Adewusi EA, Fouche G, Steenkamp V. Antioxidant, acetylcholinesterase inhibitory activity and cytotoxicity assessment of the crude extracts of *Boophane disticha*. Afri J Pharmacol Ther. 2012;1:78-83.
92. Liu Z-M, Huang X-Y, Cui M-R, Zhang X-D, Chen Z, Yang BS, Zhao XK. Amaryllidaceae alkaloids from the bulbs of *Lycoris radiata* with cytotoxic and anti-inflammatory activities. Fitoterapia. 2015;101:188-93.
93. Cortes N, Posada-Duque RA, Alvarez R, Alzate F, Berkov S, Cardona-Gómez GP, Osorio E. Neuroprotective activity and acetylcholinesterase inhibition of five Amaryllidaceae species: A comparative study. Life Sci. 2015;122:42-50.
94. El-Ansari MA, Aboutabl EA, Farrag ARH, Sharaf M, Hawas UW, Soliman GM, El-Seed GS. Phytochemical and pharmacological studies on *Leonotis leonurus*. Pharm Biol. 2009;47:894-902.
95. Lategan CA, Campbell WE, Seaman T, Smith PJ. The bioactivity of novel furanoterpenoids isolated from *Siphonochilus aethiopicus*. J Ethnopharmacol. 2009;121:92-7.
96. Kopalli SR, Noh SJ, Koppula S, Suh YH. Methylparaben protects 6-hydroxydopamine-induced neurotoxicity in SH-SY5Y cells and improved behavioural impairments in mouse model of Parkinson's disease. Neurotoxicology. 2013;34:25-32.
97. Esmaeili-Mahani S, Vazifekhah S, Pasban-Aliabadi H, Abbasnejad M, Sheibani V. Protective effect of orexin-A on 6-hydroxydopamine-induced neurotoxicity in SH-SY5Y human dopaminergic neuroblastoma cells. Neurochem Int. 2013;63:719-25.
98. Ju MS, Lee P, Kim HG, Lee KY, Hur J, Cho SH, Sung SH, Oh MS. Protective effects of standardized Thuja orientalis leaves against 6-hydroxydopamine-induced neurotoxicity in SH-SY5Y cells. Toxicol In Vitro. 2010;24:759-65.
99. Jantas D, Greda A, Golda S, Korostynski M, Grygier B, Roman A, Pilc A, Lason W. Neuroprotective effects of metabotropic glutamate receptor group II and III activators against MPP<sup>+</sup>-induced cell death in human neuroblastoma SH-SY5Y cells: the impact of cell differentiation state. Neuropharmacol. 2014;83:36-53.
100. Xie H-r, Hu L-S, Li G-Y. SH-SY5Y human neuroblastoma cell line: *In vitro* cell model of dopaminergic neurons in Parkinson's disease. Chin Med J. 2010;123:1086-92.

101. Donato MT, Martínez-Romero A, Jiménez N, Negro A, Herrera G, Castell JV, et al. Cytometric analysis for drug-induced steatosis in HepG2 cells. *Chem Biol Interact.* 2009;181:417-23.
102. Custodio JB, Moreno AJ, Wallace KB. Tamoxifen inhibits induction of the mitochondrial permeability transition by  $Ca^{2+}$  and inorganic phosphate. *Toxicol Appl Pharmacol.* 1998;152:10-7.
103. Kanski J, Aksenova M, Stoyanova A, Butterfield DA. Ferulic acid antioxidant protection against hydroxyl and peroxy radical oxidation in synaptosomal and neuronal cell culture systems *in vitro*: structure-activity studies. *J Nutr Biochem.* 2002;13:273-81.
104. Maurya DK, Devasagayam TPA. Antioxidant and prooxidant nature of hydroxycinnamic acid derivatives ferulic and caffeic acids. *Food Chem Toxicol.* 2010;48:3369-73.
105. Lee DH, Han YS, Han ES, Bang H, Lee CS. Differential involvement of intracellular  $Ca^{2+}$  in 1-methyl-4-phenylpyridinium-or 6-hydroxydopamine-induced cell viability loss in PC12 cells. *Neurochem Res.* 2006;31:851-60.
106. Fujita H, Shiosaka M, Ogino T, Okimura Y, Utsumi T, Sato EF, Akagi R, Inoue M, Utsumi K, Sasaki.  $\alpha$ -Lipoic acid suppresses 6-hydroxydopamine-induced ROS generation and apoptosis through the stimulation of glutathione synthesis but not by the expression of heme oxygenase-1. *Brain Res.* 2008;1206:1-12.
107. Blum D, Torch S, Nissou MF, Benabid AL, Verna JM. Extracellular toxicity of 6-hydroxydopamine on PC12 cells. *Neurosci Lett.* 2000;283:193-6.
108. Shim JS, Kim HG, Ju MS, Choi JG, Jeong SY, Oh MS. Effects of the hook of *Uncaria rhynchophylla* on neurotoxicity in the 6-hydroxydopamine model of Parkinson's disease. *J Ethnopharmacol.* 2009;126:361-5.
109. Tirmenstein MA, Hu CX, Scicchitano MS, Narayanan PK, McFarland DC, Thomas HC, Schwartz LW. Effects of 6-hydroxydopamine on mitochondrial function and glutathione status in SH-SY5Y human neuroblastoma cells. *Toxicol In Vitro.* 2005;19:471-9.
110. Cairns RA, Harris IS, Mak TW. Regulation of cancer cell metabolism. *Nat Rev Cancer.* 2011;11:85-95.
111. Zhu TG, Wang XX, Luo WF, Zhang QL, Huang TT, Xu XS, Liu CF. Protective effects of urate against 6-OHDA-induced cell injury in PC12 cells through antioxidant action. *Neurosci Lett.* 2012;506:175-9.

112. Rogers K, Fong W, Redburn J, Griffiths LR. Fluorescence detection of plant extracts that affect neuronal voltage-gated  $Ca^{2+}$  channels. *Eur J Pharm Sci.* 2002;15:321-30.
113. Meng H, Li C, Feng L, Cheng B, Wu F, Wang X, Li Z, Liu S. Effects of Ginkgolide B on 6-OHDA-induced apoptosis and calcium over load in cultured PC12. *Int J Dev Neurosci.* 2007;25:509-14.
114. Huang L, Xue Y, Feng D, Yang R, Nie T, Zhu G, Tao K, Gao G, Yang Q. Blockade of RyRs in the ER attenuates 6-OHDA-induced calcium overload, cellular hypo-excitability and apoptosis in dopaminergic neurons. *Front Cellular Neurosci.* 2017;11:52-64.
115. Krishna AB, Manikyam HK, Sharma VK, Sharma N. Plant cardenolides in therapeutics. *Int J Indig Med Plants.* 2015.48:1871-96.
116. Belmokhtar CA, Hillion J, Segal-Bendirdjian E. Staurosporine induces apoptosis through both caspase-dependent and caspase-independent mechanisms. *Oncogene.* 2001;20:3354-62.
117. Latchoumycandane C, Anantharam V, Jin H, Kanthasamy A, Kanthasamy A. Dopaminergic neurotoxicant 6-OHDA induces oxidative damage through proteolytic activation of PKC $\delta$  in cell culture and animal models of Parkinson's disease. *Toxicol Appl Pharmacol.* 2011;256:314-23.
118. Li L, Gao L, Song Y, Qin Z-H, Liang Z. Activated cathepsin L is associated with the switch from autophagy to apoptotic death of SH-SY5Y cells exposed to 6-hydroxydopamine. *Biochem Biophys Res Commun.* 2016;470:579-85.

# Appendix I: Ethical approval

The Research Ethics Committee, Faculty Health Sciences, University of Pretoria complies with ICH-GCP guidelines and has US Federal wide Assurance.

- FWA 00002567, Approved dd 22 May 2002 and Expires 20 Oct 2016.
- IRB 0000 2235 IORG0001762 Approved dd 22/04/2014 and Expires 22/04/2017.



UNIVERSITEIT VAN PRETORIA  
UNIVERSITY OF PRETORIA  
YUNIBESITHI YA PRETORIA

Faculty of Health Sciences Research Ethics Committee

9/05/2016

## Approval Certificate New Application

**Ethics Reference No.: 147/2016**

**Title:** Assessment of the effect of selected African plants on an in vitro model of Parkinson's disease.

Dear Keagile Lepule

The **New Application** as supported by documents specified in your cover letter dated 21/04/2016 for your research received on the 25/04/2016, was approved by the Faculty of Health Sciences Research Ethics Committee on its quorate meeting 25/03/2016.

Please note the following about your ethics approval:

- Ethics Approval is valid for 2 years **Start Date:** 01-Feb-2016 **End Date:** 30-Nov-2017 **Duration:** 2 years
- Please remember to use your protocol number (**147/2016**) on any documents or correspondence with the Research Ethics Committee regarding your research.
- Please note that the Research Ethics Committee may ask further questions, seek additional information, require further modification, or monitor the conduct of your research.

**Ethics approval is subject to the following:**

- The ethics approval is conditional on the receipt of 6 monthly written Progress Reports, and
- The ethics approval is conditional on the research being conducted as stipulated by the details of all documents submitted to the Committee. In the event that a further need arises to change who the investigators are, the methods or any other aspect, such changes must be submitted as an Amendment for approval by the Committee.

We wish you the best with your research.

Yours sincerely

Dr R Semmeré, MChB; MMed (Int); MPharm, PhD  
Deputy Chairperson of the Faculty of Health Sciences Research Ethics Committee, University of Pretoria

*The Faculty of Health Sciences Research Ethics Committee complies with the SA National Act 61 of 2003 as it pertains to health research and the United States Code of Federal Regulations Title 45 and 46. This committee abides by the ethical norms and principles for research, established by the Declaration of Helsinki, the South African Medical Research Council Guidelines as well as the Guidelines for Ethical Research: Principles Structures and Processes 2004 (Department of Health).*

☎ 012 356 3085    ✉ fhsethics@up.ac.za    🌐 <http://www.up.ac.za/healthethics>  
✉ Private Bag X323, Arcadia, 0007 - Tswelopele Building, Level 4-59, Gezina, Pretoria

**\*\* Kindly collect your original signed approval certificate from our offices, Faculty of Health Sciences, Research Ethics Committee, Tswelopele Building, Level 4-59**

## Appendix II: Reagent preparation

### **2,2'-Azobis (2-methylpropionamide) dihydrochloride (AAPH)**

AAPH powder was obtained from Sigma Aldrich (St. Louis, USA). A stock solution (400 mM) was prepared by dissolving 21.7 mg in 200  $\mu$ L of distilled water. Aliquots were stored at  $-80^{\circ}\text{C}$  and a fresh working solution prepared prior to use.

### **5,5',6,6'-Tetrachloro-1,1,3,3'- tetraethylbenzimidazolylcarbocyanine iodide (JC-1)**

5,5',6,6'-Tetrachloro-1,1,3,3'- tetraethylbenzimidazolylcarbocyanine iodide (JC-1) powder was obtained from Sigma Aldrich (St Louis, USA). Stock solutions (5 mg/ mL) were prepared by dissolving 5 mg with 1 mL DMSO.

### **5% Aqueous Sulphuric acid**

Sulphuric acid was purchased from Merck Chemical (Darmstadt, Germany). Aqueous Sulphuric acid was prepared by slowly adding 2.5 mL in 47.5 mL of deionised water.

### **6-Hydroxydopamine (6-OHDA)**

6-Hydroxydopamine powder was obtained from Sigma Aldrich (St Louis, USA). Stock solutions (121.mM) were prepared by dissolving 25 mg with 1 mL of 1% ascorbic acid. Aliquots were stored at  $-80^{\circ}\text{C}$  and fresh working solution was prepared prior to experiments.

### **1-Methyl-4-phenypyridinium (MPP<sup>+</sup>)**

1-Methyl-4-phenypyridinium (MPP<sup>+</sup>) powder was purchased from Sigma Aldrich (St. Louis, USA). Stock solutions (67.3 mM) were prepared by dissolving 20 mg in 1 mL of 0.1% ascorbic acid. The aliquots were stored at  $-80^{\circ}\text{C}$ . Working solutions were prepared freshly prior to use.

### **Aqueous 3% sodium nitrate and 1% Aluminium chloride**

Sodium nitrate and Aluminium chloride were purchased from Sigma Aldrich (St Louis, USA). The solution was prepared by dissolving 1.5 g of Sodium nitrate and 0.5 g Aluminium chloride in 50 mL of deionized water.

### **Dihydrodichlorofluorescein diacetate (H<sub>2</sub>-DCF-DA)**

Dihydrodichlorofluorescein diacetate (H<sub>2</sub>-DCF-DA) powder was purchased from Sigma Aldrich (St Louis USA). Stock solutions (20.5 mM) were prepared by dissolving 10 mg with 1 mL DMSO. Aliquots were stored at -80°C and fresh working solution was prepared prior to use.

### **Dulbecco's Modified Eagle's Medium (DMEM)**

Dulbecco's Modified Eagle's Medium was purchased from Sigma Aldrich (St Louis, USA). The mass of 48 g DMEM powder was dissolved in 5 L of sterile deionised water. The solution was filter sterilised twice using a 0.22 µm cellulose acetate filter. The medium was fortified with 1% penicillin/streptomycin and subsequently stored in 500 mL bottles at 4°C. Prior to use the medium was supplemented with 10% FCS.

### **Dragendorff's reagent**

Potassium iodide and Bismuth nitrate were purchased at Merck Chemical (Darmstadt, Germany). The Potassium iodide solution was prepared by dissolving 13 g Potassium iodide powder in 100 mL of 30% (v/v) aqueous acetic acid. Bismuth nitrate solution was prepared by dissolving 1.7 g of Bismuth nitrate powder in 100 mL 30% (v/v) aqueous acetic acid. The two solutions were mixed at a ratio of 4:1 (Bismuth nitrate:potassium iodide)

### **Foetal calf serum (FCS)**

Foetal calf serum was obtained from PAA (Pasching, Austria). The host serum complements was heat inactivated by incubating at 56°C for 45 min. This was added to culture media to a concentration of 10%.

### **Folin ciocalteau reagent**

Folin ciocalteau reagent was purchased from Sigma Aldrich (St Louis, USA) and used as undiluted.

### **Fura-2 AM**

Fura-2 AM powder was obtained from Sigma Aldrich (St Louis, USA). Stock solutions (5 mM) were prepared by dissolving 5 mg with 1 mL DMSO. Aliquots were stored at -80°C and fresh working solution were prepared prior to use.

### **Ham's F12 medium**

Ham's F12 medium powder was purchased from Sigma Aldrich (St Louis, USA). The mass of 48 g Ham's F12 medium powder was dissolved in 5 litre of sterile deionised water. The solution was filter sterilised twice using a 0.22  $\mu\text{m}$  cellulose acetate filter. The medium was fortified with 1% penicillin/streptomycin and subsequently stored in 500 mL bottles at 4°C. Prior to use the medium was supplemented with 10% FCS.

### **Loading buffer**

Loading Buffer consisted of 5.9 mM potassium chloride (KCl), 1.4 mM magnesium chloride ( $\text{MgCl}_2$ ), 10 mM HEPES, 1.2 mM monosodium phosphate ( $\text{NaH}_2\text{PO}_4$ ), 5 mM sodium bicarbonate ( $\text{NaHCO}_3$ ), 140 mM Sodium chloride (NaCl), 11.5 mM D-glucose and 1.8 mM calcium chloride ( $\text{CaCl}_2$ ). The buffer was prepared by dissolving 439.9 mg of KCl, 133.9 mg of  $\text{MgCl}_2$ , 2.38 g of HEPES, 143.98 mg of  $\text{NaH}_2\text{PO}_4$ , 420.04 mg of  $\text{NaHCO}_3$ , 8.18 g of NaCl, 2.07 g of D-glucose and 200.0 mg of  $\text{CaCl}_2$  in a litre of Tris-base. The solution was sonicated till everything was completely dissolved; the pH was adjusted with sodium hydroxide or hydrochloric acid.

### **Monochlorobimane**

Monochlorobimane (MCB) powder was purchased from Sigma Aldrich (St. Louis, USA). Stock solutions (25 mM) were prepared by dissolving 5 mg in 880  $\mu\text{L}$  of DMSO. The aliquots were stored at -80°C. Working solutions were prepared freshly prior to use.

### **Phosphate buffered saline (PBS)**

BBL™ FTA hemagglutination powder was obtained from BD biosciences (France). The buffer was prepared by dissolving 9.23 g in a litre of distilled water and subsequently stored at 4°C.

### **Saponin**

Saponin powder was obtained from Sigma Aldrich (St. Louis, USA). A 1% solution was prepared by dissolving 1 g into 100 mL of distilled water and subsequently stored at 4°C.

### **Solvents**

Organic solvents (acetone, methanol, chloroform, DMSO) were obtained from Merck Chemical (Darmstadt, Germany).

### **Staurosporine**

Staurosporine powder was obtained from Sigma Aldrich (St. Louis, USA). Stock solution (2.14 mM) was prepared by dissolving 0.5 mg in 500  $\mu$ L DMSO, aliquots were stored at  $-80^{\circ}\text{C}$ . Working solution was prepared in PBS.

### **Sulforhodamine B**

Sulforhodamine B powder was obtained from Sigma Aldrich (St. Louis, USA). Solution (0.057%) was prepared by dissolving 57 mg in 100 mL 1% acetic acid .

### **Tamoxifen**

Tamoxifen citrate was purchased from Sigma Aldrich (St. Louis, USA). Stock solutions (30 mM) were prepared by dissolving 16.90 mg into 1 mL of DMSO. Aliquots were stored at  $-80^{\circ}\text{C}$  and working solutions were prepared with medium prior to experiments.

### **Trichloroacetic acid**

Trichloroacetic acid was obtained from Merck Chemical (Darmstadt, Germany). The solution (5% w/v) was prepared by dissolving 50 g in a 100 mL of distilled water and subsequently stored at  $4^{\circ}\text{C}$ .

### **Tris-Base**

Tris-Base powder was purchased from Merck Chemicals (Darmstadt, Germany). The solution was prepared by dissolving 2.42 g in 1 L of distilled water, and was stored at  $4^{\circ}\text{C}$ . The pH was adjusted to 7.4 using sodium hydroxide and hydrochloric acid.

### **Trypan blue counting solution**

Trypan blue powder was purchased from BDH Laboratories Supplies (UK). Trypan blue counting solution (0.1% w/v) was prepared by dissolving 200 mg trypan blue powder in 50 mL PBS and subsequently the solution was filtered through a  $0.45\ \mu\text{m}$  syringe filter to remove any insoluble particulates.

### **Tyrosin/Versene**

Tyrosin/versene solution was obtained from The Scientific Group (Gauteng, RSA) in liquid form and used undiluted.

### **1% Vanillin in 5% aqueous sulphuric acid**

Vanillin powder was purchased from Sigma Aldrich (St. Louis, USA). The solution was prepared by dissolving 0.5 g vanillin powder in 50 mL 5% (v/v) aqueous sulphuric acid prior to use.